2016-06-27

The SMURF2-YY1-C-MYC Axis in the Germinal Center Reaction and Diffuse Large B Cell Lymphoma: A Dissertation

Sally E. Trabucco
University of Massachusetts Medical School

THE SMURF2-YY1-C-MYC AXIS IN THE GERMINAL CENTER REACTION AND DIFFUSE LARGE B CELL LYMPHOMA

A Dissertation Presented

By

SALLY ELIZABETH TRABUCCO

Submitted to the Faculty of the
University of Massachusetts Graduate School of Biomedical Sciences,
Worcester
in partial fulfillment of the requirements for the degree of

DOCTOR OF PHILOSOPHY

JUNE 27, 2016

CELL BIOLOGY

THE SMURF2-YY1-C-MYC AXIS IN THE GERMINAL CENTER REACTION AND DIFFUSE LARGE B CELL LYMPHOMA

A Dissertation Presented
By
SALLY ELIZABETH TRABUCCO

The signatures of the Dissertation Defense Committee signify completion and approval as to style and content of the Dissertation

_____
Hong Zhang, Ph.D, Thesis advisor

_____
Carol Schrader, Ph.D., Member of Committee

_____
Rachel Gerstein, Ph.D., Member of Committee

_____
Brian Lewis, Ph.D., Member of Committee

_____
John Manis, M.D., Member of Committee

The signature of the Chair of the Committee signifies that the written dissertation meets the requirements of the Dissertation Committee

_____
Stephen Jones, Ph.D., Chair of Committee

The signature of the Dean of the Graduate School of Biomedical Sciences signifies that the student has met all graduation requirements of the school.

_____
Anthony Carruthers, Ph.D.
Dean of the Graduate School of Biomedical Sciences

Cell Biology Program
June 27, 2016

Acknowledgments

First, I would like to thank my mentor, Hong Zhang, for his support and guidance over the last four years. He has made a welcoming lab environment and supported my many ideas and pursuits throughout graduate school. I also would like to thank past members of the Zhang lab, Hang Cui, Charusheila Ramkumar, and Yahui Kong for helping me settle into the lab, teaching me new techniques, and being supportive of experiments directly related to my thesis. I would also like to thank the Cell and Developmental Biology department which has been a wonderful place to learn and collaborate. The advice, guidance, and challenging questions my committee, Stephen Jones, Rachel Gerstein, Brian Lewis, Carol Schrader, and John Manis, provided has been greatly appreciated. My committee has gone above and beyond just advice and often provided resources for experiments and advice on new techniques, for which I am grateful.

I thank James Bradner for the JQ1 compound and advice when preparing our manuscript. I thank Andrew Evens, John Manis, and Subbarao Bondada for providing reagents for the experiments presented in chapter II. I also would like to thank Brian Lewis, Carol Schrader, and David Weaver for providing reagents for the experiments presented in chapter III.

Finally, I would like to thank the family and friends who have supported me throughout graduate school and life. I specifically want to thank my roommates through various stages in graduate school, Melissa Fulham, Justine Richardson, and Tina Kuksin, who all spend many nights at home discussing science and graduate school with me. I especially need to thank my family: my parents who spent many hours listening to me in both excitement and frustration and who have always believed I could do anything I set my mind to, my brother who was always there for a good laugh and to get my mind off school and experiments when I needed a break, my grandparents who started calling me Dr. Sal years ago knowing someday soon I would get to this point, and the rest of my extended family who have been understanding when I missed events for a time point and supportive of my educational endeavors through these past 23 years.

Abstract

Diffuse large B cell lymphoma (DLBCL) is the most common non-Hodgkin's lymphoma. Patients who fail conventional therapy (~50%) have a poor prognosis and few treatment options. It is essential to understand the underlying biological processes, the progression of the disease, and utilize this information to develop new therapeutics.

DLBCL patients with high C-MYC expression have a poor prognosis and new therapeutics for these patients are needed. This thesis describes work testing the hypothesis that JQ1, which can indirectly inhibit C-MYC in some tumors, can be used as an effective treatment for DLBCL. Some tumors have an unknown mechanism causing high C-MYC expression, leading me to investigate the underlying mechanisms. YY1 is a transcriptional regulator of *c-Myc* and has been implicated in DLBCL and as a potential regulator of the germinal center (GC) reaction. DLBCL arises from GC cells or post-GC cells. I tested the hypothesis that YY1 regulates the GC reaction. SMURF2 is an E3-ubiquitin ligase for YY1 and a tumor suppressor for DLBCL. I was interested in examining the mechanism underlying the suppression of DLBCL by SMURF2 leading to the hypothesis that SMURF2 regulates the GC.

This thesis shows JQ1 leads to cell death and cellular senescence in human DLBCL cells. I conclude that BRD4 inhibition by JQ1 or derivatives could provide a new therapeutic avenue for DLBCL patients. I also show loss of YY1 perturbs the GC by decreasing the dark zone and increasing apoptosis. Finally I show modulation of SMURF2 does not affect the GC, suggesting SMURF2 utilizes a different mechanism to act as a tumor suppressor and may not modulate YY1 in the context of the GC.

TABLE OF CONTENTS

List of Tables

List of Figures

Copyrighted Materials Produced by the Author

Some data and analysis in this thesis have been previously published. All previously published data and analysis presented in this thesis were originally obtained and analyzed by the author. Final analysis included contributions from co-authors listed.

Chapter II and some related portions of Chapters I and V have been previously published as:

Trabucco, SE., Gerstein, RM., Evens, AM., Bradner, JE., Schultz, LD., Greiner, DL., and Zhang, H. (2015) Inhibition of bromodomain proteins for the treatment of human diffuse large B-cell lymphoma. Clin. Cancer Res. *21*, 112-122

Chapter III and some related portions of Chapters I and V have been submitted as a manuscript not yet in print:

Trabucco, SE., Gerstein, RM., and Zhang, H. (2016) YY1 regulates the germinal center reaction by inhibiting apoptosis. J. Immunology.

CHAPTER I: Introduction

Diffuse Large B-cell Lymphoma

Diffuse Large B-cell Lymphoma (DLBCL) is the most common non-Hodgkin's lymphoma, accounting for 30-40% of diagnoses(1, 2). Approximately 50% of patients eventually fail the conventional treatment, a combination therapy that includes chemotherapeutic agents doxorubicin, cyclophosphamide, and vincristine, prednisone, and targeted anti-CD20 monoclonal antibody rituximab, termed R-CHOP. The inclusion of rituximab, which specifically ablates B cells, improves the cure rate of DLBCL by 10-15%, indicating the benefit of targeted therapies(3). For patients who either do not respond or relapse after treatment, prognosis is poor and few treatment options outside of stem cell transplant exist(3, 4). Unfortunately, the advanced age of patients with DLBCL predisposes them to comorbidities and confounding factors, which prevent them from tolerating high doses of chemotherapy and also render them ineligible for stem cell transplant. Recent studies have focused on understanding the underlying genetics of DLBCL in an effort to discover specific targets for new therapeutics, which may decrease the need for high doses of chemotherapy or increase the overall survival rate of patients(5) (5).

DLBCL has been separated into three distinct subtypes, termed the cell of origin classification, by gene expression profiling: activated B-cell-like (ABC), germinal center B-cell-like (GCB), and primary mediastinal B-cell lymphoma (PMBL) (6–10). These subtypes differ in molecular features and

cell of origin, each arising from distinct molecular processes that ultimately lead to neoplastic transformation. The ABC subtype has a gene expression signature that is similar to activated peripheral blood B cells, while the GCB subtype is similar to germinal center B cells (described below) and PMBL subtype arises from thymic B cells(6). Patients with ABC subtype have a worse prognosis than those with GCB subtype(6).

Mutations in *EZH2* and chromosomal translocations of *BCL2*, which leads to decreased apoptosis or *C-MYC*, leading to increased proliferation, are more common in the GCB subtype(7, 11–13). Alterations in *BLIMP1/PRDM1*, which regulates B cell differentiation(14–16), and various mutations leading to activation of the *NF-κB* pathway(17–21), are associated with the ABC subtype. Common to both GCB and ABC subtypes are *BCL6* translocations(22, 23) and mutations in *CREBBP* and *EP300*(24). Additional recurrent mutations in DLBCL have been identified recently(24–28), although the ability of these mutations to directly lead to lymphomagenesis has not been studied experimentally. In particular, a number of reports have highlighted the incidence of both *C-MYC* translocations (8.8-11%) and increased protein levels of C-MYC (29-31.8%) in DLBCL(29, 30). Once identified, these genetic alterations provide promising targets for the development of new therapeutics.

In addition to the cell of origin classification of DLBCL subtypes described above, Monti and colleagues independently identified subsets

classified as consensus clusters based on gene clustering(31). The three consensus clusters are OxPhos (related to oxidative phosphorylation), BCR/proliferation (related to cell cycle and B cell receptor (BCR) signaling cascade), and HR (related to immunological host response) (31). These consensus clusters do not significantly overlap with the cell of origin classification, and are not as effective as the cell of origin classification at predicting response to current standard therapeutics(31), which may be why the cell of origin has been more widely adopted. However, the consensus clustering classification strategy may identify tumors that would respond well to other therapies, for example OxPhos tumors may be sensitive to proteasome inhibition and HR tumors may respond well to immune modulators(31).

Germinal Centers

B cells initially differentiate from common lymphoid progenitors into early stages of development in the bone marrow. During this differentiation process progenitor B cells (pro-B cells) undergo variable-distal-joining (V(D)J) recombination in order to produce a variety of immunoglobulin molecules with affinity for different antigens. This process provides an initial step to diversify the antigens recognized by B cells. With further differentiation naïve, mature, B cells enter the peripheral lymphoid system(32). These naïve B cells can become activated to enter germinal centers (GCs).

GCs are sites in secondary lymphoid organs (such as the spleen) where affinity maturation of antibodies occurs(33). Upon encountering antigen, naïve B cells interact with T follicular helper (T_{FH}) cells and become activated to form distinct GCs within the lymphoid follicles(33–35). A recent paper from Tas and colleagues showed that GCs can be originally seeded by tens to hundreds of B cell clones, and that some of these initial clones are shared between neighboring GCs(36). They additionally went on to demonstrate that as the GC reaction progresses, many, but not all, GCs become dominated by descendants of a single clone(36).

GC B cells undergo two distinct processes in order to produce high affinity antibodies with varying effector functions: somatic hyper mutation (SHM) and class switch recombination (CSR). Both processes require activation-induced cytidine deaminase (AID) (37). SHM is the process by which point mutations are induced in the immunoglobulin (*Ig*) gene in order to introduce diversity in the variable region to drive the development of high affinity antibodies. Mutations in the GC are induced at a high rate, about 1 mutation in 1000 base pairs per division(37). AID deaminates deoxycytidine, which, depending on the repair mechanism utilized, can lead to the induction of mutations. The common repair mechanisms used in response to AID deamination are base excision repair and mismatch repair(38). These repair mechanisms can lead to single strand breaks or, when single strand breaks are in close proximity, double strand breaks. Single strand breaks can be

repaired by error-prone polymerases, which leads to the induction of mutations. Double strand breaks in the switch region of *Ig* lead to non-homologous end joining, resulting in CSR(38). AID is required for affinity maturation and CSR. Mouse models of AID deletion are unable to undergo SHM or CSR(37).

In addition to targeting the *Ig* gene locus, AID has been shown to affect more than 45% of genes expressed in GC B cells[ERROR]. This “off-targeting” of AID is believed to contribute to mutations that lead to B cell lymphoma. Understanding why some genes are targets of AID and others are not has been of interest. Recently, Duke and colleagues have shown that AID targeting in non-*Ig* genes appears to be based on the location of three binding motifs: E-box motifs, C/EBP-β motifs, and YY1 binding motifs(39). Binding sites for YY1, a transcription factor discussed in detail below, are enriched at promoter regions of highly mutated genes. Sites of the three binding motifs tend to co-localize in regions of highly mutated genes(39).

Fluorescent activated cell sorting (FACS) or immunohistochemistry (IHC) staining for cell surface markers CD95/Fas, GL7, or peanut agglutinin (PNA) allows for detection of committed GC B cells as early as 4 days after antigen encounter. By day 7 after antigen encounter, the GCs have begun to polarize into dark (DZ) and light zones (LZ). In the DZ, cells undergo rapid proliferation and SHM of the variable regions of the *Ig* genes. GC B cells then physically transit from the DZ into the LZ where they interact with T_{FH} cells

and undergo selection for high-affinity antibodies as well as CSR(35, 40–43) to allow for fine-tuning of Ig effector functions. CSR is not restricted to the GC: some evidence suggests that CSR may occur in extrafollicular regions(44, 45).

Although DZ and LZ have apparently different functions in the GC, they do not appear to be definitively separate differentiation stages, as was once believed(46). Gene expression profiling experiments have identified unique gene signatures in mouse and human DZ and LZ cells that diverge in only a relatively small set of genes(46). In particular, the LZ signature is dominated by upregulation of signatures related to *CD40* signaling, *NF-κB*, *c-Myc*, and the negative regulation of apoptosis. The DZ signature is primarily related to cell cycle progression and mitosis genes(46). These dominant signatures are unsurprising given the demonstrated dominance of LZ cells in selection and DZ cells in rapid proliferation.

Recent evidence has suggested that loss of factors essential for the polarity of the DZ and LZ, such as FOXO1(47, 48), do not completely eliminate the components of the DZ signature. Although FOXO1-negative GC B cells result in the loss of follicular dendritic cell polarity and instead have a diffuse follicular dendritic cell pattern in the GC, the FOXO-1-negative GCs are otherwise normal in size and number(47, 48). The loss of surface DZ markers is accompanied by an overall gene signature more similar to the LZ, however these ‘LZ only’ GCs still maintain rapid proliferation and SHM,

although at somewhat diminished levels compared with a normal GC(47, 48). This suggests plasticity in the DZ and LZ signatures, which provides a productive, although suboptimal due to decreased affinity maturation and CSR, GC response even in the absence of factors important for the DZ program.

Recent studies have begun to focus more on the process of selection that occurs in the LZ. Although the process by which GC B cells with auto-reactive antibodies are selected against is not fully understood, the mechanism for positive selection of GC B cells with increasingly high affinity antibodies has become more clear. Zhang and colleagues showed that antibodies from early plasma cells, which form and begin secreting antibodies prior to the formation of the GC, play an important role in ensuring the antibodies produced by GC B cells have progressively higher affinity for antigen(49). Antibodies secreted by plasma cells bind to and mask antigen presented by the follicular dendritic cells in the GC. If a GC B cell produces a higher affinity surface Ig, they will outcompete the masking antibody for access to the antigen. This continues to occur in the GC with progressively higher affinity antibodies that are produced from plasma cells as they exit the GC into circulation. This ensures that the highest affinity antibodies are produced(49).

Additionally, Gitlin and colleagues have shown that T_{FH} cells are important in the GC B cell selection process(50). As GC B cells transit from

the DZ to the LZ they capture and present antigen to T_{FH} cells, which then signal back to the GC B cells to provide pro-survival signals. Gitlin and colleagues also showed that the amount of antigen presented to the T_{FH} cells alters the GC B cell fate as they recirculate back into the DZ(50). GC B cells that capture and present a high level of antigen, suggesting a high affinity antibody, receive signals to increase the number of cell divisions initiated in the DZ. These cells with increased cell divisions consequently have increased somatic mutations, resulting in a higher likelihood of producing an even higher affinity antibody(50). GC B cells that express Ig with high-affinity for antigen are positively selected and differentiate into memory B cells or plasma cells to produce high-affinity antibodies.

A distinct gene expression signature distinguishes GC B cells from other B cell subsets at different developmental stages(51–53), suggesting specific transcriptional programs likely play an important role in GC development. C-MYC is an interesting protein with a role in the GC that is discussed in detail below.

One of the most important factors in the GC transcription program is BCL6. BCL6 is a DNA binding transcriptional repressor with a specific binding motif that recruits co-repressors including N-COR1, SMRT, BCOR, MTA3, and CTBP1(54). BCL6 can also interact with MIZ1 allowing it to bind and suppress expression of other genes including *CDKN1A*(55). It is expressed primarily in GC B cells and has been well characterized as an essential

transcription factor regulating the GC. BCL6 is required for the GC reaction but must be down regulated in order for cells to exit the GC as plasma cells.

The regulation of BCL6 is tightly controlled in the GC by different signaling pathways. IRF8 can contribute to BCL6 activation(56), while IRF4 transcriptionally represses *Bcl6* downstream of CD40 signaling in the LZ in mouse experiments. In addition, BCL6 protein is regulated by acetylation of the PEST domains, phosphorylation leading to ubiquitination and degradation, and auto-inhibition by intra-molecular binding(54). Additionally, activation of signaling in cells with high affinity BCRs leads to degradation of BCL6 and differentiation(54). The primary function of BCL6 is to repress or prevent premature activation of GC cells by repressing members of BCR/CD40 signaling, repressing differentiation genes, such as *Prdm1* and *Irf4*, and with modulating chemokine and cytokine responses(54). Importantly, BCL6 also inhibits the DNA damage response by inhibiting p53 expression, preventing apoptosis due to DNA damage(57).

BLIMP-1, which can function both as a repressor of *Bcl6*, and is itself repressed by BCL6, is required for plasma cell differentiation and is highly expressed in plasma cells. BLIMP-1 inhibits both *Bcl6* and *c-Myc* in order to maintain plasma cells in a terminally differentiated and non-proliferative state(58). Additionally, BLIMP-1 has been implicated as a tumor suppressor in DLBCL, likely due to its ability to enforce terminal differentiation(14, 16).

IRF4, which is also required for plasma cells and for *Bcl6* expression, has important roles in the GC(59, 60). IRF4 is required for CSR in *in vitro* stimulated B cells [57] , and is required for GC formation by both GC B cells(61) and T_{FH} cells(62). IRF4 seems to be required for early initiation of GC B cells, but not for their maintenance(60). IRF4 provides an example of the complex multitude of roles some factors play in the GC reaction, highlighting the difficulty in determining all the precise roles for some factors.

Apoptosis plays an important role in regulation of GCs because the balance between apoptosis and survival must be carefully maintained to produce high affinity antibodies while preventing the development of self-reactive antibodies. Vikstrom and colleagues showed that *Bcl-xL*, *Bim*, and *Mcl1* are all pro-survival factors upregulated in the GC(63). They showed that while *Bcl-xL* is dispensable for the GC reaction, *Mcl1* is required for formation of the GC. *Mcl1* appears to have a dose-dependent effect on survival of GC B cells, as mice with one intact allele of *Mcl1* display an intermediate phenotype, of about 50% decrease in GC B cells(63). Finally, Vikstrom and colleagues showed that *Mcl1* is required both for activation and persistence of the GC(63). Further studies have shown that *Mcl1* is also required for maintenance of plasma cells(64) and loss of one *Mcl1* allele can inhibit lymphomagenesis(65). This highlights the importance of *Mcl1* to promote survival of GC, plasma cells, and transformed lymphoma cells. In addition to the essential role for *Mcl1* in pro-survival, EAF2, an activator of apoptosis in

cancer cells, has also been implicated as important to promote apoptosis in GC B cells. Loss of *EAF2* in mouse GC B cells results in enlarged GCs, increased antibody production, and autoimmune symptoms(66). This emphasizes the importance of tightly controlled apoptosis in GC B cells.

BCR and NF-κB signaling are two signaling processes that play only a small role in the GC. Both signaling pathways only appear to be active in a subpopulation of LZ GC B cells(67, 68). In the case of BCR signaling, Khalil and colleagues have shown that although BCR stimulation does occur in GC B cells, the downstream signaling cascade is prevented by high phosphatase activity(69). Canonical NF-κB signaling, which is associated with cell growth and survival, is active in a subset of LZ GC B cells as indicated by translocation of RELA, C-REL, and p50 into the nucleus(68). Further, Heise and colleagues have shown that c-REL is required for maintenance of the GC, while RELA is dispensable for GC and affinity maturation, but required for plasma cells(70). This suggests that both BCR and NF-κB signaling may have a role in the selection that occurs in the LZ.

GC and DLBCL

In addition to its essential function in adaptive immunity, the GC reaction plays a critical role in B-cell lymphomagenesis. Both SHM and CSR involve error-prone DNA repair that can target genes other than *Ig* in GC B cells(71–77), leading to genetic alterations that promote tumorigenesis. Furthermore, GC B cells in DZ are among the fastest dividing mammalian

cells with an estimated cell cycle time of 6-12 hours(78–80). Accelerated proliferation of GC B cells is accompanied by attenuation of DNA damage sensing and replication checkpoints(55, 57, 81, 82), thus increasing the risk of accumulation of oncogenic mutations. Because of the high proliferation rate and high activity of mutagenic processes in GC B cells, it is not surprising that most Non-Hodgkin's lymphomas (NHLs) are derived from GC B cells or B cells that have passed through GCs(83–87).

C-MYC

Overview

c-Myc is a potent oncogene; it was first discovered as the cellular homolog to the viral *v-Myc*(88, 89), was further identified in both animal and human tumors, and was also shown to be essential for normal mouse embryonic development(88). Additionally C-MYC is one of four factors required to reprogram fibroblasts into induced pluripotent stem cells(90). C-MYC is a basic helix-loop-helix leucine zipper transcription factor that dimerizes with MAX to bind DNA. C-MYC can act to both activate and repress the transcription of targets, and it has been suggested that C-MYC may repress some targets by binding MIZ-1 and displacing the normal activating co-factors to mediate repression(90). C-MYC has been suggested to regulate at least 15% of the genome and is involved in diverse processes including cell cycle progression, ribosome biogenesis, signal transduction, vesicle trafficking, metabolism, protein folding, apoptosis, nuclear regulatory factors,

and DNA repair(91). However, some recent reports have indicated that C-MYC may play a role more as an amplifier of transcriptional signals already present in the cell, rather than as a determinant of transcription(92). Regardless of how exactly C-MYC exerts its effects on transcription, it has been well documented to be important in many cell contexts for cell cycle progression(93). Interestingly, one exception was the low level of *c-Myc* detected in GC B cells. GC B cells are considered one of the most proliferative somatic cells, making the lack of *c-Myc* expression surprising given its role in other proliferating cell types.

However, two groups recently utilized a *c-Myc-GFP* reporter system to identify a subset of Germinal Center B cells that do express *c-Myc*(94, 95). They reported that *c-Myc* has a biphasic expression pattern, being first expressed transiently in the early GC cells and then repressed by BCL6 in the highly proliferative DZ, only to be then expressed again after being selected for re-entry into the dark zone(94, 95). In addition, they showed that loss of *c-Myc* results is loss of the GC, indicating that, although only transiently expressed, *c-Myc* is required for GC formation and maintenance(94, 95).

In lymphoma

C-MYC is a common driver of carcinogenesis in many types of hematopoietic malignancies. Translocation of *C-MYC*, leading to increased expression, to the highly expressed *Ig* loci, most commonly the heavy chain

(IgH), is characteristic of Burkitt's lymphoma, which arises from GC B cells(90). *C-MYC* translocations to *Ig* loci have also been documented in multiple myeloma, which is a malignancy of plasma B cells(96). In DLBCL *C-MYC* is translocated in 8.8%-11% of cases. C-MYC has increased expression in 29-38.1% of DLBCL cases(29, 30), demonstrating the importance of C-MYC in DLBCL. Clinically, an increase in C-MYC, whether through translocation, amplification, or other methods, is an adverse prognostic factor for DLBCL(29). Currently the treatment of C-MYC-high DLBCL is an unmet medical need.

Therapeutic inhibition

Historically, transcription factors have been considered to be 'untargetable' by small molecule inhibition, which is why many small molecule-targeting strategies focus on upstream factors such as kinase inhibition. However, treatment focused on transcription factor oncogenes, such as C-MYC, would provide an ideal treatment against many types of cancer, regardless of the upstream pathways that lead to C-MYC activation. This has led to many strategies to attempt to attenuate *c-Myc* expression and eliminate tumors that are addicted to C-MYC.

One strategy has been to target the dimer C-MYC-MAX. C-MYC dimerizes with MAX to bind DNA, so inhibition strategies have focused on both limiting the dimerization event itself, as well as inhibiting its subsequent binding to

DNA. Two inhibitors stand out in these regards. 10058-F4 is an inhibitor of C-MYC-MAX dimerization and has been shown effective in many *in vitro* cell line experiments(90) as well as *in vivo* against N-MYC driven tumors(97). The other inhibitors, Celastrol and celastrol-inspired molecules, inhibit the C-MYC-MAX dimer from binding to DNA(98). Efficacy of these molecules has been shown across various cell lines *in vitro*.

Another strategy to inhibit C-MYC-addicted tumors targets effector molecules downstream of C-MYC. This strategy has been shown effective in certain situations, but is complex due to differences in downstream C-MYC target molecules depending on the cellular and oncogenic context. Many of these strategies have been proof-of-principle in nature, utilizing shRNA, which are not currently amenable to clinical applications. Some of the effective downstream targeting strategies have included shRNA or small molecule inhibition of some metabolic downstream effectors including ornithine decarboxylase (ODC), lactate dehydrogenase A (LDHA), and glutaminase (GLS) (90). These metabolic targets were chosen because of their importance downstream of C-MYC in certain tumor contexts.

Additional studies aiming to inhibit C-MYC activity have focused on modulating the effects of C-MYC on microRNA expression, specifically by adeno-associated viral expression of miR-26a in a C-MYC-induced model of liver cancer. miR-26a is repressed by C-MYC and the reintroduction of miR-26a in the liver cancer model proved efficacious by reducing the size of liver

tumors(99). These types of inhibition of C-MYC-targets may be effective in some contexts, but not in others. Although C-MYC aberration is common in up to 70% of human tumors, the important downstream functions may vary widely.

This thesis focuses on the inhibition of *C-MYC* expression and activity directly through the use of the small molecule bromodomain and extra terminal domain (BET) family inhibitor JQ1(100). JQ1 competitively interacts with BET bromodomains, thus preventing them from binding to chromatin. BET bromodomains are scaffolding factors that recognize acetylated lysines on chromatin and facilitate transcriptional activation. The four BET bromodomains for which JQ1 has high affinity are BRD4, which JQ1 has the highest affinity for, BRD2, BRD3, and BRDT. JQ1 was originally developed for use in NUT (nuclear protein in testis)-midline carcinoma, in which *BRD4* is translocated(100). Further studies identified inhibition of BET bromodomains as a potential method to inhibit C-MYC transcriptional activity. C-MYC mediated transcription is associated with acetylated lysines on chromatin and is also involved in pause release of RNA polymerase II, similarly to BRD4. These findings prompted Delmore and colleagues to investigate the utility of JQ1 in inhibition of C-MYC transcription(101). They found that not only was C-MYC-mediated transcription inhibited, but also the transcription of *C-MYC* itself was inhibited by JQ1. This finding was validated in a number of studies primarily focused on hematopoietic malignancies, including multiple myeloma,

acute myeloid leukemia, promyelocytic leukemia, B-cell acute lymphoblastic leukemia, and Burkitt's lymphoma, where C-MYC has a well-established role as a dominant oncogenic driver(102–107).

These studies began to establish JQ1 as an indirect inhibitor of C-MYC, however further investigation, particularly in some solid tumors, suggested that JQ1 could have anti-tumor effects independently of C-MYC inhibition(108, 109). Further studies suggest that BRD4 associates with enhancers and super enhancers in cancer to promote high levels of transcription from a small set of essential genes(106). Lovén and colleagues proposed that JQ1-mediated inhibition of BRD4 preferentially decreases expression of oncogenes that have been highly selected for in any specific cancer(106). This may provide an explanation for the broad efficacy seen for JQ1 inhibition across tumor types. BRD4 may be loaded preferentially at the highly expressed oncogenes to which a given tumor is addicted and when this association is disrupted, the cell survival rapidly deteriorates. A study from Chapuy and colleagues revealed highly asymmetric loading of BRD4 at super-enhancers in DLBCL cells. These super-enhancers and genes that they regulate are particularly sensitive to JQ1 inhibition, explaining the selective effect of JQ1 on oncogenic and lineage-specific transcriptional circuits(110).

Yin Yang 1

Yin Yang 1 (YY1) has been implicated in the GC transcriptional program. Additionally, high expression of YY1 is an indicator for poor prognosis in DLBCL.

The multi-functional protein

YY1 is a multi-functional protein with roles in many types of cellular processes including transcriptional activation and repression, X-chromosome inactivation, contraction of DNA loci(111), protein stability(112), viral gene expression, epigenetic regulation, and oncogenesis(113). YY1, a GLI-Kruppel class protein, has four zinc fingers that allow it to directly bind to and interact with DNA. It also has a REPO domain which allows YY1 to bind polycomb repressive complex (PRC) members, specifically YAF2(114). The core PRC has no components with DNA binding capabilities, which raises questions about how PRC is targeted to various DNA loci. It has been proposed that YY1 may act to target PRC via its DNA binding zinc finger domains(114). The carboxyl terminus region of YY1 physically interacts with other proteins important in transcription, including EP300, C-MYC, and HDAC2(113).

Loss of *YY1* causes embryonic lethality in a dose dependent manner(115, 116). YY1 is also involved in differentiation of muscle, intestinal stem cell self-renewal(117), and cell growth in many cell types(113). Schug and colleagues have suggested that YY1 could regulate as much as 10% of the total human genome, likely in a cell-dependent context(118). In order to

classify some of the YY1 targets, Affar and colleagues utilized a mouse model in which YY1 levels in mouse embryonic fibroblasts (MEFs) are decreased to 25% of normal expression(115). Microarray on these MEFs reveal changes in many genes which are primarily due to the decrease in YY1, although does not identify those which may be indirect versus direct YY1 targets. Nonetheless, this study indicates that YY1 has a role in regulation of cell cycle genes, such as *CDKN1A* (*p21*), mitosis and cytokinesis genes (including kinesin family members and aurora kinases), DNA replication and repair genes (including polymerases, *RAD18*, and *Ung*), apoptosis related genes (such as *Bcl-xL* and *FAS*), cell growth and proliferation genes (such as *Btg2*, *Fos*, and *Src*), and developmental genes (including *BMP*s and myosins) (115). Further studies have identified other, direct, transcriptional targets of YY1 including activation of *c-Myc*(119, 120) and *Xist*(121).

YY1 ChIP-Seq has been performed in a number of human cell lines(122). GM12878, a human B lymphocyte cell line, has YY1 binding peaks associated with 719 unique genes. By comparing these YY1 peaks to those in two other human cell lines (NT2-D1 and K562), I found that 50% (360/719) of genes with YY1 binding in GM12878 also have YY1 binding in the other two cell lines. Gene ontology analysis of these common targets shows enrichment for maintenance processes, including RNA metabolic processes, nucleobase-containing compound metabolic processes, and cellular component biogenesis. This suggests that, in the context of human B cells, at least half of

YY1 targets may be specific to the cell type, while the remaining targets involve common biological processes.

In addition to YY1's role in transcriptional activation and repression, it appears that the protein has other non-transcriptional roles. In particular, YY1 has been shown to disrupt p53-EP300 protein interaction by blocking EP300-dependent acetylation and stabilization of p53. YY1 also interacts with MDM2 to promote p53-MDM2 complex, which leads to increased p53 degradation(123). This interaction of YY1 with MDM2 to enhance MDM2-p53 binding can be disrupted by $p14^{ARF}$(124). YY1 can also act to alter protein localization, as in the case of AID protein. Zaprazna and Atchison showed that YY1 and AID proteins physically interact and that YY1 increases the nuclear AID levels in activated B cells by increasing AID protein stability(112). These studies provide examples in which YY1 alters protein-protein interactions or protein stability leading to post-translational regulation of protein levels.

In B-cells

Interest in the role of YY1 in B cells began when YY1 binding sites were discovered in enhancers important for variable-distal-joining (V(D)J) recombination(111). This led to the development of a conditional YY1 allele in mice to allow tissue specific deletion in order to bypass the embryonic lethality of knockout mice. Ablation of *YY1* in early B cells using *Mb1-cre*

blocks the transition from progenitor B cells to precursor B cells partially through impairing chromatin contraction at the *Ig* heavy chain locus and V(D)J recombination(111). Pan and colleagues found that the YY1 REPO domain, which is required for involvement in PRC, is necessary for progenitor to precursor B cell transition(125). Additionally, they have shown that YY1 without the REPO domain impairs *Ig* kappa chain rearrangement, but not *Ig* heavy chain, suggesting that YY1 may function to recruit PRC in *Ig* kappa rearrangement but not for *Ig* heavy chains(125). YY1 appears to require tight regulation in normal B cell development. When YY1 is overexpressed in wild type bone marrow, normal B cell development is impaired, resulting in fewer B lineage cells, while myeloid lineages remain normal(126). Together this evidence suggests that YY1 levels must be carefully controlled for normal B cell development.

Recently, binding motifs for YY1 were found to be significantly enriched in the promoter regions of genes preferentially expressed in GC B cells, suggesting that YY1 functions as a master regulator of the GC reaction(51). However, experimental evidence supporting a role for YY1 in the GC is lacking. One group attempted to define the role of YY1 in the GC by investigating the loss of YY1 in B cells stimulated *in vitro*(112). They showed that YY1 controls CSR and levels of nuclear AID, but does not effect proliferation *in vitro*(112). Although this provides some suggestion that YY1 has a role in the GC, current *in vitro* models do not represent the vast

complexity of an *in vivo* GC reaction. During the preparation of this thesis a study was published demonstrating that loss of *YY1* can diminish the GC response in mice(127).

In cancer

YY1 has been implicated as a potential oncogene. A review from Bonavida and Kaufhold(128) provides an overview of YY1 expression in various types of cancer. They indicate many cancer types including bladder, brain, breast, colon, gastic, hepatocellular carcinoma, cervical, ovarian, and prostate cancer display increased *YY1* expression compared with normal tissue. Interestingly, although YY1 expression is increased in pancreatic ductal adenocarcinoma, it appears that YY1 suppresses invasion and metastasis, meaning increased YY1 correlates with better outcome. In esophageal cancer, YY1 is down regulated compared with normal tissue, which is in contrast to all of the other cancer types surveyed(128).

YY1 has also been implicated in lymphoma. YY1 is significantly increased in human DLBCL, Burkitt's lymphoma, and follicular lymphoma compared with reactive lymph nodes or normal B cells(129–131). Further, high levels of YY1 expression correlates with a worse survival prognosis in human DLBCL and follicular lymphoma patients(130, 131).

SMURF2

Smad ubiquitin regulatory factor 2 (SMURF2) is a tumor suppressor. In DLBCL low *Smurf2* expression is a poor prognostic indicator.

The E3-ubiquitin-ligase

SMURF2 is a Nedd4 family E3-ubiquitin ligase(132) containing an amino-terminal C2 domain, two WW domains, which facilitate protein-protein interactions with PPXY motifs, and a carboxyl-terminal HECT domain which ubiquitinates the target(133). SMURF2 was originally identified for its ability to ubiquitinate and degrade members of the TGF-β family including SMAD1. Subsequent studies have shown that SMURF2 can ubiquitinate and mediate the degradation of multiple other factors including SMURF1(134), YY1(135, 136), ID1(137), ID3(137), RNF20(138), RUNX2(139), RAP1B(140), and components of the Wnt signaling pathway(141–143).

The tumor suppressor and aging factor

SMURF2 has been identified as a tumor suppressor in a number of different types of cancer including lymphoma(138, 144), hepatocellular carcinoma(138, 144), breast cancer(134), and melanoma(144). Multiple groups have shown that loss of *Smurf2* in mice results in increased cancer incidence with a long latency(138, 144). In addition low *SMURF2* expression in human lymphoma patients is predictive for poor prognosis(135). Ectopic expression of wild type *SMURF2* significantly decreases the growth of human

DLBCL cell lines in a E3-ubiquitin-ligase dependent manner. When the catalytic cysteine residue is mutated and this mutant is overexpressed there are no changes to proliferation, suggesting SMURF2 requires E3-ubiqutin-ligase activity to function as a tumor suppressor(135).

In addition to its role as a tumor suppressor, SMURF2 has been implicated as an aging factor. Loss of *Smurf2* results in increased number of hematopoietic stem cells (HSC) in both young and old mice, and in more functional HSCs(145). HSCs from old mice, although more numerous, are less able to repopulate the blood lineages and are more likely to exhaust. Through serial transplantation and competitive repopulation, *Smurf2*-deficent HSCs from both young and old mice are less likely to exhaust and are better able to compete with young wild type HSCs than either young or old wild type HSCs(145). This shows that SMURF2 is an aging factor, which when decreased, provides anti-aging properties.

The implication of SMURF2 as protective in cancer, but detrimental to stem cell aging, highlights the often dichotomous nature of human aging. In order to maximize the healthy reproductive years, the human body is programed to prevent cancer, which, as exemplified by SMURF2, can later have detrimental effects on the aging process. How SMURF2 is acting dichotomously can help advance the understanding of the underlying biology of cancer and aging and create therapies that modulate SMURF2 to promote healthy HSCs and healthy aging or inhibit cancer.

SMURF2 has an important role in regulating senescence, by mediating the degradation of ID1, which in turn results in an increase in *p16* levels(137). P16 is a well-characterized senescence factor as part of the p16-RB pathway. When SMURF2 is ectopically expressed in human fibroblasts, *p16* levels are increased and early senescence occurs(137). It has also been shown that *Smurf2*-deficent MEFs continue to proliferate long after wild type MEFs have senesced and that loss of *Smurf2* appears to promote immortalization of MEFs(144). Although there is a well-established role for SMURF2 in senescence, it is less clear if the regulation of senescence is what provides SMURF2 with tumor suppressor and aging properties.

The role of senescence in cancer is well documented, beginning with the concept of oncogene-induced senescence, which was first explored by Serrano and colleagues. They showed that oncogenic RAS expression promotes premature senescence in otherwise normal cells(146). This has subsequently been explored with additional oncogenes and tumor suppressors including B-RAF over expression(147), and PTEN loss(148). An example of oncogene-induced senescence occurring naturally *in vivo* is in the context of benign skin nevi (commonly referred to as skin moles). These abnormal melanocyte growth lesions typically harbor oncogenic mutations including *B-RAF* and *N-RAS*, however they often do not progress to malignant melanoma, or if they do progression has a very long latency(149, 150). These nevi have been shown to display markers of senescence,

providing an *in vivo* example of oncogene-induced senescence as a preventative measure in tumorigenesis. The rare nevi that progress to malignant melanoma typically have additional pathway mutations that circumvent the senescence pathway. In addition to the role senescence has in prevention of malignancy, it can also occur as a response to treatment in full malignancy, termed therapy-induced senescence. Schmitt and colleagues showed that tumor-bearing mice with therapy (or drug) induced senescence have a better outcome than those with senescence defects(151). This solidifies an important role for senescence in cancer prevention and treatment.

Ramkumar and colleagues have suggested that SMURF2 tumor suppressive activity is likely due to the decrease of senescence in the mouse tissues(144), however Blank and colleagues have suggested an alternative scenario that is also possible(138). They suggest that SMURF2 acts to promote genomic stability by targeting RNF20, an epigenetic modifier, for degradation(138). It seems most likely that in the context of tumor suppression, both control of genomic stability and promotion of senescence could likely be important.

SMURF2-YY1-C-MYC Axis

Previous studies(135, 136) have shown that SMURF2 mediates the ubiquitination and degradation of YY1. Any decrease in YY1, as a multi-

functional protein with many roles, likely results in a multitude of molecular changes in the cell, which may have broad reaching effects. In previous studies it has been shown that when SMURF2 mediates the degradation of YY1, a similar decrease in the mRNA and protein of the transcription factor C-MYC is observed. C-MYC has many diverse roles in the cell, however, in the context of many types of cancer, C-MYC has been well characterized as an oncogene with roles in proliferation, altering cell metabolism(88), and differentiation(152). This SMURF2-YY1-C-MYC axis therefore constitutes a potentially important pathway in the development and maintenance of cancer. The previous study(135, 144) showed that a decrease in *Smurf2* levels leads to increased incidence of cancer, primarily B cell lymphoma. Decreased SMURF2 protein expression in patient samples has been shown to be predictive of a poor clinical outcome in patients treated with the standard of care, R-CHOP.

DLBCL tumors with high C-MYC expression constitute an unmet clinical need. As detailed above, the small molecule inhibitor JQ1 can indirectly inhibit C-MYC activity, making it an intriguing candidate for use in high C-MYC expressing tumors. This thesis will examine the hypothesis that JQ1 is an effective treatment for human DLBCL. Some DLBCL tumors have amplification or translocation of *C-MYC*, which causes the increased C-MYC protein. However, many of the tumors with high C-MYC expression do not have a clear mechanism for the increase. Understanding the underlying

mechanism of increased C-MYC expression may provide additional therapeutic targeting opportunities.

One possibility is that *C-MYC* is controlled at the transcriptional level. YY1 has been shown to activate *C-MYC* transcription. Previously, it has been shown that knockdown of *YY1* in human DLBCL cell lines leads to a decrease in cell number(135). High YY1 expression is correlated with poor survival prognosis in lymphoma. In addition, YY1 has been suggested to be a master regulator of the GC transcriptional program(51). As discussed above, GC or post-GC cells are the cell-of-origin for most DLBCL, and perturbations in the GC may contribute to DLBCL development. This led me to investigate if YY1 regulates the GC, and test the hypothesis that YY1 is essential for the GC reaction.

Previous work established SMURF2 as an important regulator of YY1 protein stability. In this thesis I show that YY1 protein is increased in the GC (Figure 3.1). As detailed above, SMURF2 has been established as a tumor suppressor in B cell lymphoma. This led me to hypothesize that decreasing SMURF2 in the GC would perturb the GC reaction, potentially providing a mechanism for the tumor suppressive activity of SMURF2. The goal of this thesis is to further the understanding of this SMURF2-YY1-C-MYC pathway so that this knowledge may be used to advance the lymphoma field and inform treatment progression.

CHAPTER II: Inhibition of bromodomain proteins for the treatment of human diffuse large B cell lymphoma

JQ1 is a small molecule inhibitor of the bromodomain and extra-terminal (BET) family of bromodomain proteins**.** Studies have found anti-proliferative and pro-apoptotic effects of JQ1 in several types of malignancies. In some hematopoietic malignancies, this effect has been linked to inhibition of C-MYC. This led me to hypothesize that JQ1 treatment in DLBCL cells would result in decreased cell proliferation and viability in a C-MYC-dependent manner.

Results

Human DLBCL cells are sensitive to JQ1

Recent studies found anti-proliferative and pro-apoptotic effects of JQ1, particularly in hematopoietic malignancies, and these effects of JQ1 are primarily mediated through inhibition of *c-MYC*(100–102, 104, 105, 107, 109, 153, 154). Given the recently reported incidence of *c-MYC* overexpression in DLBCL(29), I hypothesized that JQ1 would inhibit human DLBCL cell proliferation and therefore might be effective in DLBCL therapy. To test this hypothesis, I used a panel of 11 human DLBCL cell lines, including four cell lines classified as the ABC subtype [HLY-1(155), HBL-1(18), OCI-Ly3 and OCI-Ly10(156)] and seven cell lines classified as the GCB subtype [SU-DHL-

4, SU-DHL-5, SU-DHL-6, SU-DHL-10, OCI-Ly8, OCI-Ly18(155), and RC-K8(28)].

I treated these 11 DLBCL cell lines with increasing doses of JQ1 for 72 hours, at which time I determined the number of viable cells by propidium iodide (PI) exclusion and flow cytometry. As shown in Figure 2.1A, total viable cells after JQ1 treatment as a percentage of DMSO-treated control cells (set to be 100%) were decreased significantly in a dose-dependent manner in all 11 DLBCL cell lines. The JQ1 dose that led to 50% inhibition of growth in DLBCL cell lines was between 25 and 160 nM, compared to 360 nM for the less sensitive human cervical cancer cell line HeLa(107). Both the ABC and GCB subtypes were sensitive to JQ1, suggesting a broad effect of JQ1 in inhibiting DLBCL cell proliferation. Furthermore, I treated four cell lines (SU-DHL-4, SU-DHL-10, OCI-Ly3 and OCI-Ly8) with two different doses of JQ1 (250 nM and 500 nM) and determined the number of viable cells at 2, 3, 4, and 7 days after treatment. As shown in Figure 2.1B, the numbers of viable cell at different time points after JQ1 treatment were significantly lower than

FIGURE 2.1 *(following page)* JQ1 treatment of human DLBCL cell lines leads to decreased cell viability. **(A)** 12 cell lines, including 11 human DLBCL cell lines and a human cervical cancer cell line HeLa, were treated with the indicated doses of JQ1 for 3 days. Viable cells were determined by PI exclusion in flow cytometry. The number of viable cells after JQ1 treatment is normalized as percent of viable cell number of DMSO-treated control. Error bars are SD of at least 3 independent experiments. **(B)** Proliferation of 4 DLBCL cell lines. Cells were treated with the indicated doses of JQ1 and doxorubicin (Dox) and viable cells were determined by PI exclusion in flow cytometry at indicated time after treatment. Error bars are SD of 3 independent experiments. Two-way ANOVA was used to compare JQ1 or Dox-treated with DMSO-treated controls. ***: $P<0.001$.

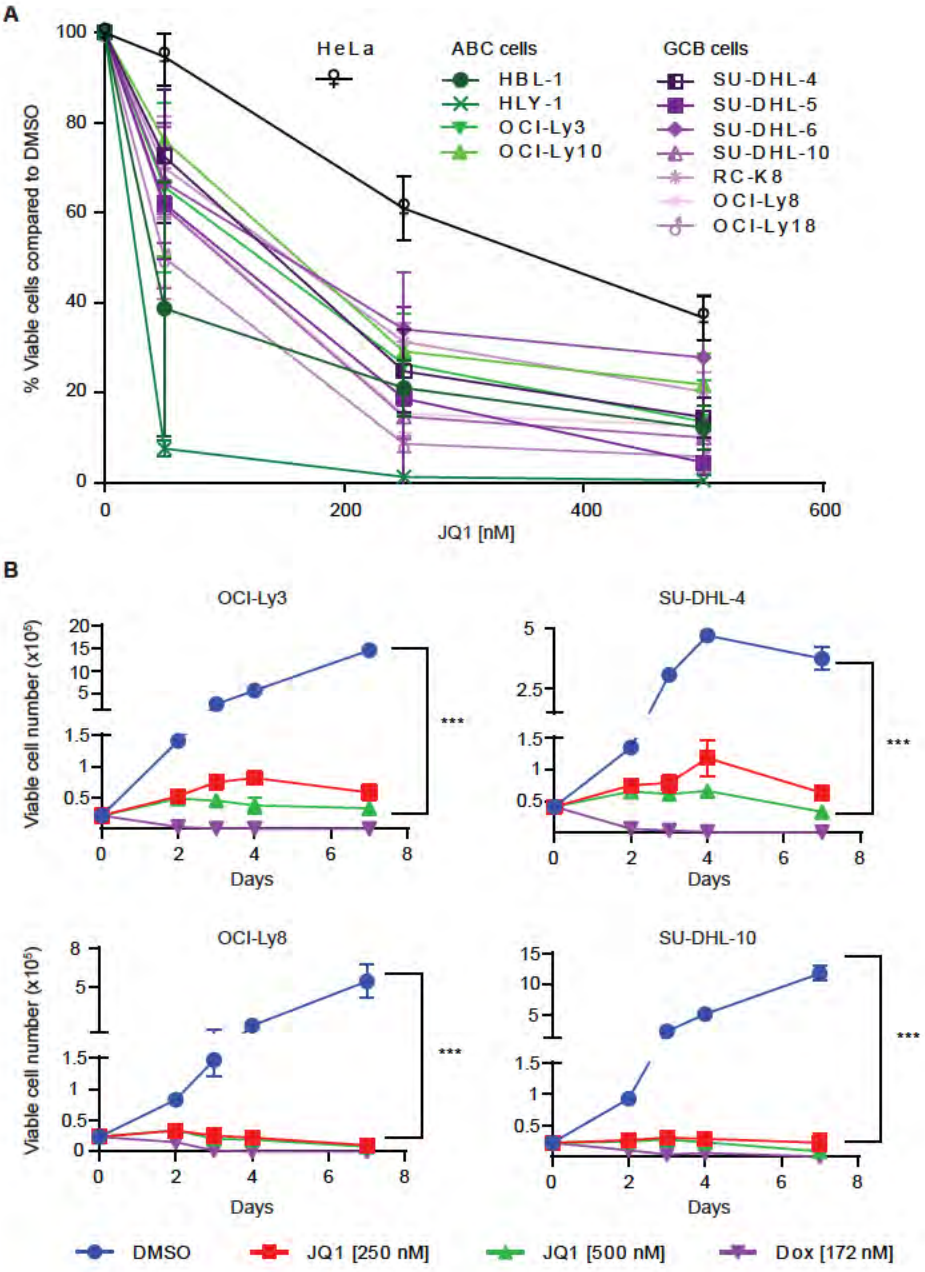
A
% Viable cells compared to DMSO
JQ1 [nM]
HeLa
ABC cells
HBL-1
HLY-1
OCI-Ly3
OCI-Ly10
GCB cells
SU-DHL-4
SU-DHL-5
SU-DHL-6
SU-DHL-10
RC-K8
OCI-Ly8
OCI-Ly18
B
OCI-Ly3
SU-DHL-4
OCI-Ly8
SU-DHL-10
Viable cell number (x10⁵)
Days
***
DMSO
JQ1 [250 nM]
JQ1 [500 nM]
Dox [172 nM]

FIGURE 2.1

those treated with the DMSO control, indicating an anti-proliferative effect of JQ1 in DLBCL cells. Doxorubicin was included as a control known to induce high levels of apoptosis at 172nM dose.

JQ1 treatment induces cell cycle arrest in DLBCL cells followed by either apoptosis or senescence

The number of viable cells after JQ1 treatment deceased more slowly in comparison to doxorubicin, which is used as a positive control for apoptosis (Figure 2.1B). To understand the mechanism underlying the anti-proliferative effect of JQ1 in DLBCL cells, I analyzed cell cycle distribution using FACS at various time points after JQ1 treatment. After 2 days of JQ1 treatment, a significant decrease in the percentage of cells in the S phase and a significant increase in percentage of cells in the G1 phase was observed (Figure 2.2). Further, there was minimal increase in the sub-G1 population (Figure 2.2), suggesting that JQ1 induces cell cycle arrest with minimal cell death after 2 days of treatment. After 4 days of JQ1 treatment, OCI-Ly8 and SU-DHL-4 cells maintained the cell cycle arrest, whereas a consistent increase in the sub-G1 population was observed in OCI-Ly3 (5.5% for 250 nM JQ1-treated

FIGURE 2.2 *(following page)* JQ1 induces cell cycle arrest and cell death in human DLBCL cells. Cell cycle analyses of DLBCL cells treated with JQ1 or doxorubicin (Dox) for 2 days and 7 days were shown. Error bars are SD of 3 independent experiments. Welch's *t*-test was used for statistical analysis. *: $P<0.05$, **: $P<0.01$, ***: $P<0.001$.

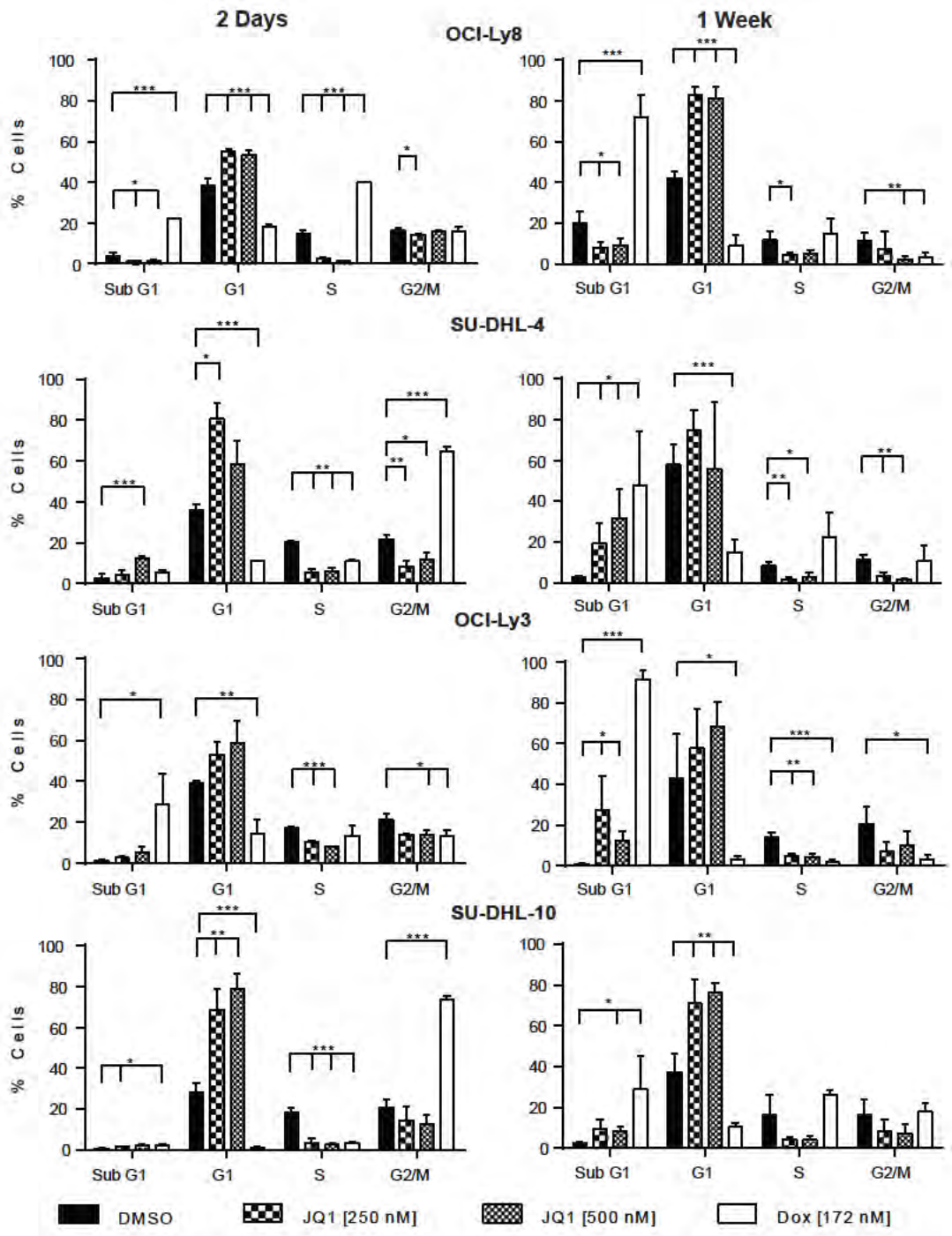
2 Days
1 Week
OCI-Ly8
SU-DHL-4
OCI-Ly3
SU-DHL-10
% Cells
Sub G1
G1
S
G2/M
DMSO
JQ1 [250 nM]
JQ1 [500 nM]
Dox [172 nM]

FIGURE 2.2

and 7.8% for 500 nM JQ1-treated compared to 0.7% for DMSO-treated control) and SU-DHL-10 (3.1% for 250 nM JQ1-treated and 3.5% for 500 nM JQ1-treated compared to 1.1% for DMSO-treated control) (Figure 2.3).

In comparison, doxorubicin treatment led to a significant increase in the sub-G1 population in SU-DHL-10, OCI-Ly3 and OCI-Ly8 cells after just 2 days of treatment (Figure 2.2 and 2.3).

Neither doxorubicin nor JQ1 induced a significant increase in the sub-G1 population in SU-DHL-4 cells up to 4 days of treatment (Figure 2.3). To further investigate cell death after JQ1 treatment, I measured caspase 3/7 activity as an indicator of apoptosis. I found a small but consistent increase in caspase 3/7 activity 4 days after treatment with 250 nM JQ1 compared with DMSO-treated control cells in OCI-Ly3 (2.8-fold increase) and SU-DHL-10 (1.6-fold increase) cells, whereas a significant increase in caspase 3/7 activity was observed in both OCI-Ly3 (12.9-fold increase) and SU-DHL-10 (353-fold increase) cells after 4 days of doxorubicin treatment compared to DMSO-treated controls (Figure 2.4A).

I found that this initial G1 cell cycle arrest was followed by either apoptosis or senescence after prolonged (7-day) treatment with JQ1. OCI-Ly3, SU-DHL-4 and SU-DHL-10 cells showed significant increases in the sub-G1 populations: 27.5% (250 nM JQ1) and 12.2% (500 nM JQ1) compared to 1.0% (DMSO) for OCI-Ly3; 19.3% (250 nM JQ1) and 31.6% (500 nM JQ1) compared to 2.8% (DMSO) for SU-DHL-4; 9.2% (250 nM JQ1) and 8.2% (500

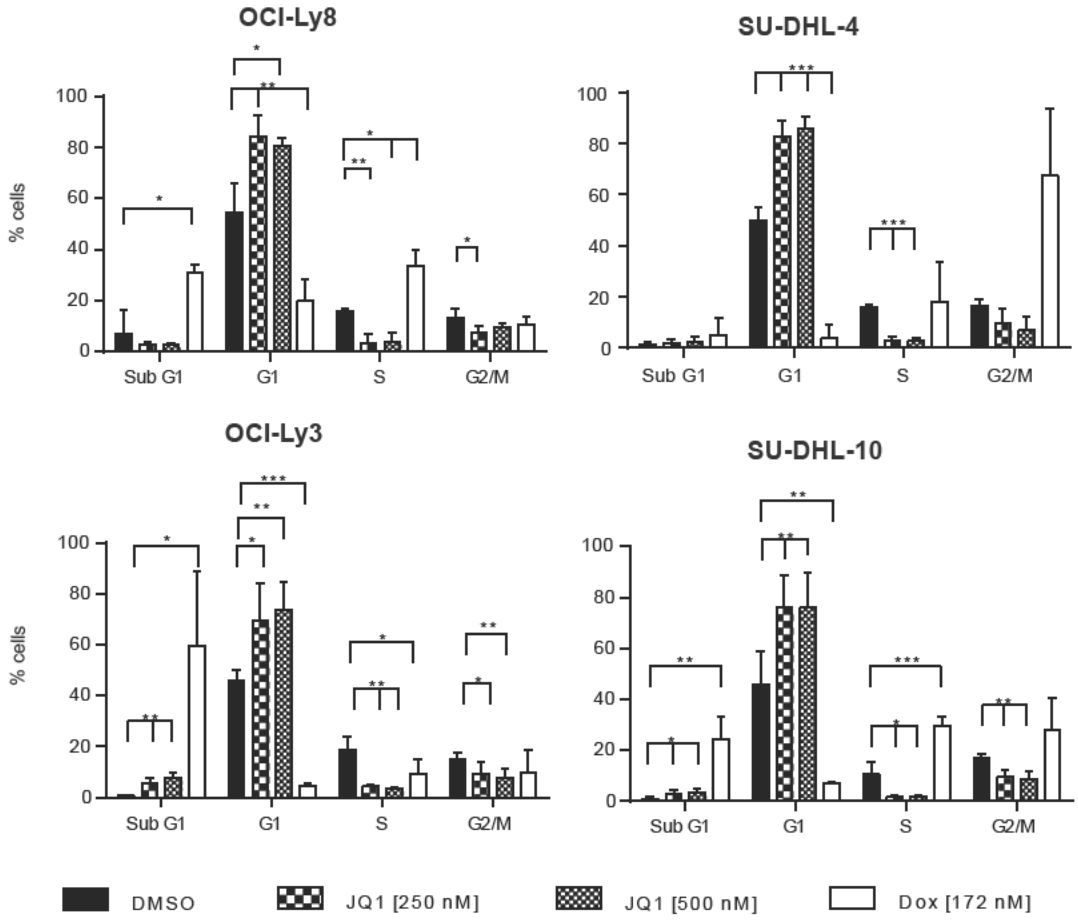

FIGURE 2.3

FIGURE 2.3 JQ1 induces cell cycle arrest and cell death after 4 days of treatment. Cell cycle analysis of 4 cell lines treated with JQ1 or doxorubicin (Dox) for 4 days. Error bars are SD of 3 independent experiments. Welch's *t*-test was used for statistical analysis. *: $P<0.05$, **: $P<0.01$, ***: $P<0.001$.

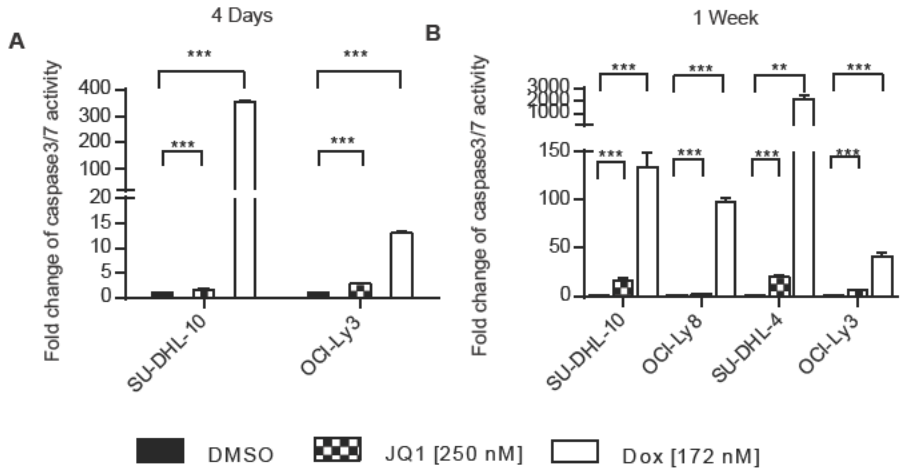

FIGURE 2.4

FIGURE 2.4 JQ1 induces apoptosis in human DLBCL cells. Caspase 3/7 activity in DLBCL cells treated with JQ1 or Dox for **(A)** 4 days or **(B)** 7 days was measured and normalized with that in cells treated with DMSO, which was set to be 1. Error bars are SD of 5 independent experiments. Welch's *t*-test was used for statistical analysis. **: $P<0.01$, ***: $P<0.001$.

nM JQ1) compared to 2.3% (DMSO) for SU-DHL-10 cells (Figure 2.2). In contrast, OCI-Ly8 did not have an increased sub-G1 population, but rather maintained a G1 arrest (Figure 2.2). Apoptosis in SU-DHL-4, SU-DHL-10 and OCI-Ly3 cells and the lack of cell death in OCI-Ly8 cells were corroborated by the analysis of caspase 3/7 activity. As shown in Figure 2.4B, a significant increase in caspase 3/7 activity was observed in SU-DHL-10, SU-DHL-4, and OCI-Ly3 cells treated with 250 nM JQ1 compared to DMSO control (16-fold, 20-fold and 6.2-fold increase, respectively). In comparison, OCI-Ly8 showed only a small increase (2.4-fold increase) in caspase 3/7 activity after 1 week of treatment with 250 nM JQ1.

To further characterize the anti-proliferative effects of JQ1, I removed JQ1 after 7 days of treatment to investigate whether removal of the drug from the cells for an extended period allowed the cells to re-enter the cell cycle. All of the four cell lines tested either maintained growth arrest, or in the case of SU-DHL-4, had decreased cell numbers (Figure 2.5A). This suggests that JQ1 treatment caused cells to permanently exit the cell cycle. To test whether these cells entered senescence, I stained them for senescence associated β-galactosidase (SA-β-gal) activity. After 7 days of treatment with 250 nM JQ1, I observed a significant percentage of cells staining positively for SA-β-gal in OCI-Ly3 and OCI-Ly8 cells (71.6% and 90.6%, respectively). In contrast, only 5.4% or no SA-β-gal positive cells were observed in SU-DHL-10 and SU-DHL-4 after JQ1 treatment for 1 week (Figure 2.5B). These data indicate that JQ1 treatment results in two independent phenotypes in human DLBCL cell lines: apoptosis and senescence.

JQ1 treatment leads to suppression of C-MYC expression

As JQ1-mediated suppression of *C-MYC* expression is responsible for its anti-proliferative effect in various types of cancer cells(101, 103, 105, 107, 157, 158), I examined C-MYC protein levels in the 11 DLBCL cell lines that were characterized for response to JQ1 treatment (Figure 2.6A). In particular, OCI-Ly3(159) and SU-DHL-4(160)cells have *C-MYC* amplifications. HBL-1(161), OCI-Ly8, OCI-Ly18(159), SU-DHL-6, and SU-DHL-10(160) cells have

FIGURE 2.5 JQ1 induces senescence in OCI-Ly8 and OCI-Ly3 cells. **(A)** DLBCL cells were treated with JQ1 for 7 days. JQ1 or DMSO was then washed away and viable cells were counted by PI exclusion in flow cytometry at 3 and 5 days after drug removal. Error bars are SD of 3 independent experiments. **(B)** Representative staining of SA-β-gal in cells treated with JQ1 for 7 days. Percent of SA-β-gal positive cells was quantified from 5-8 randomly selected fields with at least 500 cells. Error Bars are SD and Welch's *t*-test was used for statistical analysis. **: $P<0.01$, ***: $P<0.001$.

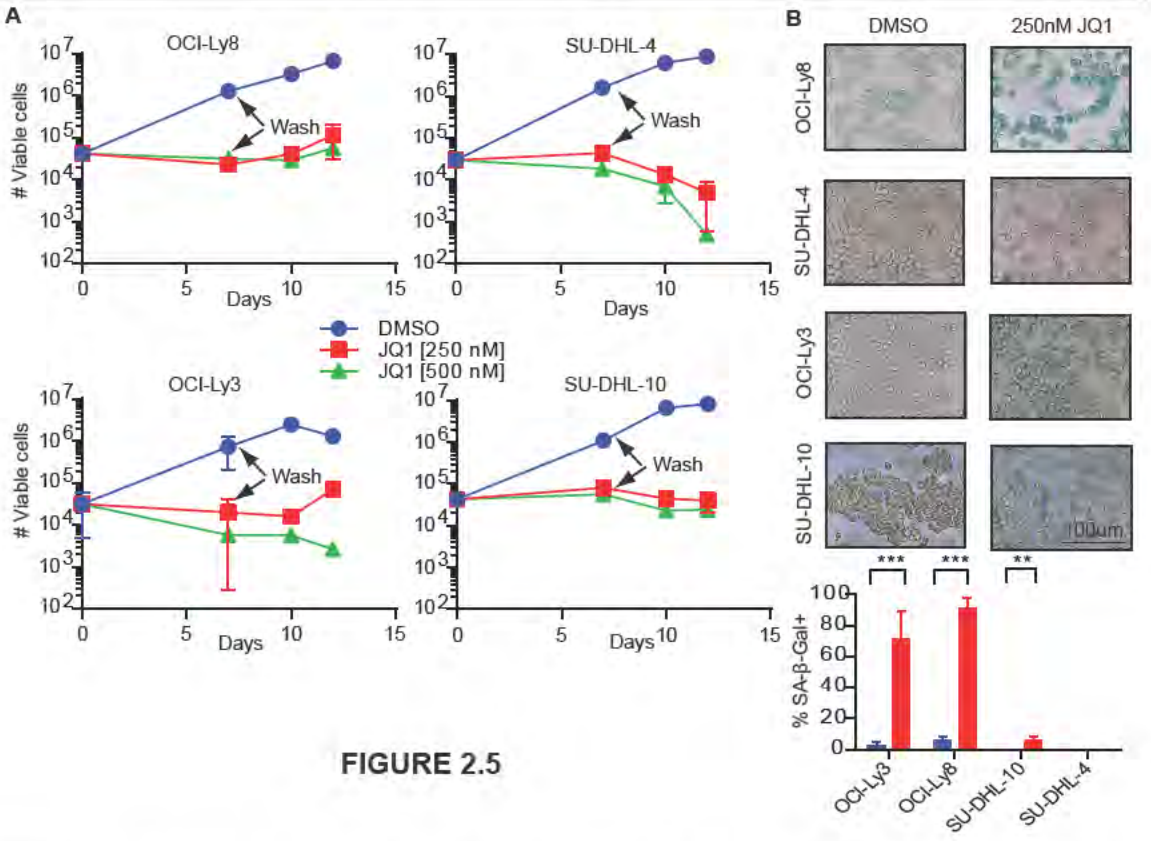

FIGURE 2.5

C-MYC translocations, whereas *C-MYC* loci in RC-K8(162), SU-DHL-5(160), OCI-Ly10 and HLY-1 (John Manis, personal communication) cells are normal. I found that these cell lines expressed varying amounts of C-MYC protein (Figure 2.6A). After 2 days of JQ1 treatment, C-MYC protein level was clearly decreased in 10 out of 11 DLBCL cell lines tested (Figure 2.6A). The C-MYC level did not change significantly in SU-DHL-10 cells after 2 days of JQ1

treatment (Figure 2.6A). However, an 88% decrease in the C-MYC protein level was observed in SU-DHL-10 cells after 7 days of JQ1 treatment (Figure 2.6B). JQ1 treatment decreased the C-MYC level in cells with *C-MYC* translocations (HBL-1, OCI-Ly8, OCI-Ly18, SU-DHL-6, and SU-DHL-10), *C-MYC* amplifications (OCI-Ly3 and SU-DHL-4) or without change in the *C-MYC* locus (RC-K8, SU-DHL-5, OCI-Ly10 and HLY-1). These data suggest that JQ1-mediated suppression of *C-MYC* can occur at the natural, chromosomally-translocated or gene amplified *C-MYC* loci.

To understand the possible mechanisms of the apoptosis versus senescence response after JQ1 treatment, I examined the expression of proteins previously implicated in these processes. Levels of the anti-apoptotic factor BCL-XL did not change upon JQ1 treatment (Figure 2.6B). In addition, proteins known to regulate senescence, such as p16, p21 and RB, were either undetectable or showed decreased expression after JQ1 treatment. Protein levels of p53 were not changed and its mutation status did not appear to correlate with response treatment, as OCI-Ly3 cells have wild type p53(163) and OCI-Ly8 cells harbor a mutated p53(159).

FIGURE 2.6 JQ1 treatment leads to suppression of C-MYC expression in DLBCL cells. **(A)** Western analysis of C-MYC protein levels in human DLBCL cell lines treated with JQ1 (250 nM) or DMSO for 2 days. The status of *C-MYC* in each cell line is indicated as: A (amplified), T (translocated) and N (normal). SU-DHL is abbreviated as SU. **(B)** Western analysis of C-MYC, BCL-XL, p16, p21, p53 and Rb protein levels in DLBCL cells treated with JQ1 (250 nM) or DMSO for 7 days.

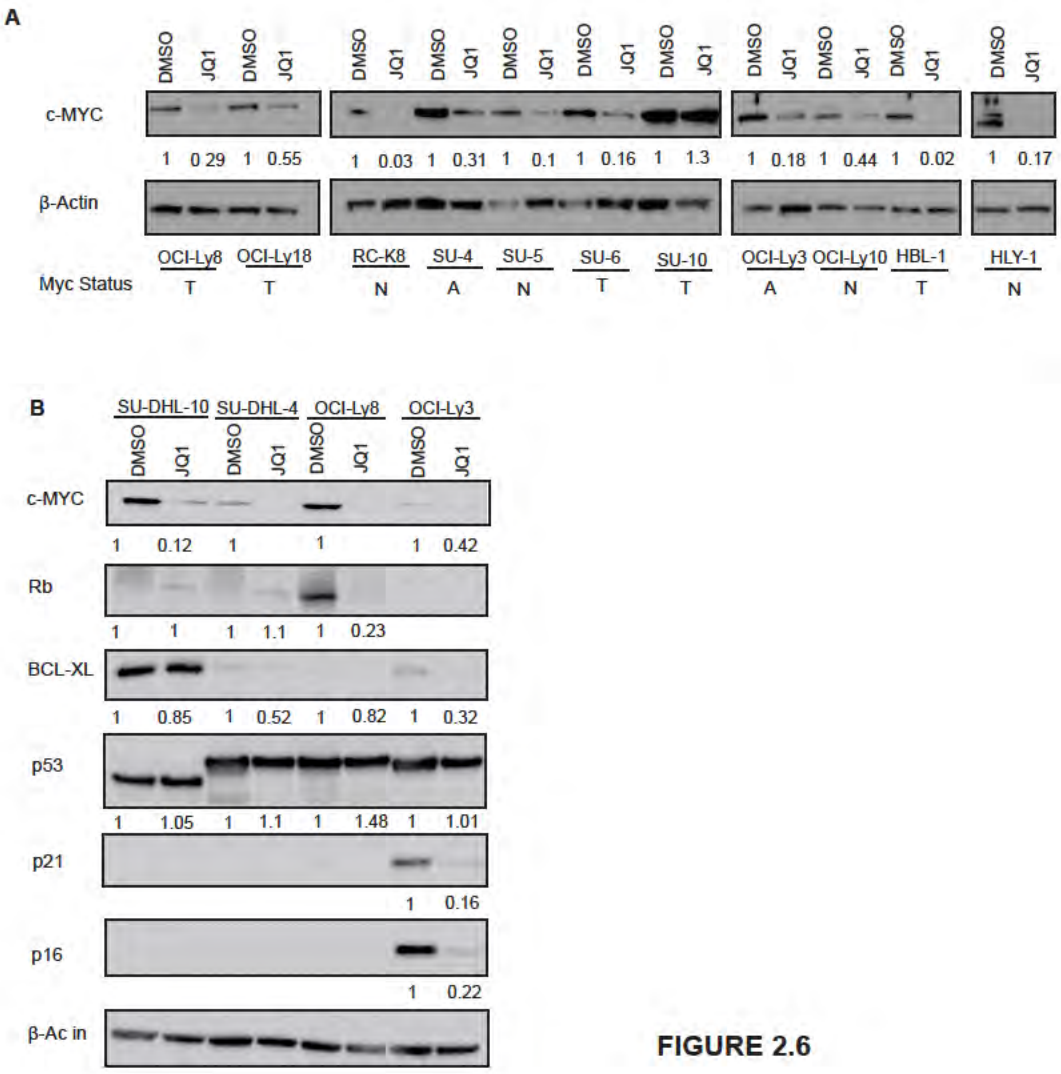

FIGURE 2.6

Although p53 in SU-DHL-10 and SU-DHL-4 cells has not been annotated, the reduced p53 protein size in SU-DHL-10 suggests a truncation (Figure 2.6B). Further studies will be required to elucidate the mechanism by which apoptosis or senescence is induced. It is currently unclear if decreasing C-

MYC causes apoptosis or senescence phenotype, or if C-MYC is rather decreased due to the decrease in proliferation.

JQ1 treatment of xenograft tumors results in significantly decreased rate of tumor growth and increased survival of mice

In order to evaluate how DLBCL cells xenografted into NSG mice would respond to a regimen of treatment with JQ1, I engrafted OCI-Ly8 cells subcutaneously into NSG mice and measured tumor volume. When at least one tumor on each mouse was detectable by palpation, I began a daily treatment of JQ1 (50 mg/kg of mouse body weight) or vehicle for 21-days. Seven mice from the vehicle-treated group and four mice from JQ1-treated group had to be euthanized before the end of treatment regimen because tumor volumes reached 1000 mm^3. Tumor growth was significantly decreased in JQ1 treated mice compared with vehicle treated (P<0.001) (Figure 2.7A). In addition to subcutaneously injected tumors, I used OCI-Ly8 cells to engraft NSG mice intraperitoneally in order to better mimic human disease. Six days after cell injection, I began daily treatment with 50 mg/kg JQ1 or vehicle for 21-days. After the completion of treatment, I monitored the mice until all were moribund and therefore had to be euthanized. JQ1 significantly (P=0.0039) increased survival time with a mean survival of 33.6 days compared with 29.5 days for vehicle (Figure 2.7B). Upon sacrifice, mice displayed infiltration of tumor cells into spleen and liver (Figure 2.7C) as well as prominent abdominal masses. Overall, these results demonstrate that treatment of DLBCL with

JQ1 results in either cell death or senescence.

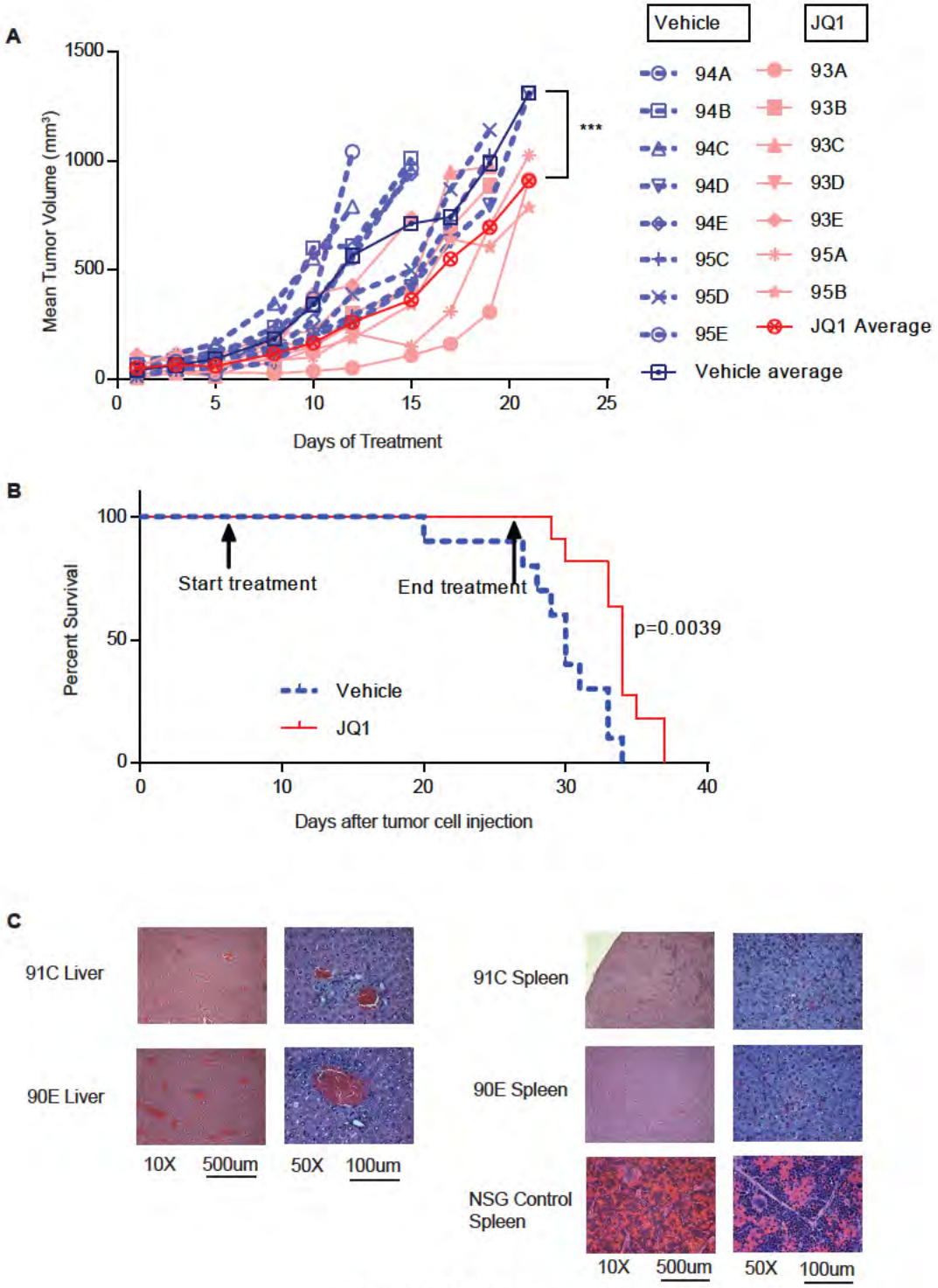

FIGURE 2.7

FIGURE 2.7 *(Previous page)* JQ1 treatment suppresses tumor growth and improves survival of NSG mice engrafted with DLBCL cells. **(A)** Growth of OCI-Ly8 tumor cells injected subcutaneously into NSG mice. Mice were treated with daily IP injections of JQ1 or vehicle for 21 days or until tumor volume reached ~1000 mm^3. Tumor growth in each individual mouse and average of tumor growth in JQ1 or vehicle treated mice are shown. Two-way ANOVA is used for statistical analysis. ***: $P<0.001$. **(B)** Kaplan-Meier survival curve of NSG mice engrafted with OCI-Ly8 tumor cells intraperitoneally and treated with JQ1 or vehicle for 21 days. Log-rank test is used for statistical analysis. **(C)** H&E staining showing evidence of tumor infiltration into liver and spleen of two representative NSG mice (90E treated with vehicle and 91C treated with JQ1) engrafted with OCI-Ly8 cells intraperitoneally. Spleen section of a normal non-engrafted NSG mouse is shown for comparison.

Materials and Methods

Cell lines and cell culture

Human DLBCL cell lines OCI-Ly18, RC-K8 and SU-DHL-5 were provided by Dr. John Manis at Harvard Medical School, cell lines HBL-1, HLY-1 and OCI-Ly8 were provided by Dr. Louis Staudt at National Cancer Institute, and cell lines OCI-Ly3, OCI-Ly10, SU-DHL-4 and SU-DHL-6 were provided by Dr. Subbarao Bondada at University of Kentucky. All DLBCL cells were maintained in RPMI media (Life Technologies) plus 10% fetal bovine serum (FBS, Sigma). Human cervical cancer cell line HeLa (ATCC) was cultured in DMEM media (Life Technologies) plus 10% FBS. All cells were cultured at 37°C and 5% CO_2. JQ1 as described previously(100) was dissolved in DMSO (Corning) and added in media to treat cells. JQ1 or DMSO was replaced

every 48 hours with fresh media to maintain the same concentrations. After a week of treatment, I removed JQ1 by spinning the cells at 1500 RPM for 5 minutes and replating the cells in fresh media.

Analyses of cell viability, cell cycle, and apoptosis

To assess cell viability, cells were collected and re-suspended in staining media: Hanks' balanced salt solution (Life Technologies), 3% FBS, 0.2% sodium azide, 1 mM EDTA and 1 μg/ml propidium iodide (PI). Viable and total cell numbers were determined using a MACSQuant analyzer (Miltenyi Biotech). For cell cycle analysis, cells were collected, re-suspended in PBS, permeabilized and fixed with 95% ice-cold ethanol overnight. PI was added before analyzing samples by flow cytometry using a FACSCalibur (BD biosciences). Flow cytometry data were analyzed using FlowJo software (Treestar). Apoptosis was analyzed using a Caspase-GLO 3/7 kit with GloMax-96 microplate luminometer (Promega) following manufacturer's recommendation.

Senescence associated β-galactosidase (SA-β-gal) staining

Cells were collected and fixed in a fixation solution (2% formaldehyde and 0.2% glutaraldehyde in PBS) for 5 min. After washing in PBS, cells were stained in SA-β-gal staining solution (40 mM citric acid/phosphate buffer, pH 6.0, 5 mM potassium ferrocynide, 5 mM potassium ferricynide, 150 mM NaCl,

2 mM $MgCl_2$, 1 mg/ml X-gal). After staining overnight at 37°C, cells were cytospun onto coverslips and examined by light microscopy.

Western blots

Whole cell lysates were isolated using RIPA buffer (50 mM Tris–HCl pH 7.5, 150 mM NaCl, 1% Triton X-100, 0.1% SDS, 0.5% deoxycholic acid and 0.02% sodium azide) plus fresh protease inhibitor complete (Roche). Lysates were run on SDS–PAGE Criterion X-gel (Bio-Rad) and transferred to nitrocellulose membranes (GE Osmonics). Membranes were probed with antibodies against BCL-XL, Rb (Cell Signaling), C-MYC, p21, p53, GAPDH, β-ACTIN (Santa Cruz Biotechnology), and p16 (Abcam). Membranes were visualized using Western lightening chemiluminescence detection (PerkinElmer) and ChemiDoc MP System with Image lab software (Bio-Rad).

Mouse studies

All mouse studies were carried out according to guidelines approved by the Institutional Animal Care and Use Committee of University of Massachusetts Medical School. Male NOD.Cg-*Prkdc*^{scid}*Il2rg*^{tm1Wjl}/SzJ (NSG) mice (2-4 months old from Jackson Laboratory) were maintained on a bi-weekly regime of antibiotic water (400 µg/ml of sulfamethoxazole and 80 µg/ml of trimethoprim oral suspension from HiTech Pharmacal). For tumor engraftment studies, 5×10^6 cells suspended in 50% matrigel (BD Biosciences) were

injected subcutaneously (SC) into the hind flank of each mouse (two sites per mouse). Tumors were measured using a digital caliper three times weekly for 21-days or until sacrifice. Tumor volumes were calculated using a formula: $\frac{4}{3}\pi r_1 r_2 r_3$, where $r_{1\text{-}3}$ are the radii for three dimensions of the tumor. For survival studies, 5 $\times 10^6$ cells were injected into mice intraperitoneally (IP). After detection of tumor by palpation (for SC injected) or 6 days after tumor cell injection (for IP injected), tumor-bearing mice were randomized and treated with daily IP injection of JQ1 (50 mg per kg of mouse body weight) for 21-days or until tumor volume reached 1000 mm^3 or mice became moribund. JQ1 was first dissolved in DMSO and subsequently mixed with 10% hydroxypropyl-β-cyclodextrin (Sigma) to improve solubility. Vehicle treated mice were injected with the equivalent volume of DMSO mixed with 10% hydroxypropyl-β-cyclodextrin. Tissues were harvested 2 hours after injection with JQ1 or vehicle in 10% neutral-buffered formalin for paraffin sections. Tissue sections were stained with Hematoxylin & Eosin.

Statistical analyses

Data were presented as mean ± SD. Welch's *t*-test and two-way ANOVA were used for statistical analyses, with $P<0.05$ considered as statistically significant. Kaplan-Meier survival curves were plotted and analyzed with the log-rank test.

CHAPTER III: YY1 regulates the germinal center reaction by inhibiting apoptosis and maintaining dark zones

Given the established connection between the GC and DLBCL, I investigated which molecular features may be important in the GC that are also implicated in DLBCL. The target of interest that I choose is YY1. YY1 is misregulated in DLBCL, is known to activate *c-Myc* transcription, and has been proposed as a master regulator of the GC transcription program. This led me to test the hypothesis that YY1 is an important regulator of the GC reaction.

Results

YY1 protein level is increased in GC B cells

Despite the observation that YY1 binding motifs are significantly enriched in the promoter regions of genes preferentially expressed in GC B cells, the *YY1* transcript is not changed in GC B cells compared to other B cell subsets(51). As the transcript level of a transcription factor is not necessarily an accurate indicator of its transcriptional activity, I examined the YY1 protein level in GC B cells. I immunized C57BL/6 wild-type mice with sheep red blood cells (sRBCs) to stimulate the GC reaction. At day 10 post-immunization, when the GC reaction is at the peak, I purified GC B cells ($B220^{+}GL7^{+}CD95^{+}$) and non-GC B cells ($B220^{+}GL7^{-}CD95^{-}$) in spleen by FACS for Western blot analysis. I found that YY1 protein levels were significantly increased (7.2-fold)

in GC B cells compared to non-GC B cells (Figure 3.1), prompting me to investigate whether YY1 is required for the GC reaction.

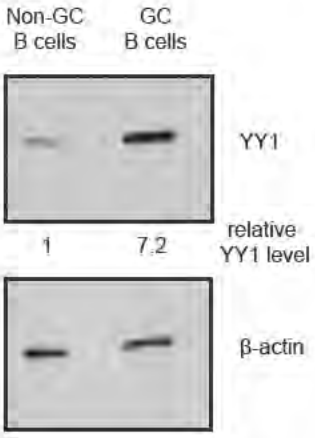

FIGURE 3.1. YY1 protein is increased in GC B cells. YY1 protein levels are determined by Western blotting in FACS-sorted GC B cells ($B220^{+}CD95^{+}GL7^{+}$) and non-GC B cells ($B220^{+}CD95^{-}GL7^{-}$) from spleens of wild-type mice (N=3) at 10 days post sRBC immunization. The relative levels of YY1 protein are quantified using β-actin as a loading control. This is representative of 2 independent experiments.

FIGURE 3.1

To facilitate the characterization of YY1 in the GC reaction, I attempted to examine YY1 protein using intracellular flow cytometry. I found that intracellular staining of YY1 was not specific, even though the same antibody detects YY1 protein specifically in Western blotting (Figure 3.2). Mouse embryonic fibroblasts (MEFs) isolated from $YY1^{Fl/Fl}$ embryos, in which exon 1 of *YY1* is flanked by two *LoxP* sites(111), were infected with adenovirus expressing the Cre recombinase. *YY1* was efficiently deleted in MEFs as indicated by decreased YY1 protein in Western blot. However, I did not detect any decrease in YY1 protein by intracellular flow cytometry (Figure 3.2). This result contrasted with a recent report using the same YY1 antibody in

intracellular flow(164). The non-specific intracellular flow prevents its use to examine YY1 protein at single-cell level during the GC reaction.

Selective deletion of *YY1* in GC B cells using *AID-Cre*

Constitutive deletion of *YY1* leads to embryonic lethality(116), and ablation of *YY1* in B cells using a floxed *YY1* allele ($YY1^{Fl}$) and *Mb1-Cre*

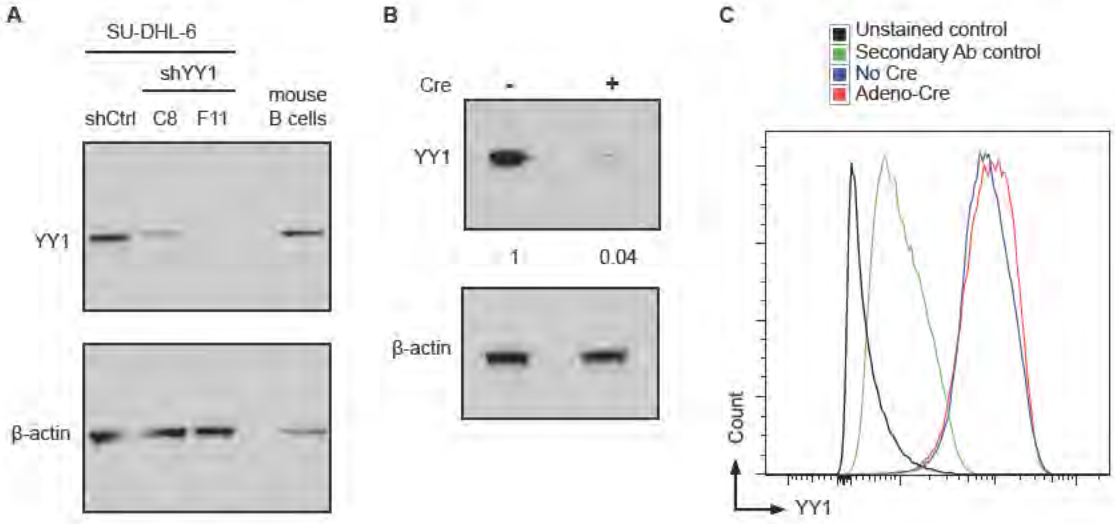

FIGURE 3.2

FIGURE 3.2. Flow cytometry analysis indicates that YY1 intracellular staining is not specific. (**A**) Western blot analysis of YY1 protein levels in human diffuse large B-cell lymphoma SU-DHL-6 cells infected with non-silencing control shRNA or shRNA targeting YY1 (C8 and F11), and mouse splenic B cells isolated from wild-type C57BL/6 mice. β-actin is included as a loading control. (**B**) Western blot analysis of YY1 protein levels in $YY1^{Fl/Fl}$ MEFs with or without infection with Adeno-Cre virus as indicated. The relative levels of YY1 protein are quantified using β-actin as a loading control. (**C**) Intracellular flow of $YY1^{Fl/Fl}$ MEFs with or without infection with Adeno-Cre virus. This figure represents data from 1 independent experiment.

blocks the transition from progenitor B cells to precursor B cells(111). As this block prevents the formation of mature B cells in secondary lymphoid organs, the use of *Mb1-Cre* or *CD19-Cre*(165) to delete *YY1* in B cells is not suitable to study the role of YY1 in the GC reaction.

To ablate *YY1* selectively in mature B cells or particularly in GC B cells, I used *AID-Cre*. The *Aicda* gene encodes activation-induced cytidine deaminase (AID), which is essential for SHM and CSR in GCs(37). AID expression is induced to high levels in GC B cells and then turned off during post-GC differentiation into plasma or memory B cells(166). In the *AID-Cre* mice, the *Cre* gene is inserted to replace exon 1 of *Aicda*, resulting in *Cre* expression under control of the *Aicda* locus and simultaneous disruption of *Aicda*(74). *AID-Cre* thus mediates recombination between *loxP* sites in GC B cells, and the resulting recombined allele is carried over when GC B cells differentiate into memory or plasma B cells(74, 166). It has previously been reported that loss of one *Aicda* allele, as in this *AID-Cre* model, causes a slight decrease in the functionality of the GC reaction and a slight increase in size of GC(167), which does not appear to have an effect in our system (Figure 3.3E). To determine the dynamics of *AID-Cre* activity in GCs, I utilized a Cre reporter *mT/mG* mouse strain, in which membrane-targeted fluorescent protein mTomato (mT) is expressed under the control of the *ROSA26* promoter prior to Cre-mediated recombination, while mGFP (mG) is expressed after Cre-mediated deletion of *mT*(168). I crossed the *AID-Cre*

mice with the *mT/mG* mice to track cells that had undergone Cre-mediated recombination at *ROSA26* at various time points after immunization with sRBCs. Mice that were not immunized with sRBCs exhibited a low but detectable level of the GC reaction (Figure 3.3A). About 50% of GC B cells in unimmunized mice were GFP positive (Figure 3.3C), indicating these cells had undergone Cre-mediated recombination. Furthermore, the GFP^+ population in unimmunized mice was enriched for GC B cells, whereas very few cells (<1%) in the GFP^- population were GC B cells (Figure 3.4). These observations are consistent with the notion that AID is induced in GC B cells and *AID-Cre* selectively mediates recombination in GC B cells. Because of the low background GC reaction, unimmunized mice do not represent true "day 0" time points where no GC B cell is detected. After sRBC immunization, there was a significant increase in GC B cells ($B220^+GL7^+CD95^+$) between day 4 and day 5 post-immunization (Figure 3.3A and 3.3E). Coinciding with this increase in GC B cells, I found a substantial increase in GFP^+ cells, in particular the mG^+mT^+ population (Figure 3.3B). These double positive cells were newly recombined as mGFP was expressed but mTomato protein was not yet degraded. Within the GC B cell population, I found a dramatic increase in the newly recombined mG^+mT^+ cells between day 4 and day 5 (Figure 3.3C and 3.3G), suggesting that *AID-Cre* is active as early as day 4 in GC B cells. In contrast, very few GFP^+ cells were found in non-GC B cells ($B220^+CD95^-GL7^-$) or non-B cells ($B220^-$) (Figure 3.3D and 3.3F), suggesting

very low levels of *AID-Cre* activity in other subsets of cells. Collectively, these results suggest that *AID-Cre* is active as early as day 4 post-immunization and carries out recombination selectively and efficiently in GC B cells.

FIGURE 3.3 *(Following page) AID-Cre* mediates efficient recombination in GC B cells. (**A**) Representative flow cytometry analysis of GC B cells ($B220^+CD95^+GL7^+$) in *AID-Cre;mT/mG* mice at different days post sRBC immunization. Cells were gated on live $B220^+$ cells. Frequency of each gated population as a percent of displayed cells is shown. (**B**) Representative flow cytometry analysis of mGFP and mTomato expression in total live splenic cells after immunization. (**C**) Representative flow cytometry analyses of mGFP and mTomato expression in GC B cells after immunization. (**D**) Representative flow cytometry analysis of mGFP and mTomato expression in non-B cells ($B220^-$) after immunization. (**E**) Quantitation of percentage of GC B cells in live B cells ($B220^+$) in response to immunization. (**F**) Percentage of $mGFP^+$ population in GC B cells (gray circles), non-B cell (dashed gray squares) or non-GC B cells (black diamonds). (**G**) Percentage of $mGFP^+mTomato^+$ population in GC B cells. Unimmunized: N=4, day 2: N=3, day 3: N=3, day 4: N=5, day 5: N=4, day 6: N=3, day 10: N=8. Error bars indicate standard deviations. This figure presents data from 6 independent experiments.

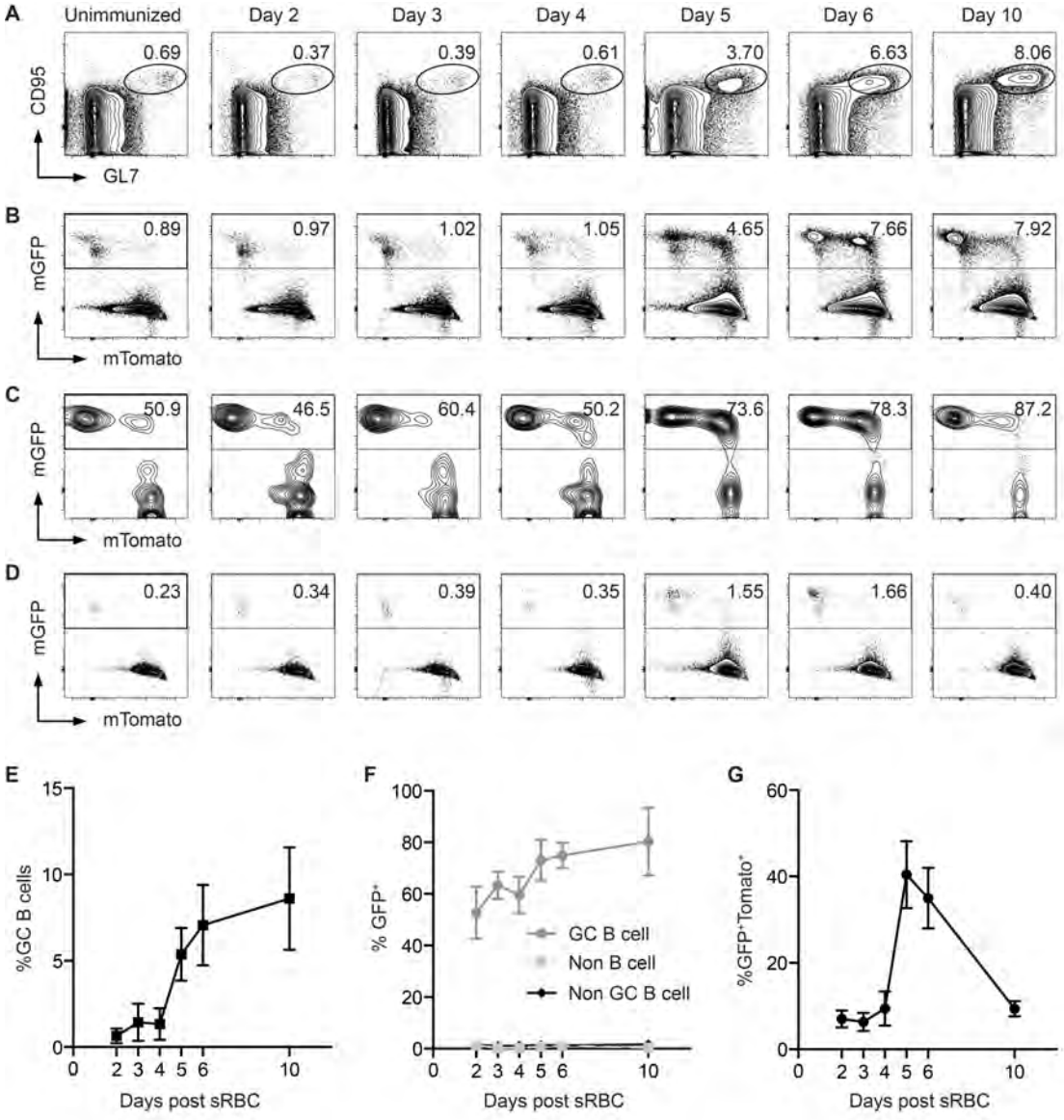
A
Unimmunized
Day 2
Day 3
Day 4
Day 5
Day 6
Day 10
CD95
GL7
0.69
0.37
0.39
0.61
3.70
6.63
8.06
B
mGFP
mTomato
0.89
0.97
1.02
1.05
4.65
7.66
7.92
C
50.9
46.5
60.4
50.2
73.6
78.3
87.2
D
0.23
0.34
0.39
0.35
1.55
1.66
0.40
E
%GC B cells
Days post sRBC
F
% GFP+
GC B cell
Non B cell
Non GC B cell
Days post sRBC
G
%GFP+Tomato+
Days post sRBC

FIGURE 3.3

FIGURE 3.4. GFP-positive population in unimmunized *AID-Cre;mT/mG* mice is enriched for GC B cells. (**A**) Representative flow cytometry analysis of GC B cells ($B220^+CD95^+GL7^+$) in GFP^+ and GFP^- populations in *AID-Cre;mT/mG* mice that were not immunized with sRBCs. Frequency of each gated population as a percent of displayed cells is shown. (**B**) Average percentages of $B220^+$ cells and GC B cells in GFP^+ and GFP^- populations (N=4 from 3 independent experiments). Error bars indicate standard deviation.

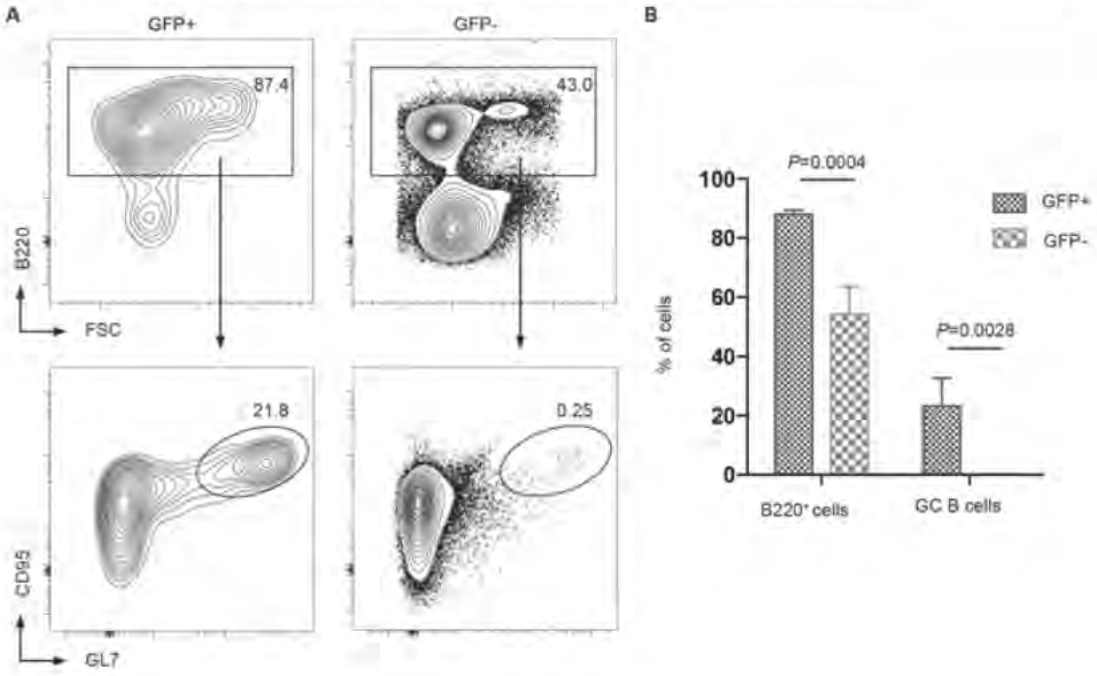

FIGURE 3.4

Deletion of *YY1* leads to an impaired GC reaction

To investigate the role of YY1 in the GC reaction, I generated $YY1^{Fl/Fl}$; *AID-Cre* (referred as $YY1^{CKO}$ hereafter) mice and compared them with $YY1^{Fl/Fl}$ alone, *AID-Cre* alone, or C57BL/6 wild-type mice for the GC reaction in response to sRBC immunization. I examined GC B cells ($B220^+CD95^+GL7^+$ or $B220^+PNA^+$) by flow cytometry at different time points after immunization (Figures 3.5 and 3.6). Day 4 post-immunization represents the earliest time

point that newly formed GC B cells can be reliably detected by flow cytometry using cell surface markers. Day 6 is a time during which GCs are still maturing, whereas day 10 is at the peak of the GC reaction(33–35).

After sRBC immunization, $B220^{+}$ populations remained largely unchanged (Figure 3.5). Starting at day 4 post-immunization, I observed a gradual increase in the frequency and total number of GC B cells ($B220^{+}CD95^{+}GL7^{+}$) in spleens of wild type, *YY1*$^{Fl/Fl}$, or *AID-Cre* control mice compared to unimmunized mice (Figure 3.5). However, a significant decrease in the frequency of GC B cells was observed in *YY1*^{CKO} mice compared to *YY1*$^{Fl/Fl}$, *AID-Cre,* or wild-type mice at day 4 (Figure 3.5A). This decrease resulted in 30-70% reduction of total GC B cells in the spleens of *YY1*^{CKO} mice compared to control mice. Significant decreases in the frequency and number of GC B cells in *YY1*^{CKO} mice was observed at day 6 and day 10 post-immunization (Figure 3.5B and 3.5C). Further, at day 10 post-immunization, I found that the frequency and number of GC B cells in *YY1*^{CKO} mice continued to decrease (by 3-fold) compared to day 6, while control mice had largely maintained their GC B cells (Figure 3.5C). The decrease in GC B cells in *YY1*^{CKO} mice was similar when I used $B220^{+}PNA^{+}$ for GC B cells (Figure 3.6) or stained with PNA in immunohistochemistry for the presence of

GCs (Figure 3.5).

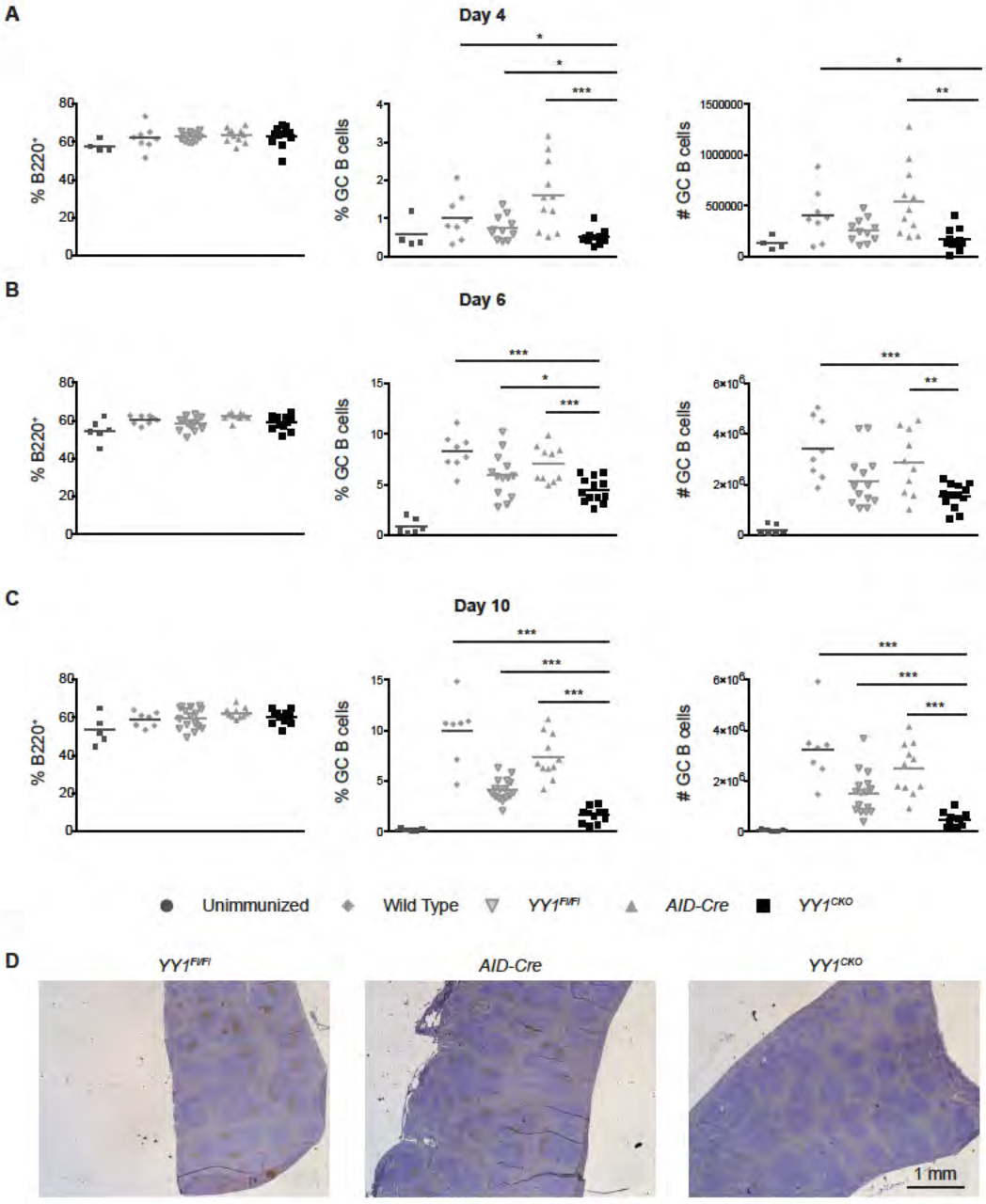

FIGURE 3.5

FIGURE 3.5. *(Previous page)* Loss of *YY1* leads to an impaired GC reaction using GL7 and CD95. Percent of B cells ($B220^+$), GC B cells ($B220^+CD95^+GL7^+$) in live B cells ($B220^+$) and total number of GC B cells (right panels) in spleens of mouse at (**A**) day 4 (4 independent experiments), (**B**) day 6 (8 independent experiments) and (**C**) day 10 (7 independent experiments) post sRBC immunization. Each point represents data from a single mouse. Horizontal bar indicates mean of data. (**D**) Representative immunohistochemical staining of spleen sections with PNA at day 10 post immunization. *: $P<0.05$, **: $P<0.01$, ***: $P<0.001$.

Collectively, these data indicate that YY1 is required for an efficient GC reaction and loss of *YY1* leads to an impaired GC reaction.

GCs are polarized into DZ and LZ during GC reaction. Given the diminished GC reaction in $YY1^{CKO}$ mice, I wanted to determine if *YY1* deletion preferentially altered DZ vs. LZ. As shown in Figure 3.7, DZ cells ($B220^+CD95^+GL7^+CXCR4^{hi}CD86^{lo}$) outnumbered LZ cells ($B220^+CD95^+GL7^+CXCR4^{lo}CD86^{hi}$) in control mice as previously reported(169). In contrast, a significant decrease in the frequency of DZ cells and a concomitant increase in the frequency of LZ cells were found in $YY1^{CKO}$ mice at 10 day after immunization compared to control mice (Figure 3.7), which resulted in a 2-fold decrease in the ratio of DZ versus LZ cells. These data suggest that YY1 regulates the balance between DZ and LZ cells in GCs.

FIGURE 3.6 *(Following page)* Loss of *YY1* leads to an impaired GC reaction using PNA. (**A**) Representative flow cytometry analyses of GC B cells ($B220^+PNA^+$) at day 10 post sRBC immunization. Frequency of each gated population as a percent of displayed cells is shown. (**B**) Percent of GC B cells ($B220^+PNA^+$) in live B cells ($B220^+$) and total number of GC B cells in spleens at day 4 (4 independent experiments), day 6 (7 independent experiments) and day 10 (5 independent experiments) post-sRBC immunization. Each point represents data from a single mouse. Horizontal bar indicates mean of data. Statistical significance is determined by two-tailed unpaired Student's *t*-test (*: $P<0.05$, **: $P<0.01$, ***: $P<0.001$).

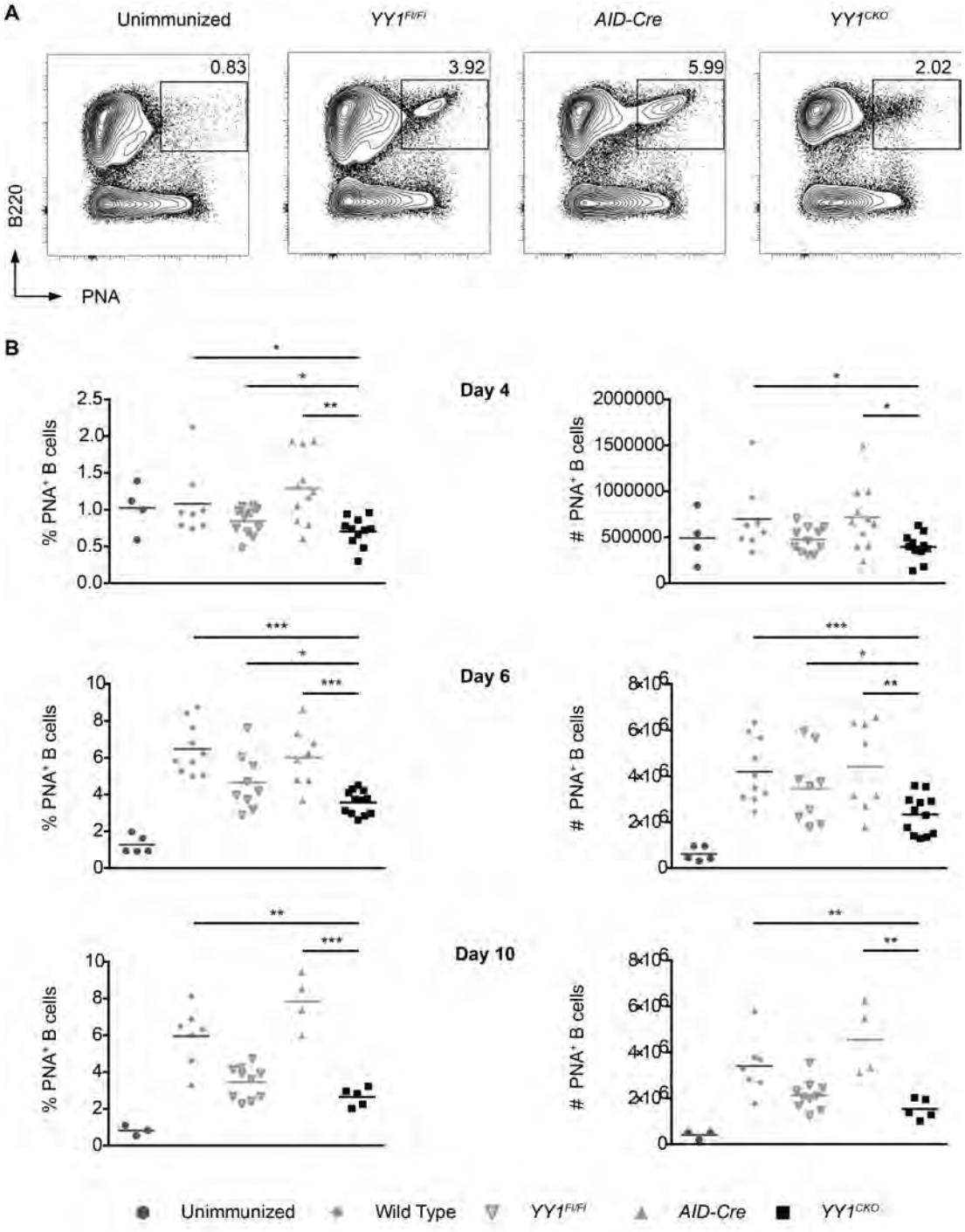
A
Unimmunized
YY1F/F/
AID-Cre
YY1CKO
0.83
3.92
5.99
2.02
B220
PNA
B
Day 4
Day 6
Day 10
% PNA+ B cells
# PNA+ B cells
Unimmunized
Wild Type
YY1F/F/
AID-Cre
YY1CKO

FIGURE 3.6

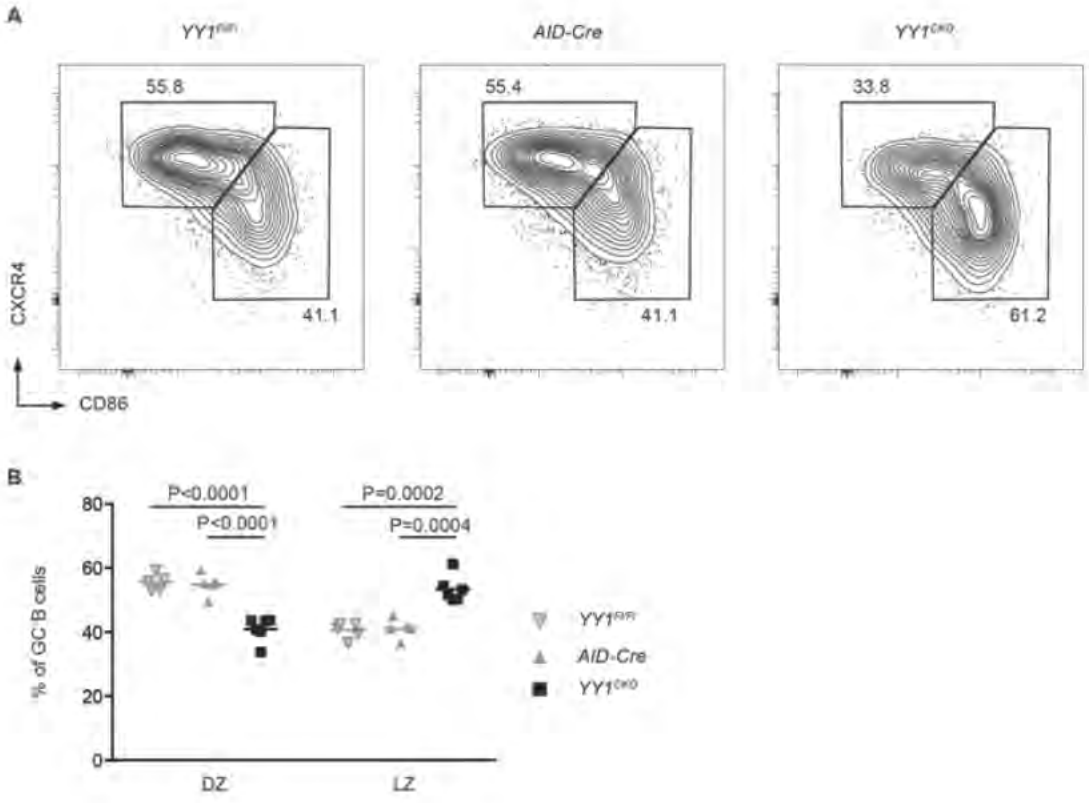

FIGURE 3.7

FIGURE 3.7 Loss of *YY1* leads to decreased DZ cells. (**A**) Representative flow cytometry analysis of DZ cells ($B220^{+}CD95^{+}GL7^{+}CXCR4^{hi}CD86^{lo}$) and LZ cells ($B220^{+}CD95^{+}GL7^{+}CXCR4^{lo}CD86^{hi}$) in $YY1^{CKO}$ mice at 10 day after sRBC immunization compared to control mice. Cells were gated on GC B cells ($B220^{+}CD95^{+}GL7^{+}$). Frequency of each gated population as a percent of displayed cells is shown. (**B**) Percent of DZ and LZ cells in GC B cells in $YY1^{CKO}$ mice at 10 day after sRBC immunization compared to control mice. Each point represents data from a single mouse. Horizontal bar indicates mean of data. This figure represents data from 2 independent experiments.

Because there were still small numbers of GC B cells present in response to sRBC immunization in *YY1*^{CKO} mice even at day 10 (Figure 3.5), I sought to determine whether these GC B cells had undergone complete deletion of both *YY1* alleles, or whether one or both alleles of *YY1* still remained intact. I sorted GC B cells from *YY1*^{CKO} mice and used single-cell PCR to determine the status of the *YY1* locus (Figure 3.8). At day 4 post-immunization, 73% of GC B cells had both *YY1* alleles deleted, whereas 10.8% and 16.2% of GC B cells had only one *YY1* allele deleted or no *YY1* deletion in *YY1*^{CKO} mice, respectively (Table 3.1). Despite increased *AID-Cre* activity from day 4 to day 10 (Figure 3.3), the frequency of GC B cells with both *YY1* alleles deleted did not increase at day 10 (69.6%) compared to day 4. Furthermore, the fraction of GC B cells without *YY1* deletion was similar at day 4 (16.2%) and day 10 (21.6%), suggesting a counter selection against cells with deletion in both *YY1* alleles. Collectively, these data indicate that although *YY1*-null GC B cells are generated, *YY1* ablation greatly reduces the magnitude of the GC response.

To investigate whether *YY1*-null GC B cells could be identified using flow cytometry instead of single-cell PCR, I crossed the *mT/mG* reporter allele into *YY1*^{CKO} mice. Similar to what is shown in Figure 3.5, the GC reaction was impaired in *YY1*^{CKO}; *mT/mG* mice (Figure 3.9). I found that 41.4% of GC B cells at day 4 post-sRBC immunization were GFP positive in *YY1*^{CKO}*; mT/mG* mice compared to 56.1% in *AID-Cre; mT/mG* control mice.

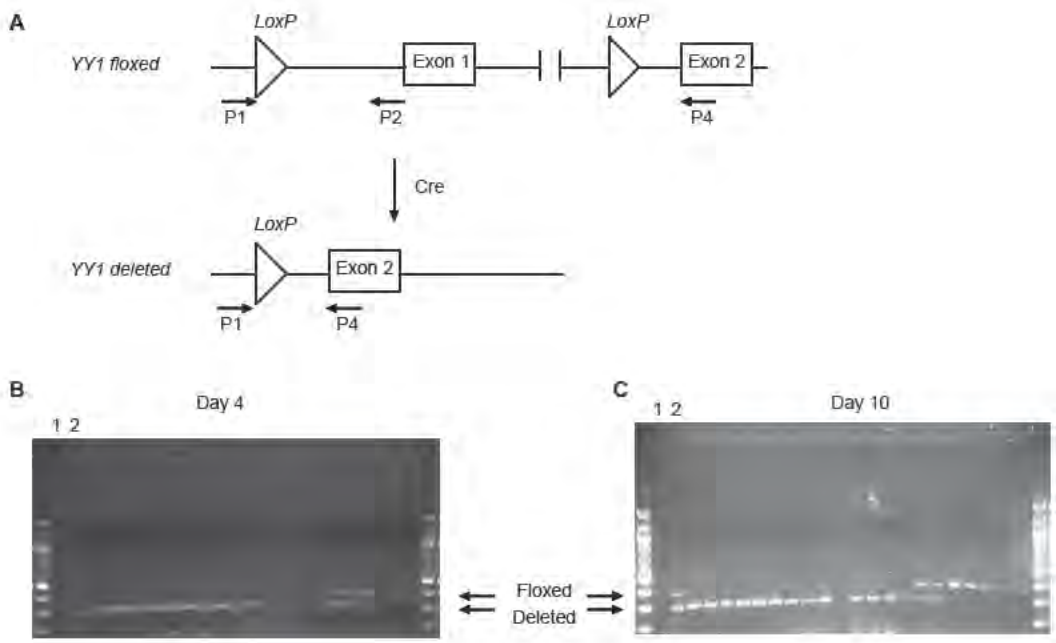

FIGURE 3.8

FIGURE 3.8 Single-cell genomic PCR to detect *YY1* deletion. (**A**) Schematics of floxed and deleted *YY1* loci. Primers used to amplify YY1 loci are indicated as P1, P2 and P4. Representative single-cell PCR results of FACS-sorted GC B cells ($B220^+GL7^+CD95^+$) from $YY1^{CKO}$ mice at (**B**) day 4 and (**C**) day 10 post sRBC immunization. Lane 1 is a negative control with water as template. Lane 2 is a positive control using genomic DNA equally mixed from $YY1^{Fl/Fl}$ and *YY1*-deleted MEFs by adeno-Cre virus.

At day 10, 58.2% of GC B cells were GFP^+ in $YY1^{CKO}$; *mT/mG* mice compared to 80.2% GFP^+ in *AID-Cre; mT/mG* control mice (Figure 3.9). Furthermore, I examined the *YY1* status in GC B cells in $YY1^{CKO}$; *mT/mG* mice. Among GC B cells that had both YY1 alleles deleted, 63.2% were GFP^+ and 36.7% were GFP^-. These data indicate GC B cells with both *YY1* alleles

deleted cannot be easily identified based on the *mT/mG* reporter, thus limiting its use to identify *YY1*-null GC B cells.

Table 3.1 *AID-Cre* mediated deletion of *YY1* alleles in GC B cells

Days post immunization	Deletion of both *YY1* alleles	Deletion of only one *YY1* allele	No *YY1* deletion
4	73.0% (54/74)	10.8% (8/74)	16.2% (12/74)
10	69.6% (71/102)	8.8% (9/102)	21.6% (22/102)

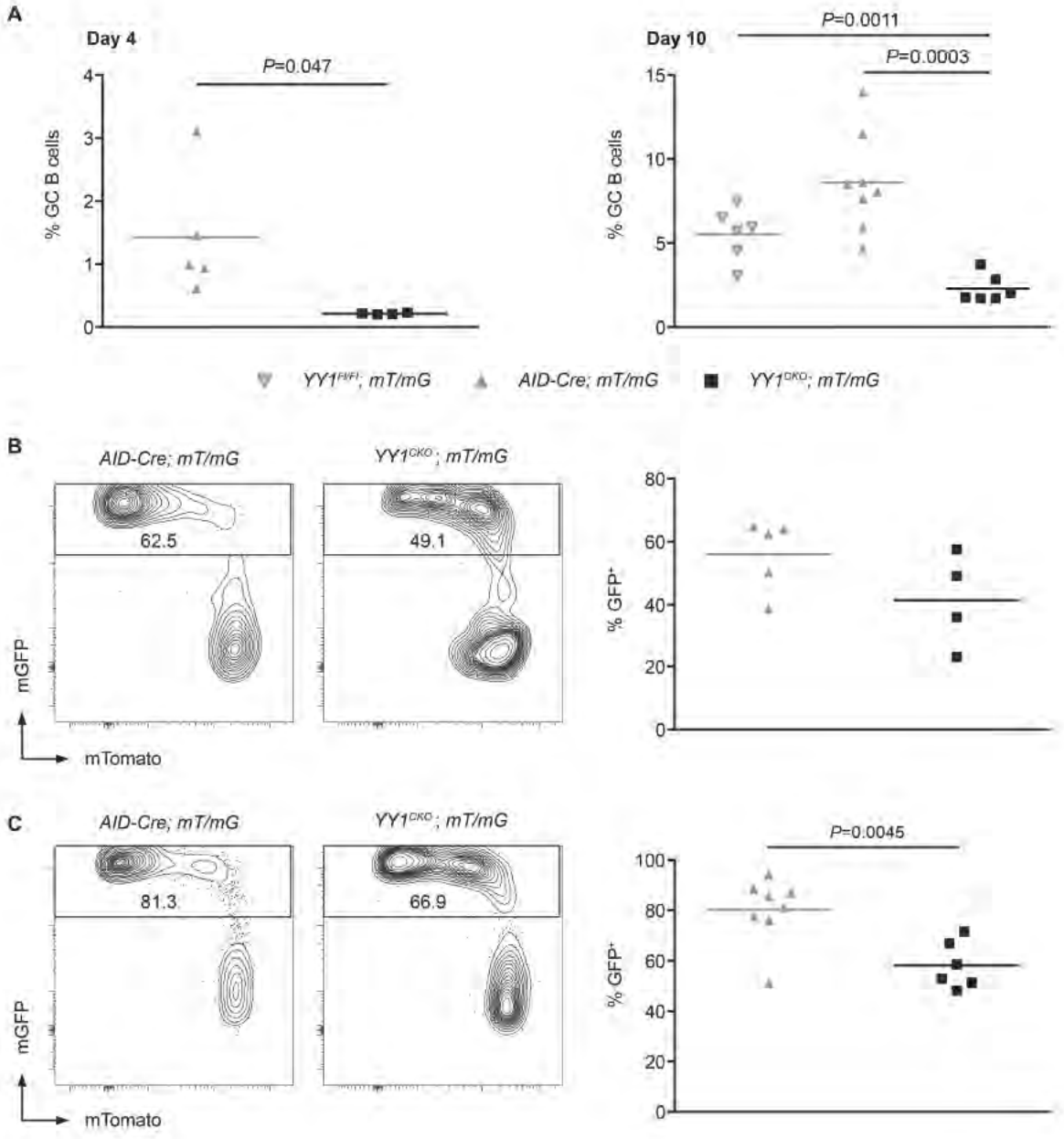

FIGURE 3.9

FIGURE 3.9 Analysis of the GC reaction in *YY1*^{CKO};*mT/mG* mice. (**A**) Percent GC B cells (B220^{+}CD95^{+}GL7^{+}) of live B cells (B220^{+}) in spleens at day 4 and day 10 post sRBC immunization. Representative flow cytometry analysis and quantitation of mGFP and mTomato expression in GC B cells at (**B**) day 4 (1 independent experiment) and (C) day 10 (2 independent experiments) post sRBC immunization. Each point represents data from a single mouse. Horizontal bar indicates mean of data.

YY1 does not affect cell proliferation but prevents apoptosis in GC B cells

The presence of small numbers of GC B cells with both *YY1* alleles deleted suggests that YY1 is likely not required for the initiation of the GC reaction. The decrease in DZ cells and the decrease of GC B cells in $YY1^{CKO}$ mice from day 6 to day 10 (average of 1.5×10^6 cells at day 6 vs. 0.48×10^6 cells at day 10) post-immunization suggest that impairment of the GC reaction in $YY1^{CKO}$ mice is due to a defect in maintaining or amplifying GC B cell numbers. I suspected this defect could be the result of altered proliferation and/or apoptosis of GC B cells in $YY1^{CKO}$ mice. To test this hypothesis, I first examined the consequence of loss of *YY1* on cell proliferation and cell cycle. As shown in Figure 3.10A, BrdU incorporation was significantly decreased in GC B cells in $YY1^{CKO}$ mice compared to control mice ($YY1^{Fl/Fl}$ or *AID-Cre*) at day 10 post-sRBC immunization. In contrast, proliferation of non-GC B cells ($B220^+CD95^-GL7^-$) or non-B cells ($B220^-$) was low and there was no difference in BrdU incorporation in these cells between $YY1^{CKO}$ and control mice (Figure 3.10A). Interestingly, Ki-67 and DAPI staining indicated there was no significant difference in cell cycle distribution of GC B cells between $YY1^{CKO}$ and control mice (Figure 3.10B and 3.10C).

As DZ cells undergo rapid proliferation(50, 78–80, 169), the altered DZ/LZ ratio in $YY1^{CKO}$ mice (Figure 3.7) prompted an investigation into whether decreased BrdU incorporation in GC B cells in $YY1^{CKO}$ mice was due

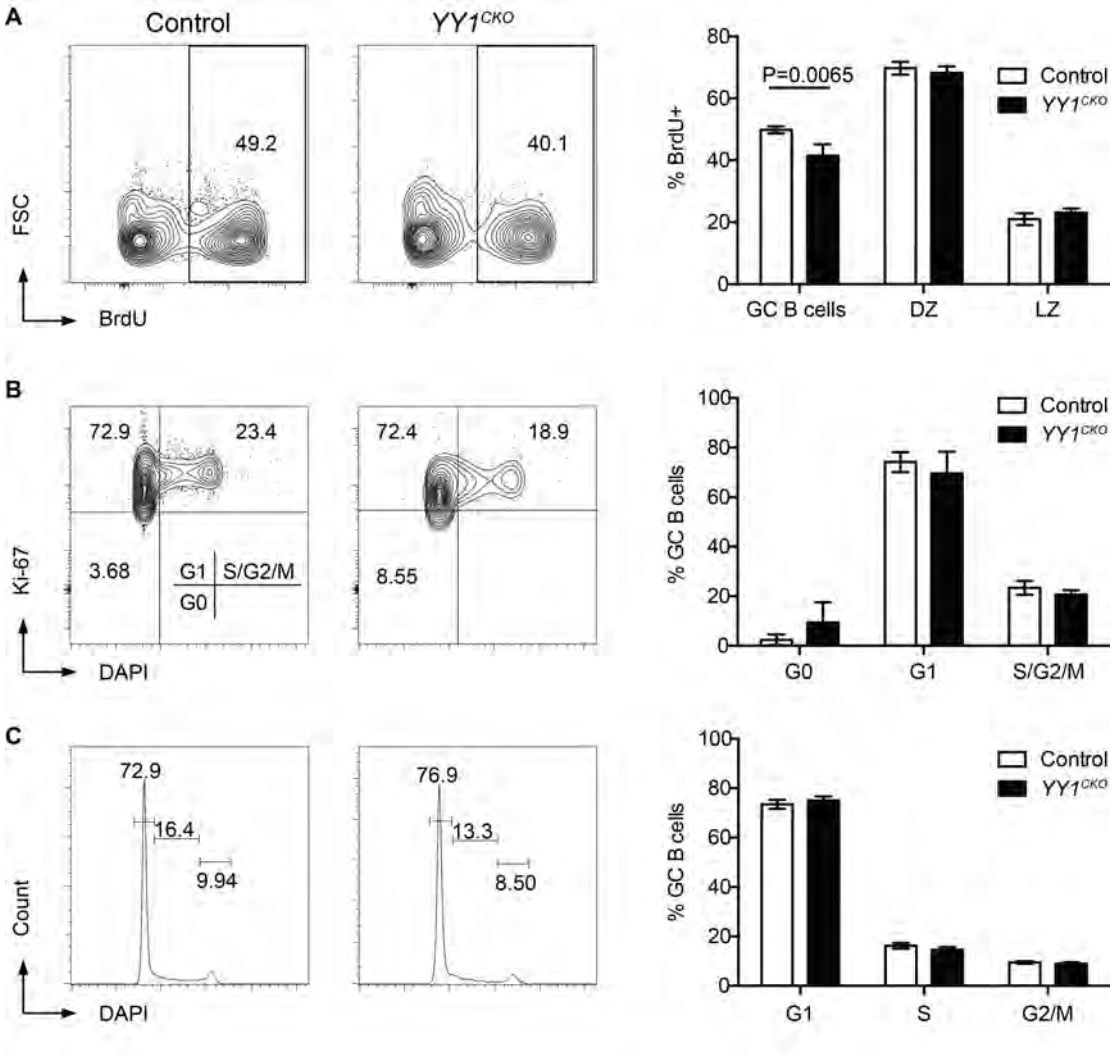

FIGURE 3.10

to decreased proliferation in DZ and LZ cells, or due to a decrease in DZ cells. I found no significant difference in BrdU incorporation in DZ or LZ cells between *YY1*^{CKO} mice and control mice (Figure 3.10A). Because LZ cells proliferate slower than DZ cells and incorporate less BrdU (Figure 3.10A), these data argue that altered distribution of DZ and LZ cells rather than

FIGURE 3.10 *(Previous page)* Loss of *YY1* does not directly affect proliferation of GC B cells. (**A**) Representative flow cytometry analysis of BrdU incorporation in GC B cells ($B220^+CD95^+GL7^+$) at day 10 post sRBC immunization in control ($YY1^{Fl/Fl}$ or *AID-Cre*), $YY1^{CKO}$, or negative controls (samples injected with BrdU but stained without anti-BrdU antibody, or samples without BrdU injection but stained with anti-BrdU antibody). Average percentages of BrdU incorporation in GC B cells, DZ cells ($B220^+CD95^+GL7^+CXCR4^{hi}CD86^{lo}$), LZ cells ($B220^+CD95^+GL7^+CXCR4^{lo}CD86^{hi}$), non-B cells and non-GC B cells are shown below. Controls ($YY1^{Fl/Fl}$ or *AID-Cre*): N=4, $YY1^{CKO}$: N=3. (**B**) Representative flow cytometry analysis of Ki-67 and DAPI staining of GC B cells at day 10 post immunization and averages of 6 controls ($YY1^{Fl/Fl}$ or *AID-Cre*) and 4 $YY1^{CKO}$ mice are shown at right. (**C**) Representative cell cycle analysis of GC B cells at day 10 post immunization and averages of 6 controls ($YY1^{Fl/Fl}$ or *AID-Cre*) and 4 $YY1^{CKO}$ mice are shown at right. Error bars are standard deviations. This figure represents data from 1 independent experiment.

change in proliferation *per se* is responsible for the decreased BrdU incorporation in GC B cells of $YY1^{CKO}$ mice.

From day 6 to day 10 post-immunization, GC B cells in $YY1^{CKO}$ mice continued to decrease (1.5×10^6 vs 0.48×10^6) suggesting that cell death is responsible for the loss of GC B cells in $YY1^{CKO}$ mice. I investigated whether loss of *YY1* in GC B cells activates apoptosis by staining cells with an apoptotic marker activated caspase-3(170, 171). As shown in Figure 3.11A, activated caspase-3 was increased more than two-fold in GC B cells in $YY1^{CKO}$ mice compared to controls. This increase in apoptosis was limited to GC B cells, as non-GC-B cells and non-B cells displayed very low activated caspase-3 staining and there was no difference between control and $YY1^{CKO}$ mice (Figure 3.11A and 3.11B). In addition, I used TUNEL staining to detect late stages of apoptosis and found that apoptosis was significantly increased

in GC B cells (PNA^+ cells in follicles) in $YY1^{CKO}$ mice compared to control mice (Figure 3.11C and 3.11D). Together these data indicate that loss of *YY1* in GC B cells leads to an increase in apoptosis and therefore is required for the proper maintenance of a robust GC reaction. Overall, I conclude that YY1 regulates the GC by inhibiting apoptosis and maintaining normal DZ.

FIGURE 3.11 *(Following page)* Loss of *YY1* leads to increased apoptosis. (**A**) Representative flow cytometry analysis of activated Caspase-3 staining in GC B cells ($B220^+CD95^+GL7^+$) at day 10 post sRBC immunization. Samples stained without Caspase-3 antibody were used as negative controls and samples from a mouse irradiated (5 Gy) were used as positive controls for Caspase-3 staining. (B) Average percentages of Caspase-3 positive population in non-B cells ($B220^-$), non-GC B cells ($B220^+CD95^-GL7^-$) and GC B cells. Controls ($YY1^{Fl/Fl}$ or *AID-Cre*): N=6, $YY1^{CKO}$: N=4. (**C**) Representative immunofluorescent staining of TUNEL (green), PNA (red) and DAPI (blue) of spleen sections. (**D**) Averages of TUNEL positive cells as a percent of PNA positive cells in controls ($YY1^{Fl/Fl}$ or *AID-Cre*: N=5) and $YY1^{CKO}$ mice (N=3). About 600-800 PNA^+ cells were counted per genotype. Error bars are standard deviations. This figure represents data from 1 independent experiment.

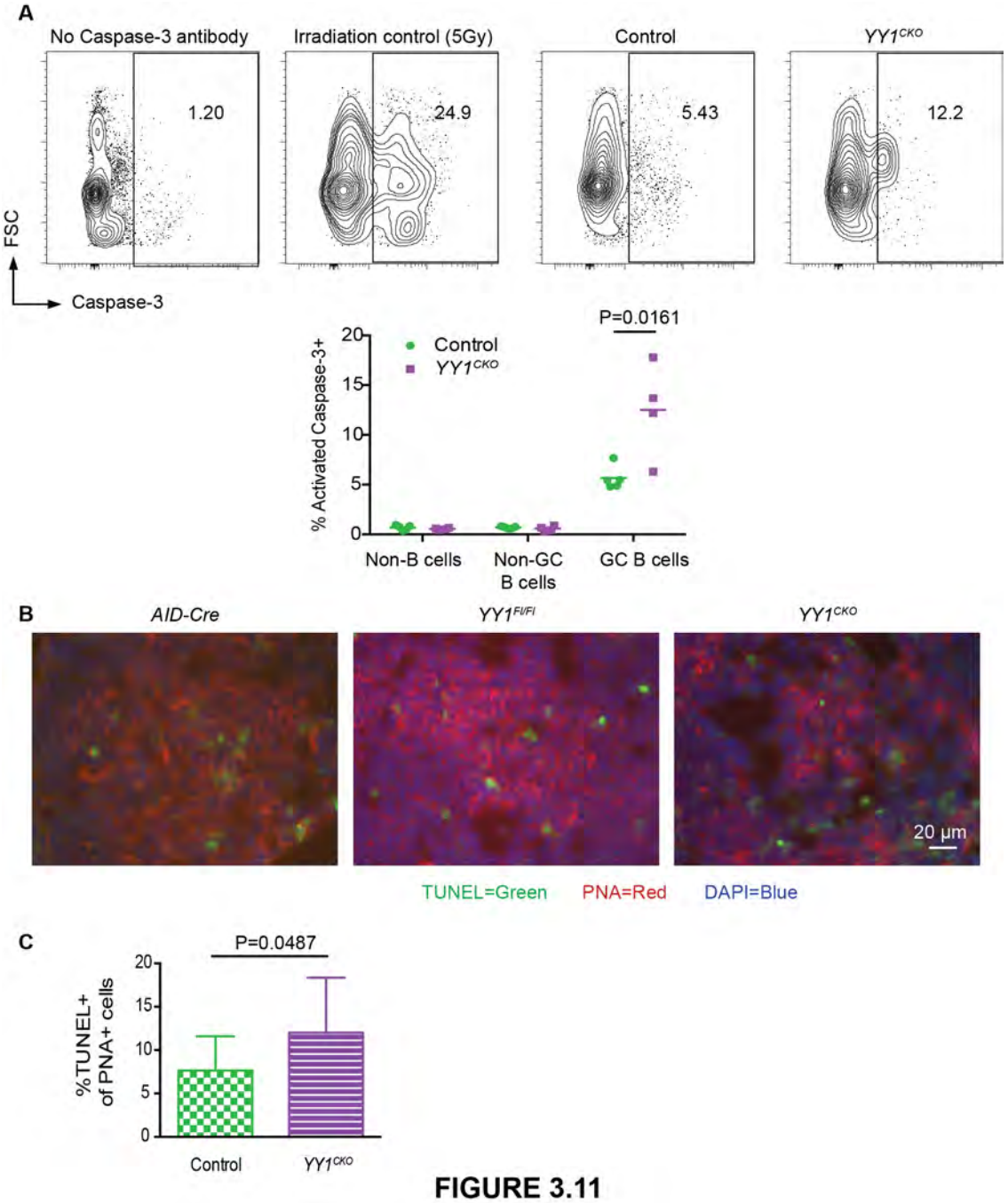
A
No Caspase-3 antibody
Irradiation control (5Gy)
Control
YY1CKO
1.20
24.9
5.43
12.2
FSC
Caspase-3
P=0.0161
Control
YY1CKO
% Activated Caspase-3+
20
15
10
5
0
Non-B cells
Non-GC B cells
GC B cells
B
AID-Cre
YY1Fl/Fl
YY1CKO
20 μm
TUNEL=Green
PNA=Red
DAPI=Blue
C
P=0.0487
%TUNEL+ of PNA+ cells
20
15
10
5
0
Control
YY1CKO

FIGURE 3.11

Materials and Methods

Mouse strains

Mouse strains *YY1*$^{Fl/Fl}$ (B6;129S4-*Yy1*^{tm2Yshi}/J), *AID-Cre* (B6.129P2-*Aicda*$^{tm2(cre)Mnz}$/J), *mT/mG* (B6.129(Cg)-*Gt(ROSA)26Sor*$^{tm4(ACTB-tdTomato,-EGFP)Luo}$/J) and C57BL/6 wild-type were obtained from Jackson laboratories. Mouse studies were approved by the Institutional Animal Care and Use Committee of University of Massachusetts Medical School.

Immunization

Sheep red blood cells (1.5×10^9) (Cocalico Biologicals) were injected intraperitoneally into 8 to 10-week old mice of both sexes. At various days after immunization, spleens were collected for FACS staining, fixed in formalin or frozen in OCT for sectioning.

Flow Cytometry

Spleens were prepared into single cell suspension and red blood cells were lysed in cold distilled water. After filtered through 70-μm nylon mesh and counting using a MACSQuant analyzer (Miltenyi Biotec), cells were incubated with anti-CD16/32 antibody (BioXCell) to block Fc receptors and stained with fixable viability dye eFluor 780 (eBioscience). Cells were then stained for 20 min in staining media (Hank's balanced salt solution, 3% FBS, 0.02% sodium azide, 1 mM EDTA) with primary antibodies, including B220-FITC, B220-

eVolve 655 (clone RA3-6B2), GL7-eFluor 660, GL7-eFluor 450 (clone GL7), CD95-PE, CD95-APC (clone 15A7) (eBioscience), PNA-biotin (Vector Laboratories), CD86-Pe-Cy7 (clone GL-1; BioLegend) or CD184-biotin (2b11/CXCR4; BD Bioscience). Cells stained with biotin-labeled antibodies were incubated with streptavidin-eFluor 450 (eBioscience). For intracellular staining, cells were stained with fixable viability dye eFluor 780, permeabilized and fixed using a cytofix/cytoperm plus kit (BD Bioscience) according to manufacturer suggested protocol. Cells were then stained with YY1 antibody (H-414; Santa Cruz Biotechnology) and DyLight 594-conjugated secondary antibody (Jackson ImmunoResearch). Flow cytometry analysis was performed on an LSRII FACS or a FACSAria cell sorter (BD Bioscience), and analyzed using FlowJo software (FlowJo).

Single-cell PCR of floxed and deleted *YY1* alleles

GC B cells ($B220^{+}CD95^{+}GL7^{+}$) were sorted into sterile water (5-10 µl) as one cell per well in 96-well plates. Cells were lysed by 3 freeze-thaw cycles followed by heating to 98°C for 10 minutes. PCR to amply the *YY1* locus was performed using Phusion hot start flex DNA polymerase (New England Biolabs) and primers: P1 (5'-ACCTGGTCTATCGAAAGGAAGCAC-3'), P2 (5'-GCTTCGCCTATTCCTCGCTCATAA-3'), and P4 (5'-CCAAAGTTCGAAACCTGCTTTCCT-3') as described(111).

BrdU incorporation and cell cycle analysis

Mice were injected intraperitoneally with 1 mg BrdU. 6-16 hours later, spleen cells were stained for GC B cells as described above. After being fixed and permeabilized using a BrdU flow kit (BD Bioscience), cells were stained with anti-BrdU-FITC (BD Bioscience) or anti-Ki-67-PerCp-Cy5.5 (Sola15) (eBioscience) antibody. Cells stained for Ki-67 were further incubated with DAPI. Stained cells were analyzed by flow cytometry as described above.

Activated Caspase-3 staining

Spleen cells were collected and stained for GC B cells as described above. An active Caspase-3 apoptosis kit and anti-activated caspase-3-PE antibody (BD Bioscience) were used following manufacturer suggested protocol. Stained cells were analyzed by flow cytometry as described above.

Immunofluorescence and immunohistochemistry staining

Frozen spleen sections (5 μm) were fixed in 4% paraformaldehyde and extracted in 0.5% Triton-X 100. Sections were stained with PNA-biotin and streptavidin-DyLight 594 (Jackson ImmunoResearch). TUNEL staining was performed after PNA surface staining using an *in situ* cell death detection kit (Roche) following manufacturer's recommendations. Fluorescence images were obtained using a microscope (Axiovert 200 Carl Zeiss, Inc.) equipped with a 40x objective and multi-bandpass dichroic and emission filter sets

(model 83000; Chroma Technology Corp.) set up in a wheel to prevent optical shift. Images were captured with the AxioVision software (Carl Zeiss, Inc.) and a camera (Orca-ER; Hamamatsu Photonics). Formalin fixed spleens were embedded in paraffin and sections stained with PNA-biotin. Immunohistochemistry images were obtained using a microscope (Axiovert 40 CFL Carl Zeiss, Inc.) equipped with a 2.5x objective. Images were captured with QCapture Pro 7 software (QImaging) and a camera (QImaging QI Click).

Cell Culture and viral infection

Mouse embryonic fibroblasts (MEFs) were isolated from E13.5 embryos and cultured as described(144). MEFs were infected with Adeno-Cre-GFP virus (University of Iowa) with a multiplicity of infection of 100. Four days later, cells were harvested for flow cytometry and Western blotting. SU-DHL-6 cells infected with lentiviral shRNA targeting YY1 (V2LHS_219592, V2LHS_389741) and a non-silencing shRNA control (RHS4346) were described previously(135).

Western blots

Whole cell lysates were isolated using RIPA buffer (50 mM Tris–HCl pH 7.5, 150 mM NaCl, 1% Triton X-100, 0.1% SDS, 0.5% deoxycholic acid and 0.02% sodium azide) plus fresh protease inhibitor complete (Roche). Lysates

were run on SDS–PAGE Criterion X-gel (Bio-Rad) and transferred to nitrocellulose membranes (GE Osmonics). Membranes were probed with antibodies against YY1 (H414) and β-actin (Santa Cruz Biotechnology). Membranes were visualized using Western lightening chemiluminescence detection (PerkinElmer) and ChemiDoc MP System with Image lab software (Bio-Rad).

Statistical Analysis

Data were presented as mean ± standard deviation. Two-tailed and unpaired Student's *t*-test was used for pairwise comparisons with $P<0.05$ considered statistically significant.

CHAPTER IV: SMURF2 does not regulate the GC reaction

The important role of YY1 in the GC led to the investigation of factors upstream of YY1 in the regulation of the GC. SMURF2 has been shown to mediate the ubiquitination and degradation of YY1(135, 136). SMURF2 is also a tumor suppressor in B cell lymphoma and has been implicated as prognostically significant in human DLBCL(135, 138). For these reasons I tested the hypothesis that *Smurf2* regulates a normal GC reaction by suppressing the GC response.

Results

Smurf2-deficent mice mount a normal GC response

Previous studies have shown that *Smurf2*-deficient mice have a small increase in splenic B cells and an increase in proliferation both *in vivo* and in response to LPS stimulation *in vitro*(135). Given the established role of *Smurf2* as a tumor suppressor in B cell lymphoma and the connection between the GC and lymphoma, I investigated whether *Smurf2* regulates the GC reaction. I hypothesized that *Smurf2* could act as a negative regulator of the GC, suppressing the GC to maintain a tightly controlled response. Utilizing the previously described(144) *Smurf2*-deficient (hereafter referred to as $Smurf2^{T/T}$) mice, I investigated the effect of decreased *Smurf2* levels on the GC reaction. I injected $Smurf2^{T/T}$ and wild type mice with sRBC to induce GC and examined the response by flow cytometry 6, 10, or 21 days later. Day

6 provides information about the state of the early establishment of the reaction, day 10 represents the peak of the reaction, and day 21 is the point when the reaction has greatly diminished but is still detectable. Day 21 would provide a point at which to examine if *Smurf2* loss affects the persistence of the reaction. Figure 4.1 shows that loss of *Smurf2* does not have an effect on the frequency or number of GC B cells at any of the three assayed time points.

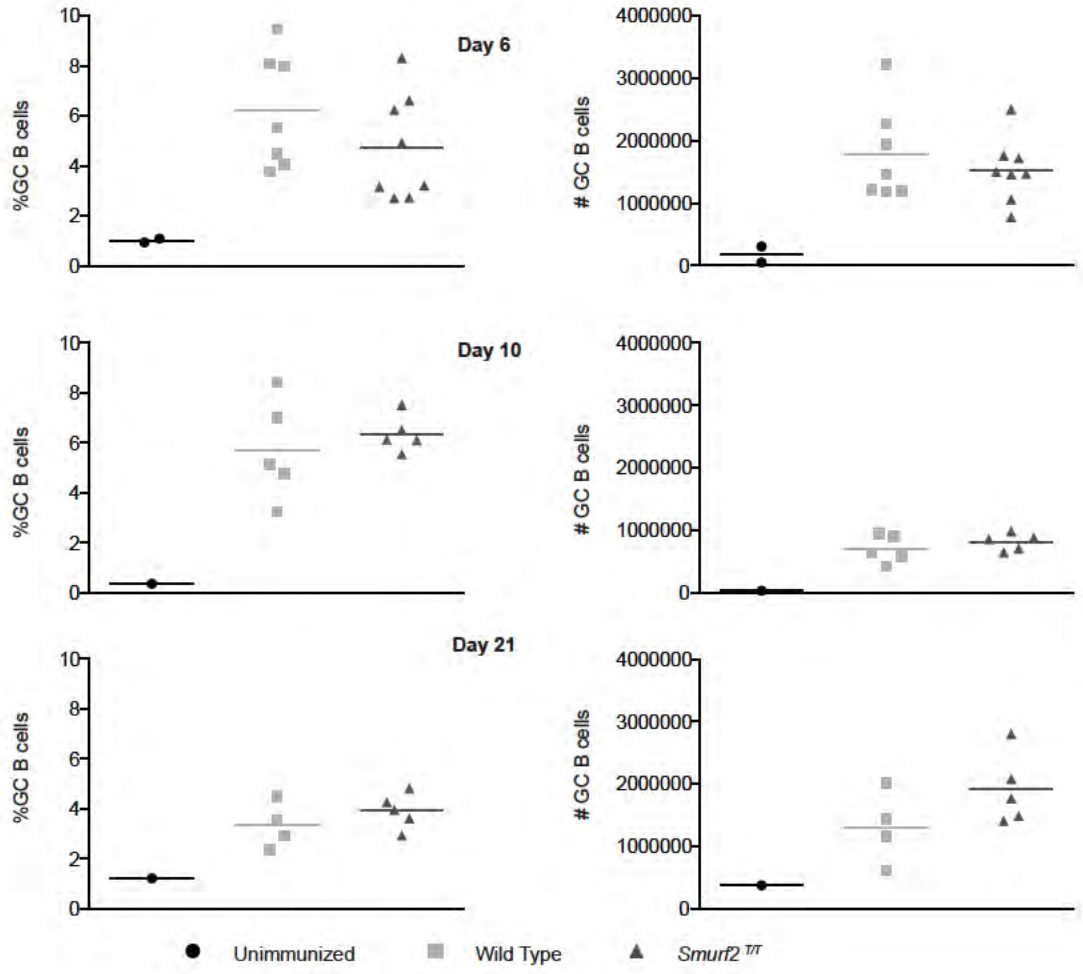

FIGURE 4.1

***Smurf2* is dispensable for normal dark zone and light zone establishment**

Given that recent studies(47, 48) have provided evidence that the DZ and LZ can be perturbed in GCs that otherwise appear normal in frequency and cell number, I was interested in determining if *Smurf2* has a role in the DZ and LZ. First, utilizing the dataset published by Sander and colleagues(48), I determined *Smurf2* mRNA levels are the same between DZ and LZ cells (Figure 4.2A). However, given that SMURF2 can be regulated at a post-translational level, I examined the DZ and LZ response in $Smurf2^{T/T}$ mice. I found no alteration in the DZ or LZ response at 6 days post-sRBC injection (Figure 4.2B). This suggests that decreased SMURF2 does not affect the cellularity or polarity of the GC reaction.

FIGURE 4.1 *(Previous page)* Smurf2-deficiency does not alter the GC reaction. (**A**) Percent of GC B cells ($B220^{+}CD95^{+}GL7^{+}$) at day 6 (left), day 10 (middle), and day 21 (right) post sRBC immunization. (**B**) Total number of GC B cells in spleens of mice at day 6 (left), day 10 (middle), and day 21 (right) post sRBC immunization. Each point represents data from a single mouse. Horizontal bar indicates mean of data. Day 6 represents data from two independent experiments; day 10 and day 21 each represent a single independent experiment.

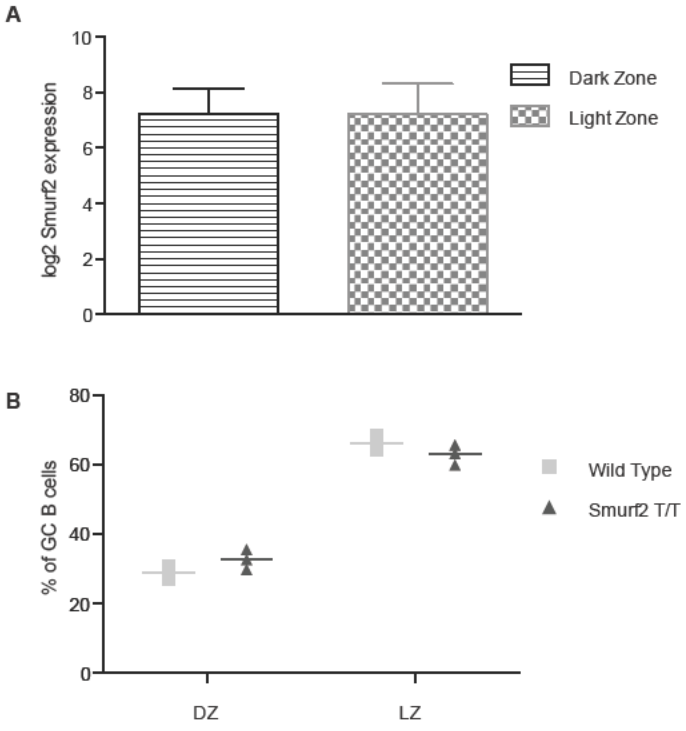

FIGURE 4.2 Smurf2-deficency does not alter the DZ or LZ. (**A**) Log_2 expression of Smurf2 from microarray dataset from Sander and colleagues (cite Sander 2015). (**B**) Percent of DZ and LZ cells in GC B cells in *Smurf2*$^{T/T}$ mice at day 6 post sRBC immunization compared to wild type mice. Each point represents data from a single mouse. Horizontal bar indicates mean of data.

FIGURE 4.2

Smurf2 loss does not affect mutation frequency

I have shown that loss of *Smurf2* does not affect the DZ and LZ distribution, nor does it alter the frequency or cell number of the GC. This led me to investigate the possibility that SMURF2 may function as a tumor suppressor by altering the mutation frequency in GC B cells. I sorted GC B cells from mice via FACS 10 days after sRBC injection in order to PCR amplify and sequence the JH4 3' intron region to determine the number of mutations. I chose this region because as part of the *Ig* locus it is targeted by AID, but as an intron there is no selective pressure on the area, which could alter the mutation profile. I found there was no difference between the

frequency of mutations in cells isolated from wild type (0.0065 mutations/base pair) mice compared with the frequency of mutations in cells isolated from *Smurf2*$^{T/T}$ (0.0061 mutations/base pair) mice (Figure 4.3). Additionally the number of unique clones with a given number of mutations had little variation, with the number of mutations per clone ranging from 1-8 and the most frequent number of mutations being one regardless of genotype (Figure 4.3).

FIGURE 4.3 Somatic hypermutation in JH4 intron is not altered by the loss of Smurf2. Mutation of JH4 introns cloned from GC B cells from wild type (left) or *Smurf2*$^{T/T}$ mice on day 10 after sRBC immunization. The center of each graph is the number of unique clones with nucleotide mutations in JH4 (those with 0 mutations were not included). Total number of nucleotides sequenced for Wild Type is 14760 nucleotides, for Smurf2 T/T is 14268 nucleotides. Circle segment size is proportional to the number of sequences with mutations indicated in the legend. Below each graph is the overall mutation frequency for each genotype in mutations/base pair.

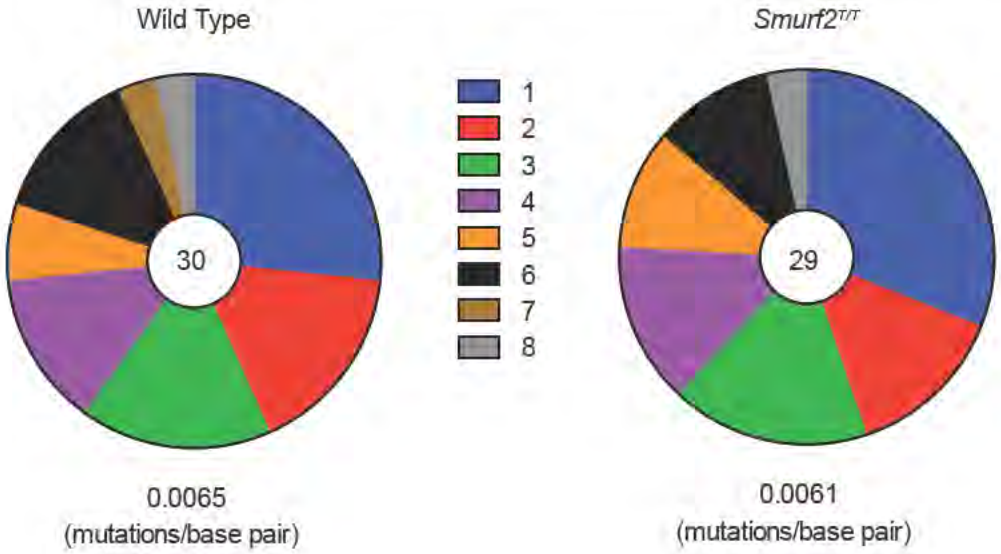

FIGURE 4.3

Increased SMURF2 expression does not affect the GC or YY1 levels

Given that the results of the studies using the *Smurf2*$^{T/T}$ mice indicate that *Smurf2* is not necessary to suppress the GC reaction, I investigated whether *Smurf2* is sufficient to suppress the GC reaction. To achieve this goal I utilized a mouse model in which *Smurf2* cDNA is inserted downstream of a lox-stop-lox site in the Rosa26 locus. This construct results in ubiquitous *Smurf2* expression in addition to endogenous levels when cre-recombinase mediates the recombination and deletion of the stop cassette. I crossed this mouse to a *CD19-Cre* mouse (hereafter referred to as *Smurf2*^{CKI}) in which cre-recombinase is inserted to replace the first exon of CD19, preventing CD19 expression from that allele and instead expressing cre in cells which normally express CD19. CD19 is normally expressed in B cells starting from early B cell development. This results in ubiquitous expression of *Smurf2* in B cells. I find that SMURF2 protein levels are increased 16.5 fold in CD19^{+} isolated splenocytes from *Smurf2*^{CKI} over CD19^{+} isolated splenocytes from *CD19-Cre* control mice (Figure 4.4A). However, despite this dramatic increase in SMURF2 protein, I found no change in levels of YY1 protein (Figure 4.4A). This suggests that SMURF2 levels are likely not the limiting factor in mediating YY1 degradation.

Utilizing these mice with high SMURF2 levels in the B cells, I investigated the peak of the GC response at day 10 post-sRBC immunization. I found no alteration in frequency or number of GC B cells (Figure 4.4B),

indicating that enforced SMURF2 expression is not sufficient to suppress the GC reaction. Overall I can conclude from these data that SMURF2 does not regulate the GC reaction, suggesting perturbation of GC dynamics does not underlie the development of B cell lymphoma in *Smurf2*$^{T/T}$ mice.

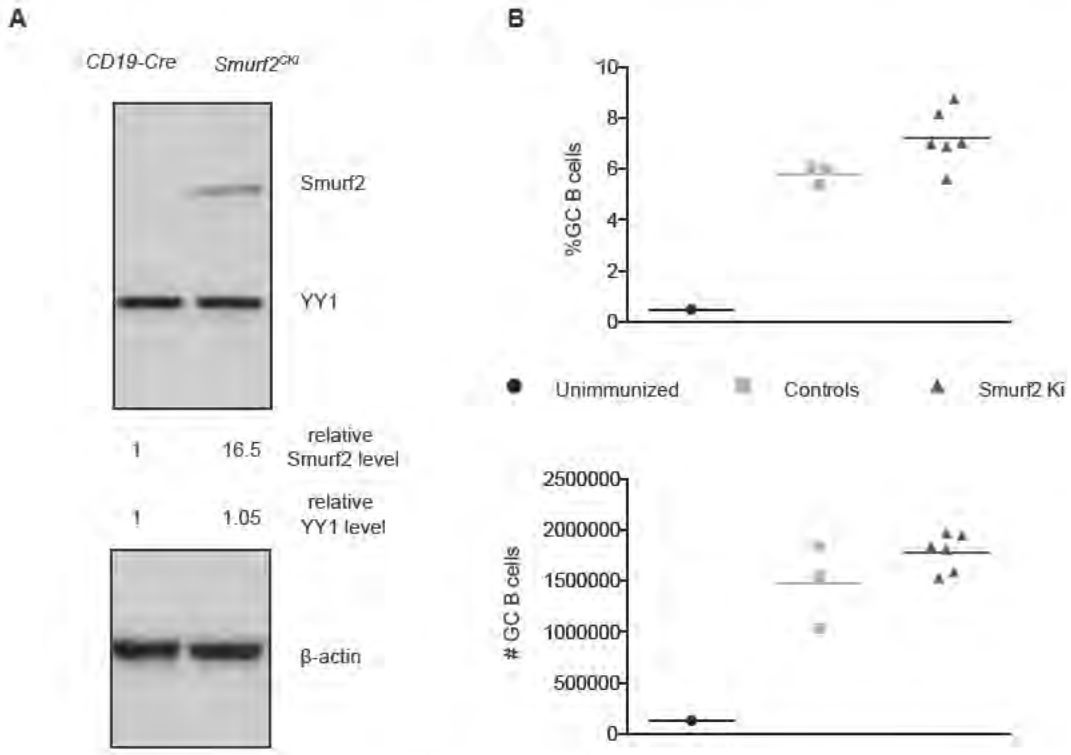

FIGURE 4.4

FIGURE 4.4 *(Previous page)* Exogenous expression of *Smurf2* is sufficient to increase protein level but does not affect the GC. (**A**) Smurf2 and YY1 protein levels determined by western blotting in $CD19^{+}$ isolated B cells from *CD19-Cre* controls and $Smurf2^{CKI}$ mice. The relative levels of Smurf2 and YY1 protein are quantified using β-actin as a loading control. (**B**) percent (left) and number (right) of GC B cells ($B220^{+}CD95^{+}GL7^{+}$) at day 10 post sRBC immunization. Controls include wild type and $Smurf2^{Ki}$ (no cre) mice. Each point represents data from a single mouse. Horizontal bar indicates mean of data.

Materials and Methods

Mouse strains

Mouse strains *CD19-Cre* (B6.129P2(C)-$Cd19^{tm1(cre)Cgn}$/J) and C57BL/6 wild-type were obtained from Jackson laboratories. $Smurf2^{T/T}$ mice were described previously(144). $Smurf2^{KI}$ mice were established utilizing a targeting vector, which included the ROSA26 genomic sequence with a floxed PGK-neo just 5' of *Smurf2* cDNA followed by an internal ribosomal entry site (IRES) and mCherry with a poly-A tail. This provides for ubiquitous expression of *Smurf2* cDNA from the ROSA26 locus after cre-mediate deletion of the PGK-neo cassette. Mouse studies were approved by the Institutional Animal Care and Use Committee of University of Massachusetts Medical School.

Immunization

Sheep red blood cells (1.5×10^9) (Cocalico Biologicals) were injected intraperitoneally into 8 to 10-week old mice of both sexes. At various days after immunization, spleens were collected for FACS staining.

Flow Cytometry

Mouse spleens were prepared into single cell suspension and red blood cells were lysed in cold distilled water. After filtering through 70-μm nylon mesh and counting using a MACSQuant analyzer (Miltenyi Biotec), cells were incubated with anti-CD16/32 antibody (BioXCell) to block Fc receptors. Cells were then stained for 20 min in staining media (Hank's balanced salt solution, 3% FBS, 0.02% sodium azide, 1 mM EDTA) with primary antibodies, including B220-FITC (clone RA3-6B2), GL7-eFluor 660 (clone GL7), CD95-PE (clone 15A7) (eBioscience), CD86-Pe-Cy7 (clone GL-1; BioLegend) or CD184-biotin (2b11/CXCR4; BD Bioscience). Cells stained with biotin-labeled antibodies were incubated with streptavidin-eFluor 450 (eBioscience). Flow cytometry analysis was performed on an LSRII FACS or a FACSAria cell sorter (BD Bioscience), and analyzed using FlowJo software (FlowJo).

Western blots

Whole cell lysates were isolated using RIPA buffer (50 mM Tris–HCl pH 7.5, 150 mM NaCl, 1% Triton X-100, 0.1% SDS, 0.5% deoxycholic acid and 0.02% sodium azide) plus fresh protease inhibitor complete (Roche). Lysates were run on SDS–PAGE Criterion X-gel (Bio-Rad) and transferred to

nitrocellulose membranes (GE Osmonics). Membranes were probed with antibodies against SMURF2 (EP629Y3) (Abcam), YY1 (H414) and β-ACTIN (Santa Cruz Biotechnology). Membranes were visualized using Western lightening chemiluminescence detection (PerkinElmer) and ChemiDoc MP System with Image lab software (Bio-Rad).

Magnetic bead isolation of $CD19^+$ cells

Cells were processed to single cell suspension and red blood cells were lysed as described above. Cells were incubated with anti-CD16/32 antibody to block Fc receptor as above. Cells were incubated with anti-CD19-Biotin antibody (ebioscience) and anti-biotin MACS microbeads following manufacturer's recommendations (Militenyi Biotec). Samples were then run on autoMACS Pro Separator (Militenyi Biotec) to achieve separation of $CD19^+$ containing fraction. These cells were washed with PBS and processed as above to isolate whole cell lysate.

Gene Expression Analysis

Utilizing the publically available dataset GSE68043(48) the values for *Smurf2* probes (1429045_at, 1429046_at, 1454894_at) for all three control DZ and three control LZ samples were obtained. These values represent $\log_2$ transformed intensity values from Affymetrix Mouse Genome 430 2.0 Array platform. The values for all *Smurf2* probes were averaged across all three DZ or LZ samples and mean with standard deviation was plotted.

SHM analysis

GC B cells ($B220^+$, $GL7^+$, $CD95^+$) were FACS sorted on day 10 post-sRBC immunization. From these sorted cells DNA was isolated by incubating in 100 µl STE (0.1M NaCl, 20mM Tris pH 8.0, 1mM EDTA) with 100 µg proteinase K and SDS (2.5 µl of 20%) for 2 hours at 55°C. Samples were then cooled to room temperature and 100 µM sodium acetate at pH 5.2 and 95% ethanol was added. After incubating overnight at -20°C, DNA was pelleted and supernatant replaced with 70% ethanol. The precipitated DNA was then pelleted again and resuspended in water. PCR was performed using hotstart Phusion DNA polymerase (New England BioLabs Inc.) and the following primers: JH4-Fwd: 5'-AGC CTG ACA TCT GAG GAC-3'; JH4-Rev: 5'-GTG TTC CTT TGA AAG CTG GAC-3'(172). The resulting DNA was separated on a 1% agarose gel and the ~600BP band was visualized using crystal violet staining and excised. The DNA was purified using Qiagen gel extraction kit. To facilitate quick cloning dA overhangs were added using taq polymerase. The resulting DNA was cloned using TOPO TA-cloning kit (ThermoFisher Scientific) following manufacturer recommendations. The resulting cloned DNA was transformed into XL-10 competent cells and colony sequencing was performed (Macrogen USA). Resulting sequences were aligned using ClustalW. Sequences were included in further analysis only if they were unique clones and if they contained at least one mutation. Python 2.7.8 was

used to compare aligned sequences to consensus sequence and determine the number and type of mutations for each clone.

CHAPTER V: Discussion

Inhibition of bromodomain proteins is effective for the treatment of human diffuse large B cell lymphoma

In chapter II of this thesis, I demonstrated that targeting BRD proteins by JQ1 in human DLBCL cells resulted in cell death or cell senescence. Sensitivity to JQ1 treatment was found in various molecular subtypes of DLBCL (ABC or GCB) and with various status of the *C-MYC* or *BCL2* locus (translocated, amplified or unchanged), suggesting that JQ1 has a broad effect in DLBCL. This broad effect is especially encouraging for the potential clinical utility of JQ1 for the treatment of DLBCL. Recent studies have found anti-proliferative and pro-apoptotic effects of JQ1, particularly in hematopoietic malignancies, and these effects of JQ1 are primarily mediated through inhibition of *C-MYC*(100–102, 104, 105, 107, 109, 153, 154). Consistent with these findings, I showed that JQ1-mediated suppression of *C-MYC* expression, regardless of whether it is from an un-perturbed *C-MYC* loci (HLY-1, OCI-Ly10, RC-K8, and SU-DHL-5), or from a chromosomally-translocated (HBL-1, OCI-Ly8, OCI-Ly18, SU-DHL-6, and SU-DHL-10), or amplified (OCI-Ly3 and SU-DHL-4) loci. Collectively, my studies suggest that inhibition of C-MYC via BET bromodomain family proteins by JQ1 provides a promising therapeutic model for patients with DLBCL.

Previously it had been shown that cancer cells respond to JQ1 primarily with rapid cell cycle arrest and apoptosis(100–102, 104, 107, 109,

173). These studies demonstrate increased apoptotic markers within 2-3 days of JQ1 treatment. I found two distinct phenotypes in response to JQ1: senescence or apoptosis. OCI-Ly8 cells displayed G1 arrest and positive staining for SA-β-gal without increases in sub-G1 population and apoptosis following JQ1 treatment, indicating that senescence is the main response to JQ1 in OCI-Ly8 cells. SU-DHL-4 and SU-DHL-10 cells showed little or no positive SA-β-gal staining but increased sub-G1 population and apoptosis, indicating that apoptosis is the prominent response to JQ1 in these two cell lines. Both apoptosis and senescence were observed in OCI-Ly3 cells. The apoptosis versus senescence phenotype did not correlate with the parameters that I examined, including molecular subtype (ABC: OCI-Ly3 vs. GCB: OCI-Ly8, SU-DHL-4 and SU-DHL-10), p53 mutation status (wild type: OCI-Ly3 vs. mutated: OCI-Ly8), *C-MYC* translocation and expression level (unperturbed: SU-DHL-4; amplified: OCI-Ly3; translocated: SU-DHL-10 and OCI-Ly8), *BCL2* translocation status (translocated: SU-DHL-4, SU-DHL-10(160) and OCI-Ly8(159); amplified: OCI-Ly3(159)), or expression of p16, p21, p53, Rb or BCL-XL.

In this study I utilized doxorubicin as a positive control for induction of apoptosis in these cell lines. As doxorubicin is a component of R-CHOP therapy it is interesting to consider if JQ1, by comparison, truly could provide additional therapeutic advantages. It is difficult to directly compare the two therapies *in vitro* with their potential efficacies *in vivo*. The effective dose of

doxorubicin in cell culture is likely much higher than could be realistically achieved in patients given the high toxicities associated with chemotherapeutic agents such as doxorubicin. Unfortunately, the NSG mouse model utilized in this study is not amenable to studies of doxorubicin *in vivo* compared with JQ1. NSG mice are not able to tolerate doxorubicin, making direct comparisons between the two drugs *in vivo* in this mouse model not feasible. This suggests there is potential value to JQ1 in treatment of DLBCL, especially given its lack of apparent adverse effects. As discussed below, combination therapies with JQ1 and doxorubicin appear to be promising, further solidifying the potential value of continued studies of JQ1 in DLBCL.

A recent study revealed highly asymmetric loading of BRD4 at super-enhancers in DLBCL cells. These super-enhancers and genes that they regulate are particularly sensitive to JQ1 inhibition, explaining the selective effect of JQ1 on oncogenic and lineage-specific transcriptional circuits(110). It will be interesting to understand how this selectivity of BRD4 loading at super-enhancers and inhibition by JQ1 are responsible for the different responses (apoptosis vs. senescence) to JQ1 in DLBCL cells.

I showed that JQ1 significantly suppresses growth of DLBCL cells engrafted in NSG mice and improves survival of tumor-bearing mice, demonstrating a potential use of JQ1 in treatment of DLBCL. I found that JQ1 alone with single daily dosing of 50mg/kg for 21 days was not sufficient to

cure the disease. The differences in JQ1 effectiveness observed between *in vitro* and *in vivo* studies could be due to a number of issues, one of which is bioavailability *in vivo*. The half-life of JQ1 in plasma is relatively low: 0.9 hours (intravenous injection of 5 mg/kg) or 1.4 hours (oral administration of 10 mg/kg(100)). When dosed every 24 hours, it is likely that very little JQ1 remains after 8 hours. Although it has not been previously measured, the effective concentration of JQ1 at the site of tumors is likely even lower than in the plasma, because the typically poor vasculature in tumor tissues could prevent JQ1 from being effectively delivered to the tumor cells. A recent study using 2 daily doses of JQ1 treatment for 30 days (vs. 1 daily dose for 21 days in our study) shows a median survival advantage of 9 days(110) compared to 4 days in our study, suggesting that more frequent dosing to maintain plasma concentration of JQ1 over time may increase its effectiveness *in vivo*, especially given that no adverse effects have been reported for JQ1 use in mouse models. Additional modifications to the structure of JQ1 that maintain its specificity while increasing the half-life will make JQ1 more effective *in vivo* and in clinical use.

It is possible to combine JQ1 with the current standard therapy to increase the efficacy of treatment. A recent study by Emadali and colleagues showed that the addition of JQ1 to Rituximab increases sensitivity of Rituximab-resistant DLBCL cell lines(154). This study provides proof-of-principal that adding JQ1 to current treatments may be beneficial to patients

with DLBCL. Another study has demonstrated the value of JQ1 in combination with other novel therapies for DLBCL. Zhao and colleagues showed that treating DLBCL cell lines with EZH2-inhibitor DZNep and JQ1 reduces cell viability in a synergistic manner(153) . I propose that JQ1 should be examined clinically in patients with DLBCL. I speculate that the addition of JQ1 as a component of salvage therapy or even potentially added to R-CHOP therapy, may result in the effective treatment of DLBCL. Continued examination of JQ1 alone and in combination with other novel therapeutic agents is warranted.

Recent advances in BET inhibition

In the past few years, advancements have been made which have built upon the work published from Chapter II of this thesis. The major areas these advancements have focused on include mechanisms of potential resistance and combination treatments. Xu and colleagues have shown that the apoptosis induced by JQ1 or other BET family inhibitors requires the repression of the miR 17-92 family which in turn drives Bim expression, leading to apoptosis; Bim is required for apoptosis in this context. The authors suggest that overexpression of BCL2, a potent anti-apoptotic factor, or inactivation of Bim may be a potential mechanism for resistance to apoptosis induced by JQ1-like molecules(174). Although in the study described in Chapter II I did not investigate the protein levels of BCL2, my results may be in contrast to the suggested resistance to apoptosis when BCL2 is

overexpressed. Of the cell lines selected for advanced study, three (Oci-Ly8, SU-DHL-4, and SU-DHL-10) have documented BCL2 translocations(159, 160), while the fourth (Oci-Ly3) has a documented amplification of BCL2(159). While all four of these cell lines likely have overexpression of BCL2 given the cytogenetic abnormalities, two (Oci-Ly3 and Oci-Ly8) respond to JQ1 treatment by preferentially senescing with only low levels of apoptosis, while the remaining two (SU-DHL-4 and SU-DHL-10) have high levels of apoptosis. If the hypothesis that BCL2 overexpression prevents JQ1-induced apoptosis is correct, these cells must have low BCL2 levels, despite the documented BCL2 translocations.

Ceribelli and colleagues focused on the role of BET inhibitors in ABC subtype DLBCL. They showed that the combination of BET inhibition with ibrutinib, a BTK inhibitor, results in the synergistic killing of ABC DLBCL both *in vitro* and in mouse xenografts(175). Cinar and colleagues focused on combination treatments in the difficult to treat double or triple-hit lymphoma. Double and triple-hit lymphomas have translocations of *C-MYC*, *BCL2*, and/or *BCL6* (two events for double-hit, all three for triple-hit) and are considered aggressive and have a poor prognosis. Cinar and colleagues showed that the combination of BCL2 inhibition and C-MYC inhibition (with BET inhibitors) suppressed growth in double and triple-hit lymphomas better than single treatments alone. They additionally showed that combination therapy with vincristine or doxorubicin (components of the standard of care, R-CHOP) and

BET inhibition or BCL2 inhibition was additive(176). The synergistic effect of BCL2 and C-MYC inhibition in double-hit lymphoma was independently confirmed(177). These recent studies have provided advancements on the work presented in Chapter II, and underscore the important nature of that work.

YY1 regulates the GC reaction by inhibiting apoptosis and maintaining DZ

As described in Chapter III of this thesis, I selectively deleted *YY1* in GC B cells using *AID-Cre* and found that loss of *YY1* significantly impaired the GC reaction as indicated by decreased frequency and number of GC B cells in spleen in response to sRBC immunization. The decrease in GC B cells was observed as early as day 4 post-sRBC immunization and exacerbated throughout the GC reaction (Figures 3.5 and 3.6). Previously, YY1 has been implicated as a regulator of the GC reaction based on the enrichment of YY1 target genes in the GC B cell-specific transcriptional signature(51). A study published after the completion of this experimental work provided evidence that deletion of YY1 results in a dramatic reduction in GC B cells(127). Now our studies provide additional experimental evidence indicating that YY1 is required for a normal robust GC reaction. Because the *AID-Cre* allele that was used is activated in GCs around day 4 after antigen encounter (Figure 3.3), I cannot completely rule out the possibility that

deleting *YY1* in naïve mature B cells before antigen encounter will affect the commitment of these cells to become GC B cells. However, our finding that ~70% of the remaining GC B cells in *YY1*^{CKO} mice at day 4 or day 10 after immunization had both *YY1* alleles deleted (Table 3.1) suggests that YY1 is not necessarily required for the initiation of the GC reaction, but rather is required to maintain a robust GC reaction.

To understand the defects in the GC reaction in the absence of YY1, I investigated whether loss of *YY1* affected proliferation of GC B cells, as YY1 has been shown to regulate proliferation in MEFs or HeLa cells(115). GC B cells in *YY1*^{CKO} mice showed a significant decrease in BrdU incorporation compared to GC B cells in control mice (Figure 3.10A). However, Ki-67 and DAPI staining indicated there was no significant difference in cell cycle distribution in GC B cells between *YY1*^{CKO} and control mice (Figure 3.10B and 3.10C), suggesting that YY1 does not directly affect proliferation of GC B cells. This finding is consistent with a previous report that ablation of *YY1* in splenic B cells activated by lipopolysaccharide *ex vivo* does not alter cell division and proliferation(112). I further found that loss of *YY1* resulted in a decrease of DZ cells and a concomitant increase in LZ cells (Figure 3.7). In DZ, GC B cells undergo rapid cell proliferation(50, 80, 169). I found that there was no significant difference in BrdU incorporation in DZ or LZ cells between *YY1*^{CKO} mice and control mice. These results argue that YY1 does not directly affect proliferation of GC B cells, but rather the altered distribution of DZ and

LZ cells is responsible for the decreased BrdU incorporation in GC B cells of *YY1*^{CKO} mice.

My finding that YY1 regulates the relative distribution of DZ and LZ in GCs is intriguing, as not much is known about how GC polarity is regulated. A large body of work supports a model in which GC B cells transit between DZ and LZ to undergo SHM in DZ and affinity selection as well as CSR in LZ(33, 80). It has been shown that DZ cells express high levels of CXCR4 and CXCR4 deficiency leads to an absence of DZ without altering the size and number of GCs(178, 179). More recently, two groups independently found that FOXO1 and phosphoinositide-3 kinase (PI3K) play a critical role in GC polarity(47, 48). FOXO1 is highly expressed in DZ, and its activity is down regulated in LZ. Deletion of *FOXO1* or activation of PI3K results in a loss of DZ with LZ-only GCs, partly due to down-regulation of CXCR4(47, 48). In addition, a small number of LZ cells were found to express FOXO1 and C-MYC(48). C-MYC is required to initiate the GC reaction and the re-entry of LZ cells into DZ for additional rounds of SHM(94, 95). FOXO1 is likely involved in both regulation of targets necessary for the formation of DZ and the cyclic re-entry of LZ cells into DZ. The latter function is possibly through up-regulation of *c-Myc*. YY1 has been found to transactivate *c-Myc*(119, 120) in splenic B cells(135). It is plausible that YY1-mediated transactivation of *c-Myc* plays a similar role in the re-entry of LZ cells into the DZ. Loss of *YY1* would impair the re-entry of LZ cells, leading to decreased DZ cells in *YY1*^{CKO} mice.

At day 10 post-immunization, the frequency and number of GC B cells in *YY1*^{CKO} mice continued to decrease by 3-fold compared to day 6, while control mice had largely maintained their GC B cells (Figure 3.5C). Apoptosis was increased in GC B cells in the absence of *YY1* (Figure 3.11), providing a plausible mechanism for the reduction of GC B cells in *YY1*^{CKO} mice. The GC-specific transcriptional profile is enriched for genes involved in cell death(51). In particular, the BCL2 family anti-apoptotic protein MCL1, which is upregulated in GC B cells, is a potential transactivation target of YY1(51). MCL1 has been shown to be the pro-survival factor in GCs. It is required for survival of GC B cells and essential for GC formation(63). It will be interesting to investigate whether *Mcl1* is the critical downstream target through which YY1 regulates the survival of GC B cells.

The GC reaction is not only critical in order to produce high-affinity antibodies for a robust adaptive immune response, but it also can lead to pathogenesis of B-cell lymphoma. Because of their high proliferation rate and highly mutagenic processes, GC B cells are susceptible targets of B-cell malignancies. Most non-Hodgkin's lymphomas are derived from GC B cells or B cells that have passed through GCs(80, 84–87). My finding that dysregulation of YY1 leads to an impaired GC reaction suggests a potential oncogenic role for YY1 in lymphomagenesis. Consistent with this notion, the expression of YY1 is increased significantly in human DLBCL, Burkitt's lymphoma, and follicular lymphoma compared to reactive lymph nodes or

normal B cells(129–131). Further, high levels of YY1 expression correlate with a worse survival prognosis in human DLBCL and follicular lymphoma patients(130, 131).

SMURF2 does not regulate the GC

In Chapter IV of this thesis, I demonstrated that SMURF2 does not have a clear role in the GC. I showed that *Smurf2*-deficiency does not alter the number or frequency of the GC regardless of when during the reaction I examined (day 6, 10, or 21). I also showed that the DZ and LZ populations are not perturbed by the loss of *Smurf2*. I had hypothesized that decreased *Smurf2* would result in an increase in the GC number and frequency or extend the persistence of the reaction. Any of these phenotypes would suggest SMURF2 has a role in suppressing the GC. Additionally, an increase in GC B cells or an extension of the persistence of the reaction would provide a logical mechanism for the increased incidence of B cell lymphoma observed in these mice. Given that I did not observe any alteration in the GC reaction in the *Smurf2*$^{T/T}$ mice, I must accept that these hypotheses are not correct.

In trying to understand the underlying mechanism that renders *Smurf2* a tumor suppressor, I tested the hypothesis that loss of *Smurf2* would increase the SHM frequency. An increased SHM frequency would likely correlate with increased non-*Ig*, “off-target” mutation frequency. This would provide a logical mechanism for the increased likelihood of cancer in

Smurf2$^{T/T}$ mice. Although this provides an attractive, logical hypothesis, unfortunately the data suggest that decreased *Smurf2* does not alter SHM.

Based on the data gathered from *Smurf2*$^{T/T}$ mice, it appears that *Smurf2* loss-induced lymphoma is not caused by an underlying increase in the GC, increase in SHM, alteration in the DZ and LZ polarity of the GC, or a more persistent GC reaction (as indicated by day 21 post-immunization). This leaves an open question as to the underlying mechanism that renders SMURF2 a tumor suppressor. One possibility proposed in the past is that the decrease in senescence in *Smurf2*$^{T/T}$ mice may be sufficient to render these mice more vulnerable to tumorigenesis. Previous work has shown a decrease in senescent cells in the spleens of *Smurf2*$^{T/T}$ mice as well as an increased likelihood for MEFs from these mice to become immortalized(144). A decrease in senescence may allow cells with DNA damage or other issues that would normally cause them to become post-mitotic and senescent to instead continue to proliferate and accumulate additional mutations. Another likely mechanism underlying the increased tumorigenesis in *Smurf2*$^{T/T}$ mice is that there is simply an increase in proliferation of B cells in these mice(135). Increased proliferation is a hallmark of cancer(180) and is often an initiating step in tumorigenesis, which provides an increase in potential target cells for additional mutations. In addition to the evidence that B cells are more proliferative in *Smurf2*$^{T/T}$ mice, it has also been shown that as these mice age the hematopoietic stem cells are more proliferative and do not display the

skewing away from the lymphoid lineages that is normally seen in aged mice(145). This may suggest that as these mice age, there are more B cells, providing more potential target cells for mutations and subsequent transformation. Finally, Blank and colleagues suggest that SMURF2 acts as a tumor suppressor by regulating genomic stability through its regulation of RNF20(138). Although the studies presented in this thesis serve to rule out some possible hypotheses for the tumor suppressive role for SMURF2, I cannot distinguish between the other possibilities presented here or others that have not been considered.

In Chapter III of this thesis I showed that loss of YY1 disrupts the GC and leads to greatly diminished frequency and number of GC B cells. I investigated whether SMURF2 could be an important upstream regulator of YY1 in this context. In order to test the hypothesis that increased SMURF2 would decrease YY1 and mimic the phenotypes observed in Chapter III I utilized the *Smurf2*^{CKI} mice. I first showed that the 16-fold increase in SMURF2 protein in these mice is not sufficient to alter the YY1 protein levels. It is currently unclear why this is the case, but it is possible that SMURF2 is not the limiting factor in the ubiquitination and degradation of YY1, therefore simply increasing SMURF2 may not alter its ability to degrade YY1. Although previous work in our lab has shown that YY1 is increased in the spleens of *Smurf2*$^{T/T}$ mice(135), it is possible that YY1 is not regulated by SMURF2 in the CD19^{+} B cells that I investigated in Figure 4.4. It is also possible that

although a decrease in SMURF2 protein increases YY1, that the subsequent increase in SMURF2 may not have the reciprocal effect. Previous work has shown that increased expression of *SMURF2* in a human DLBCL cell line does decrease YY1 protein level by about 50%(135). SMURF2 has an autoinhibitory function, mediated by the interaction between the C2 and HECT domains, which leads to inhibition of activity but stabilization of SMURF2 protein(181). This could be the reason I observe very high levels of SMURF2 protein but no apparent indication of increased SMURF2 activity. This conclusion would be strengthened by investigation of protein levels of additional SMURF2 targets. Given the possibility that this increased SMURF2 may still be functioning, and simply not targeting YY1, I investigated the frequency and number of GC B cells in these mice 10 days after sRBC immunization. I found no alteration in the GC in these mice, suggesting that either increased SMURF2 expression does not increase the SMURF2 activity in the cell, or that increased SMURF2 does not affect the GC. This highlights the need for an easy and effective assay to determine SMURF2 activity within the cell.

SMURF2-YY1-C-MYC as a pathway in lymphoma

Throughout this thesis I have demonstrated supporting evidence that the SMURF2-YY1-C-MYC axis is important to the development of lymphoma. In Chapter III I showed that YY1 has an essential role in maintaining the

normal GC reaction. Given the established link between the GC and DLBCL development, this result has implications for therapeutics. Understanding the underlying basic biological processes that occur in cells that go on to develop cancer can provide insight into new avenues for treatment and prevention. In this case, the essential nature of YY1 in the GC and the fact that it is often highly expressed in DLBCL, suggests a link worth exploring in the context of lymphoma. It seems possible that inhibition of YY1 may be effective in the context of cancer, especially given our result that YY1 appears to decrease apoptosis in GC B cells. When pursing this hypothesis investigators should also consider the potential detrimental effects loss of YY1 may have on the adaptive immune system, particularly in the context of older patients or those who may be experiencing other treatments that make them at increased susceptibility to infection. Although no YY1-specific inhibitors have been developed, evidence suggests that the anti-CD20 antibody, rituximab, which is part of R-CHOP standard of care, acts partially by inhibiting YY1(182).

Another way to utilize the data presented in Chapter III to suggest therapeutically relevant targets would be to consider possible downstream effectors of YY1. In particular, I demonstrated that YY1 promotes survival in GC B cells, suggesting YY1 could play a similar role in lymphoma. I suggest that YY1 may prevent apoptosis by activating transcription of the essential pro-survival factor *Mcl1*. MCL1 has been demonstrated as a resistance factor for BCL2 inhibition in lymphoma(183). Recently Leverson and colleagues

identified a MCL1 inhibitor that is effective in various cancer cell lines, both independently and in concert with BCL2 inhibitors(183). This could provide a potential therapeutic intervention downstream of high YY1 expression. This highlights the importance of understanding the underlying biological processes and the potential for this information to help identify relevant therapeutic targets in cancer.

Given that I also suggest the activation of *c-Myc* by YY1 may be important for the phenotypes observed in Chapter III, targeting of *c-Myc* therapeutically may be another avenue worth pursuing. As I demonstrated in Chapter II, inhibition of C-MYC indirectly by JQ1 is effective in inhibiting DLBCL cell line growth, regardless of the mechanism leading C-MYC to become oncogenic. It has been previously shown that SMURF2 can inhibit C-MYC indirectly through direct inhibition of YY1 and that exogenous expression of *SMURF2* in a human DLBCL cell line can decrease *c-Myc* levels(135). Therefore, another possible method for inhibition of C-MYC could be through the activation of SMURF2. I have begun to pursue efforts to therapeutically modulate *SMURF2* expression, although to date no small molecules have been validated.

In Chapter IV I showed that SMURF2 does not exert its tumor suppressor activity by suppressing the GC. This suggests that the SMURF2-YY1-C-MYC axis is not be the only important pathway that SMURF2 utilizes for its tumor suppressive activity. It is likely that the SMURF2-YY1-C-MYC

axis plays a role in tumor suppression that is independent of the role for YY1 and C-MYC in the GC. The precise mechanism for SMURF2 as a tumor suppressor and what downstream effectors may be important has yet to be determined. This will be an interesting area for future work.

Future Directions

The three areas of focus covered in this thesis provide starting points for interesting future investigation. The results in Chapter II have already provided a baseline for further investigation in the field. Therefore the proposed areas for further study will focus on the other two chapters. The work focused on YY1 as a factor in the GC should be expanded to investigate the mechanism by which YY1 exerts its effect. Future work should focus on how YY1 regulates the GC with particular focus on *Mcl1* and *c-Myc* as factors I have hypothesized may be involved. It will also be interesting to investigate what may occur upstream of YY1 to induce upregulation as cells commit to GC B cells. One hypothesis is that SMURF2 activity may decrease allowing YY1 protein to accumulate. Along the same lines, it would be interesting to investigate if overexpression of YY1 increases the GC. Given that YY1 is highly expressed in some lymphomas it would also be interesting to investigate if overexpression of YY1 in GC cells causes lymphoma. These two lines of investigation could be studied by utilizing a YY1 transgene to

model enforced expression with a possible REPO-domain deleted transgene as a control to probe the role of PRC recruitment in these processes.

In addition to investigating the involvement of YY1 in these various processes, it will be important to continue the work characterizing SMURF2 as a tumor suppressor. Although previously it has been established SMURF2 is a tumor suppressor(138, 144), the mechanism through which SMURF2 functions is still not clear. In Chapter IV I established that SMURF2 does not appear to have a role in the GC or in altering the mutation rate. This leaves many possible mechanisms to explore, some of which are discussed above. Identifying the mechanism through which SMURF2 acts as a tumor suppressor will advance our understanding of how SMURF2 loss contributes to tumorigenesis and may help identify potential therapeutic opportunities.

Bibliography

1. Campo, E., S. H. Swerdlow, N. L. Harris, S. Pileri, H. Stein, and E. S. Jaffe. 2011. The 2008 WHO classification of lymphoid neoplasms and beyond: evolving concepts and practical applications. *Blood* 117: 5019–32.

2. Coiffier, B. 2001. Diffuse large cell lymphoma. *Current Opinion in Oncology* 13: 325.

3. Coiffier, B., C. Thieblemont, E. Van Den Neste, G. Lepeu, I. Plantier, S. Castaigne, S. Lefort, G. Marit, M. Macro, C. Sebban, K. Belhadj, D. Bordessoule, C. Fermé, and H. Tilly. 2010. Long-term outcome of patients in the LNH-98.5 trial, the first randomized study comparing rituximab-CHOP to standard CHOP chemotherapy in DLBCL patients: a study by the Groupe d'Etudes des Lymphomes de l'Adulte. *Blood* 116: 2040–5.

4. Friedberg, J. 2011. Relapsed/Refractory Diffuse Large B-Cell Lymphoma. *ASH Education Program Book* 2011: 498–505.

5. Morrison, Hamlin, Soubeyran, Stauder, Wadhwa, Aapro, and Lichtman. 2015. Approach to therapy of diffuse large B-cell lymphoma in the elderly: the International Society of Geriatric Oncology (SIOG) expert position commentary. *Ann Oncol* 26: 1058–1068.

6. Alizadeh, A., M. Eisen, E. Davis, C. Ma, I. Lossos, A. Rosenwald, J. Boldrick, H. Sabet, T. Tran, X. Yu, J. Powell, L. Yang, G. Marti, T. Moore, J. Hudson, L. Lu, D. Lewis, R. Tibshirani, G. Sherlock, W. Chan, T. Greiner, D. Weisenburger, J. Armitage, R. Warnke, R. Levy, W. Wilson, M. Grever, J. Byrd, D. Botstein, P. Brown, and L. Staudt. 2000. Distinct types of diffuse

large B-cell lymphoma identified by gene expressionprofiling. *Nature* 403: 503–511.

7. Rosenwald, A., G. Wright, W. Chan, J. Connors, E. Campo, R. Fisher, R. Gascoyne, K. Muller-Hermelink, E. Smeland, J. Giltnane, E. Hurt, H. Zhao, L. Averett, L. Yang, W. Wilson, E. Jaffe, R. Simon, R. Klausner, J. Powell, P. Duffey, D. Longo, T. Greiner, D. Weisenburger, W. Sanger, B. Dave, J. Lynch, J. Vose, J. Armitage, E. Montserrat, A. López-Guillermo, T. Grogan, T. Miller, M. LeBlanc, G. Ott, S. Kvaloy, J. Delabie, H. Holte, P. Krajci, T. Stokke, and L. Staudt. 2002. The Use of Molecular Profiling to Predict Survival after Chemotherapy for Diffuse Large-B-Cell Lymphoma. *The New England Journal of Medicine* 346: 1937–1947.

8. Wright, G., B. Tan, A. Rosenwald, E. Hurt, A. Wiestner, and L. Staudt. 2003. A gene expression-based method to diagnose clinically distinct subgroups of diffuse large B cell lymphoma. *Proceedings of the National Academy of Sciences* 100: 9991–9996.

9. Savage, Monti, Kutok, Cattoretti, and Neuberg. 2003. The molecular signature of mediastinal large B-cell lymphoma differs from that of other diffuse large B-cell lymphomas and shares features with classical …. .

10. Shipp, M. A., K. N. Ross, P. Tamayo, A. P. Weng, J. L. Kutok, R. C. Aguiar, M. Gaasenbeek, M. Angelo, M. Reich, G. S. Pinkus, T. S. Ray, M. A. Koval, K. W. Last, A. Norton, T. A. Lister, J. Mesirov, D. S. Neuberg, E. S. Lander, J. C. Aster, and T. R. Golub. 2002. Diffuse large B-cell lymphoma outcome prediction by gene-expression profiling and supervised machine learning. *Nat. Med.* 8: 68–74.

11. Morin, R. D., N. A. Johnson, T. M. Severson, A. J. Mungall, J. An, R. Goya, J. E. Paul, M. Boyle, B. W. Woolcock, F. Kuchenbauer, D. Yap, R. K. Humphries, O. L. Griffith, S. Shah, H. Zhu, M. Kimbara, P. Shashkin, J. F. Charlot, M. Tcherpakov, R. Corbett, A. Tam, R. Varhol, D. Smailus, M. Moksa, Y. Zhao, A. Delaney, H. Qian, I. Birol, J. Schein, R. Moore, R. Holt, D. E. Horsman, J. M. Connors, S. Jones, S. Aparicio, M. Hirst, R. D. Gascoyne, and M. A. Marra. 2010. Somatic mutations altering EZH2 (Tyr641) in follicular and diffuse large B-cell lymphomas of germinal-center origin. *Nat. Genet.* 42: 181–5.

12. Savage, Johnson, Ben-Neriah, and Connors. 2009. MYC gene rearrangements are associated with a poor prognosis in diffuse large B-cell lymphoma patients treated with R-CHOP chemotherapy. .

13. Iqbal, J., W. G. Sanger, D. E. Horsman, A. Rosenwald, D. L. Pickering, B. Dave, S. Dave, L. Xiao, K. Cao, Q. Zhu, S. Sherman, C. P. Hans, D. D. Weisenburger, T. C. Greiner, R. D. Gascoyne, G. Ott, H. K. Müller-Hermelink, J. Delabie, R. M. Braziel, E. S. Jaffe, E. Campo, J. C. Lynch, J. M. Connors, J. M. Vose, J. O. Armitage, T. M. Grogan, L. M. Staudt, and W. C. Chan. 2004. BCL2 translocation defines a unique tumor subset within the germinal center B-cell-like diffuse large B-cell lymphoma. *Am. J. Pathol.* 165: 159–66.

14. Mandelbaum, J., G. Bhagat, H. Tang, T. Mo, M. Brahmachary, Q. Shen, A. Chadburn, K. Rajewsky, A. Tarakhovsky, L. Pasqualucci, and R. Dalla-Favera. 2010. BLIMP1 is a tumor suppressor gene frequently disrupted in activated B cell-like diffuse large B cell lymphoma. *Cancer Cell* 18: 568–79.

15. Pasqualucci, and Compagno. 2006. Inactivation of the PRDM1/BLIMP1 gene in diffuse large B cell lymphoma. .

16. Tam, Gomez, Chadburn, Lee, and Chan. 2006. Mutational analysis of PRDM1 indicates a tumor-suppressor role in diffuse large B-cell lymphomas. .

17. Compagno, M., W. K. Lim, A. Grunn, S. V. Nandula, M. Brahmachary, Q. Shen, F. Bertoni, M. Ponzoni, M. Scandurra, A. Califano, G. Bhagat, A. Chadburn, R. Dalla-Favera, and L. Pasqualucci. 2009. Mutations of multiple genes cause deregulation of NF-kappaB in diffuse large B-cell lymphoma. *Nature* 459: 717–21.

18. Davis, R. E., V. N. Ngo, G. Lenz, P. Tolar, R. M. Young, P. B. Romesser, H. Kohlhammer, L. Lamy, H. Zhao, Y. Yang, W. Xu, A. L. Shaffer, G. Wright, W. Xiao, J. Powell, J.-K. K. Jiang, C. J. Thomas, A. Rosenwald, G. Ott, H. K. Muller-Hermelink, R. D. Gascoyne, J. M. Connors, N. A. Johnson, L. M. Rimsza, E. Campo, E. S. Jaffe, W. H. Wilson, J. Delabie, E. B. Smeland, R. I. Fisher, R. M. Braziel, R. R. Tubbs, J. R. Cook, D. D. Weisenburger, W. C. Chan, S. K. Pierce, and L. M. Staudt. 2010. Chronic active B-cell-receptor signalling in diffuse large B-cell lymphoma. *Nature* 463: 88–92.

19. Lenz, G., R. E. Davis, V. N. Ngo, L. Lam, T. C. George, G. W. Wright, S. S. Dave, H. Zhao, W. Xu, A. Rosenwald, G. Ott, H. K. Muller-Hermelink, R. D. Gascoyne, J. M. Connors, L. M. Rimsza, E. Campo, E. S. Jaffe, J. Delabie, E. B. Smeland, R. I. Fisher, W. C. Chan, and L. M. Staudt. 2008. Oncogenic CARD11 mutations in human diffuse large B cell lymphoma. *Science* 319: 1676–9.

20. Ngo, V. N., R. M. Young, R. Schmitz, S. Jhavar, W. Xiao, K.-H. H. Lim, H. Kohlhammer, W. Xu, Y. Yang, H. Zhao, A. L. Shaffer, P. Romesser, G. Wright, J. Powell, A. Rosenwald, H. K. Muller-Hermelink, G. Ott, R. D.

Gascoyne, J. M. Connors, L. M. Rimsza, E. Campo, E. S. Jaffe, J. Delabie, E. B. Smeland, R. I. Fisher, R. M. Braziel, R. R. Tubbs, J. R. Cook, D. D. Weisenburger, W. C. Chan, and L. M. Staudt. 2011. Oncogenically active MYD88 mutations in human lymphoma. *Nature* 470: 115–9.

21. Kato, M., M. Sanada, I. Kato, Y. Sato, J. Takita, K. Takeuchi, A. Niwa, Y. Chen, K. Nakazaki, J. Nomoto, Y. Asakura, S. Muto, A. Tamura, M. Iio, Y. Akatsuka, Y. Hayashi, H. Mori, T. Igarashi, M. Kurokawa, S. Chiba, S. Mori, Y. Ishikawa, K. Okamoto, K. Tobinai, H. Nakagama, T. Nakahata, T. Yoshino, Y. Kobayashi, and S. Ogawa. 2009. Frequent inactivation of A20 in B-cell lymphomas. *Nature* 459: 712–6.

22. Iqbal, J., S. Gupta, Q. H. Chen, J. P. Brody, and P. Koduru. 2007. Diffuse large B-cell lymphoma with a novel translocation involving BCL6. *Cancer Genet. Cytogenet.* 178: 73–6.

23. Iqbal, J., T. C. Greiner, K. Patel, B. J. Dave, L. Smith, J. Ji, G. Wright, W. G. Sanger, D. L. Pickering, S. Jain, D. E. Horsman, Y. Shen, K. Fu, D. D. Weisenburger, C. P. Hans, E. Campo, R. D. Gascoyne, A. Rosenwald, E. S. Jaffe, J. Delabie, L. Rimsza, G. Ott, H. K. Müller-Hermelink, J. M. Connors, J. M. Vose, T. McKeithan, L. M. Staudt, and W. C. Chan. 2007. Distinctive patterns of BCL6 molecular alterations and their functional consequences in different subgroups of diffuse large B-cell lymphoma. *Leukemia* 21: 2332–43.

24. Pasqualucci, L., D. Dominguez-Sola, A. Chiarenza, G. Fabbri, A. Grunn, V. Trifonov, L. H. Kasper, S. Lerach, H. Tang, J. Ma, D. Rossi, A. Chadburn, V. V. Murty, C. G. Mullighan, G. Gaidano, R. Rabadan, P. K. Brindle, and R. Dalla-Favera. 2011. Inactivating mutations of acetyltransferase genes in B-cell lymphoma. *Nature* 471: 189–95.

25. Pasqualucci, L., V. Trifonov, G. Fabbri, J. Ma, D. Rossi, A. Chiarenza, V. A. Wells, A. Grunn, M. Messina, O. Elliot, J. Chan, G. Bhagat, A. Chadburn, G. Gaidano, C. G. Mullighan, R. Rabadan, and R. Dalla-Favera. 2011. Analysis of the coding genome of diffuse large B-cell lymphoma. *Nat. Genet.* 43: 830–7.

26. Morin, R. D., M. Mendez-Lago, A. J. Mungall, R. Goya, K. L. Mungall, R. D. Corbett, N. A. Johnson, T. M. Severson, R. Chiu, M. Field, S. Jackman, M. Krzywinski, D. W. Scott, D. L. Trinh, J. Tamura-Wells, S. Li, M. R. Firme, S. Rogic, M. Griffith, S. Chan, O. Yakovenko, I. M. Meyer, E. Y. Zhao, D. Smailus, M. Moksa, S. Chittaranjan, L. Rimsza, A. Brooks-Wilson, J. J. Spinelli, S. Ben-Neriah, B. Meissner, B. Woolcock, M. Boyle, H. McDonald, A. Tam, Y. Zhao, A. Delaney, T. Zeng, K. Tse, Y. Butterfield, I. Birol, R. Holt, J. Schein, D. E. Horsman, R. Moore, S. J. Jones, J. M. Connors, M. Hirst, R. D. Gascoyne, and M. A. Marra. 2011. Frequent mutation of histone-modifying genes in non-Hodgkin lymphoma. *Nature* 476: 298–303.

27. Lohr, J., P. Stojanov, M. Lawrence, D. Auclair, B. Chapuy, C. Sougnez, P. Cruz-Gordillo, B. Knoechel, Y. Asmann, and S. Slager. 2012. Discovery and prioritization of somatic mutations in diffuse large B-cell lymphoma (DLBCL) by whole-exome sequencing. *Proceedings of the National Academy of Sciences* 109: 3879–3884.

28. Zhang, J., V. Grubor, C. Love, A. Banerjee, K. Richards, P. Mieczkowski, C. Dunphy, W. Choi, W. Au, G. Srivastava, P. Lugar, D. Rizzieri, A. Lagoo, L. Bernal-Mizrachi, K. Mann, C. Flowers, K. Naresh, A. Evens, L. Gordon, M. Czader, J. Gill, E. Hsi, Q. Liu, A. Fan, K. Walsh, D. Jima, L. Smith, A. Johnson, J. Byrd, M. Luftig, T. Ni, J. Zhu, A. Chadburn, S. Levy, D. Dunson,

and S. Dave. 2013. Genetic heterogeneity of diffuse large B-cell lymphoma. *Proceedings of the National Academy of Sciences* .

29. Horn, H., M. Ziepert, C. Becher, T. F. Barth, H.-W. W. Bernd, A. C. Feller, W. Klapper, M. Hummel, H. Stein, M.-L. L. Hansmann, C. Schmelter, P. Möller, S. Cogliatti, M. Pfreundschuh, N. Schmitz, L. Trümper, R. Siebert, M. Loeffler, A. Rosenwald, and G. Ott. 2013. MYC status in concert with BCL2 and BCL6 expression predicts outcome in diffuse large B-cell lymphoma. *Blood* 121: 2253–63.

30. Johnson, Slack, and Savage. 2012. Concurrent expression of MYC and BCL2 in diffuse large B-cell lymphoma treated with rituximab plus cyclophosphamide, doxorubicin, vincristine, and …. .

31. Monti, S., K. Savage, J. Kutok, F. Feuerhake, P. Kurtin, M. Mihm, B. Wu, L. Pasqualucci, D. Neuberg, R. Aguiar, P. Cin, C. Ladd, G. Pinkus, G. Salles, N. Harris, R. Dalla-Favera, T. Habermann, J. Aster, T. Golub, and M. Shipp. 2005. Molecular profiling of diffuse large B-cell lymphoma identifies robust subtypes including one characterized by host inflammatory response. *Blood* 105: 1851–1861.

32. Nagasawa, T. 2006. Microenvironmental niches in the bone marrow required for B-cell development. *Nature Reviews Immunology* 6: 107–116.

33. Victora, G., and M. Nussenzweig. 2012. Germinal Centers. *Immunology* .

34. Silva, N., and U. Klein. 2015. Dynamics of B cells in germinal centres. *Nature Reviews Immunology* .

35. Klein, U., and R. Dalla-Favera. 2008. Germinal centres: role in B-cell physiology and malignancy. *Nature Reviews Immunology* 8: 22–33.

36. Tas, J., L. Mesin, G. Pasqual, S. Targ, J. Jacobsen, Y. Mano, C. Chen, J.-C. Weill, C.-A. Reynaud, E. Browne, M. Meyer-Hermann, and G. Victora. 2016. Visualizing antibody affinity maturation in germinal centers. *Science* 351: 1048–1054.

37. Muramatsu, M., K. Kinoshita, S. Fagarasan, S. Yamada, Y. Shinkai, and T. Honjo. 2000. Class Switch Recombination and Hypermutation Require Activation-Induced Cytidine Deaminase (AID), a Potential RNA Editing Enzyme. *Cell* .

38. Kuraoka, M., L. McWilliams, and G. Kelsoe. 2011. AID expression during B-cell development: searching for answers. *Immunologic Research* 49: 3–13.

39. Duke, Liu, Yaari, Khalil, Tomayko, and Shlomchik. 2013. Multiple transcription factor binding sites predict AID targeting in non-Ig genes. *J Immunol* .

40. Liu, Y., F. Malisan, O. de Bouteiller, C. Guret, S. Lebecque, J. Banchereau, F. Mills, E. Max, and H. Martinez-Valdez. 1996. Within Germinal Centers, Isotype Switching of Immunoglobulin Genes Occurs after the Onset of Somatic Mutation. *Immunity* 4: 241–250.

41. Shan, H., M. Shlomchik, and M. Weigert. 1990. Heavy-chain class switch does not terminate somatic mutation. *J. Exp. Med.* 172: 531–6.

42. Xu, Z., H. Zan, E. Pone, T. Mai, and P. Casali. 2012. Immunoglobulin

class-switch DNA recombination: induction, targeting and beyond. *Nature Reviews Immunology* 12: 517–531.

43. McHeyzer-Williams, M., S. Okitsu, N. Wang, and L. McHeyzer-Williams. 2011. Molecular programming of B cell memory. *Nature Reviews Immunology* 12: 24–34.

44. Pape, K., V. Kouskoff, D. Nemazee, L. Tang, J. Cyster, L. Tze, K. Hippen, T. Behrens, and M. Jenkins. 2003. Visualization of the Genesis and Fate of Isotype-switched B Cells during a Primary Immune Response. *The Journal of Experimental Medicine* 197: 1677–1687.

45. Cunningham, A., F. Gaspal, K. Serre, E. Mohr, I. Henderson, A. Scott-Tucker, S. Kenny, M. Khan, K.-M. Toellner, P. Lane, and I. MacLennan. 2007. Salmonella Induces a Switched Antibody Response without Germinal Centers That Impedes the Extracellular Spread of Infection. *The Journal of Immunology* 178: 6200–6207.

46. Victora, G., D. Dominguez-Sola, A. Holmes, S. Deroubaix, R. Dalla-Favera, and M. Nussenzweig. 2012. Identification of human germinal center light and dark zone cells and their relationship to human B-cell lymphomas. *Blood* 120: 2240–2248.

47. Dominguez-Sola, D., J. Kung, A. Holmes, V. Wells, T. Mo, K. Basso, and R. Dalla-Favera. 2015. The FOXO1 Transcription Factor Instructs the Germinal Center Dark Zone Program. *Immunity* .

48. Sander, S., V. Chu, T. Yasuda, A. Franklin, R. Graf, D. Calado, S. Li, K. Imami, M. Selbach, M. Di Virgilio, L. Bullinger, and K. Rajewsky. 2015. PI3

Kinase and FOXO1 Transcription Factor Activity Differentially Control B Cells in the Germinal Center Light and Dark Zones. *Immunity* .

49. Zhang, Y., M. Meyer-Hermann, L. A. George, M. T. Figge, M. Khan, M. Goodall, S. P. Young, A. Reynolds, F. Falciani, A. Waisman, C. A. Notley, M. R. Ehrenstein, M. Kosco-Vilbois, and K.-M. M. Toellner. 2013. Germinal center B cells govern their own fate via antibody feedback. *J. Exp. Med.* 210: 457–64.

50. Gitlin, A., Z. Shulman, and M. Nussenzweig. 2014. Clonal selection in the germinal centre by regulated proliferation and hypermutation. *Nature* 509: 637–40.

51. Green, M., S. Monti, R. Dalla-Favera, L. Pasqualucci, N. Walsh, M. Schmidt-Supprian, J. Kutok, S. Rodig, D. Neuberg, K. Rajewsky, T. Golub, F. Alt, M. Shipp, and J. Manis. 2011. Signatures of murine B-cell development implicate Yy1 as a regulator of the germinal center-specific program. *Proceedings of the National Academy of Sciences* .

52. Klein, U., Y. Tu, G. A. Stolovitzky, J. L. Keller, J. Haddad, V. Miljkovic, G. Cattoretti, A. Califano, and R. Dalla-Favera. 2003. Transcriptional analysis of the B cell germinal center reaction. *Proc. Natl. Acad. Sci. U.S.A.* 100: 2639–44.

53. Shaffer, A. L., A. Rosenwald, E. M. Hurt, J. M. Giltnane, L. T. Lam, O. K. Pickeral, and L. M. Staudt. 2001. Signatures of the immune response. *Immunity* 15: 375–85.

54. Basso, K., and R. Dalla-Favera. 2012. Roles of BCL6 in normal and

transformed germinal center B cells. *Immunol. Rev.* 247: 172–83.

55. Phan, R., M. Saito, K. Basso, H. Niu, and R. Dalla-Favera. 2005. BCL6 interacts with the transcription factor Miz-1 to suppress the cyclin-dependent kinase inhibitor p21 and cell cycle arrest in germinal center B cells. *Nature Immunology* 6: 1054–1060.

56. Lee, C. H., M. Melchers, H. Wang, T. A. Torrey, R. Slota, C.-F. F. Qi, J. Y. Kim, P. Lugar, H. J. Kong, L. Farrington, B. van der Zouwen, J. X. Zhou, V. Lougaris, P. E. Lipsky, A. C. Grammer, and H. C. Morse. 2006. Regulation of the germinal center gene program by interferon (IFN) regulatory factor 8/IFN consensus sequence-binding protein. *J. Exp. Med.* 203: 63–72.

57. Phan, R., and R. Dalla-Favera. 2004. The BCL6 proto-oncogene suppresses p53 expression in germinal-centre B cells. *Nature* 432: 635–639.

58. Crotty, S., R. Johnston, and S. Schoenberger. 2010. Effectors and memories: Bcl-6 and Blimp-1 in T and B lymphocyte differentiation. *Nature Immunology* 11: 114–120.

59. Klein, U., S. Casola, G. Cattoretti, Q. Shen, M. Lia, T. Mo, T. Ludwig, K. Rajewsky, and R. Dalla-Favera. 2006. Transcription factor IRF4 controls plasma cell differentiation and class-switch recombination. *Nature immunology* 7: 773–82.

60. Ochiai, K., M. Maienschein-Cline, G. Simonetti, J. Chen, R. Rosenthal, R. Brink, A. S. Chong, U. Klein, A. R. Dinner, H. Singh, and R. Sciammas. 2013. Transcriptional regulation of germinal center B and plasma cell fates by dynamical control of IRF4. *Immunity* 38: 918–29.

61. Willis, S. N., K. L. Good-Jacobson, J. Curtis, A. Light, J. Tellier, W. Shi, G. K. Smyth, D. M. Tarlinton, G. T. Belz, L. M. Corcoran, A. Kallies, and S. L. Nutt. 2014. Transcription factor IRF4 regulates germinal center cell formation through a B cell-intrinsic mechanism. *J. Immunol.* 192: 3200–6.

62. Bollig, N., A. Brüstle, K. Kellner, W. Ackermann, E. Abass, H. Raifer, B. Camara, C. Brendel, G. Giel, E. Bothur, M. Huber, C. Paul, A. Elli, R. Kroczek, R. Nurieva, C. Dong, R. Jacob, T. Mak, and M. Lohoff. 2012. Transcription factor IRF4 determines germinal center formation through follicular T-helper cell differentiation. *Proc Natl Acad Sci* 109: 8664–8669.

63. Vikstrom, I., S. Carotta, K. Lüthje, V. Peperzak, P. J. Jost, S. Glaser, M. Busslinger, P. Bouillet, A. Strasser, S. L. Nutt, and D. M. Tarlinton. 2010. Mcl-1 is essential for germinal center formation and B cell memory. *Science* 330: 1095–9.

64. Peperzak, V., I. Vikström, J. Walker, S. Glaser, M. LePage, C. Coquery, L. Erickson, K. Fairfax, F. Mackay, A. Strasser, S. Nutt, and D. Tarlinton. 2013. Mcl-1 is essential for the survival of plasma cells. *Nature Immunology* 14: 290–297.

65. Grabow, S., A. Delbridge, B. Aubrey, C. Vandenberg, and A. Strasser. 2016. Loss of a Single Mcl-1 Allele Inhibits MYC-Driven Lymphomagenesis by Sensitizing Pro-B Cells to Apoptosis. *Cell Reports* 14: 2337–2347.

66. Li, Y., Y. Takahashi, S. Fujii, Y. Zhou, R. Hong, A. Suzuki, T. Tsubata, K. Hase, and J.-Y. Wang. 2016. EAF2 mediates germinal centre B-cell apoptosis to suppress excessive immune responses and prevent autoimmunity. *Nature*

Communications 7: 10836.

67. Mueller, Matloubian, and Zikherman. 2015. Cutting Edge: An In Vivo Reporter Reveals Active B Cell Receptor Signaling in the Germinal Center. *The Journal of Immunology* 194: 2993–2997.

68. Basso, K., U. Klein, H. Niu, G. Stolovitzky, Y. Tu, A. Califano, G. Cattoretti, and R. Dalla-Favera. 2004. Tracking CD40 signaling during germinal center development. *Blood* 104: 4088–4096.

69. Khalil, A. M., J. C. Cambier, and M. J. Shlomchik. 2012. B cell receptor signal transduction in the GC is short-circuited by high phosphatase activity. *Science* 336: 1178–81.

70. Heise, N., N. Silva, K. Silva, A. Carette, G. Simonetti, M. Pasparakis, and U. Klein. 2014. Germinal center B cell maintenance and differentiation are controlled by distinct NF-κB transcription factor subunits. *The Journal of Experimental Medicine* 211: 2103–2118.

71. Pasqualucci, L., A. Migliazza, N. Fracchiolla, C. William, A. Neri, L. Baldini, R. S. Chaganti, U. Klein, R. Küppers, K. Rajewsky, and R. Dalla-Favera. 1998. BCL-6 mutations in normal germinal center B cells: evidence of somatic hypermutation acting outside Ig loci. *Proc. Natl. Acad. Sci. U.S.A.* 95: 11816–21.

72. Pasqualucci, L., P. Neumeister, T. Goossens, G. Nanjangud, R. S. Chaganti, R. Küppers, and R. Dalla-Favera. 2001. Hypermutation of multiple proto-oncogenes in B-cell diffuse large-cell lymphomas. *Nature* 412: 341–6.

73. Staszewski, O., R. E. Baker, A. J. Ucher, R. Martier, J. Stavnezer, and J. E. Guikema. 2011. Activation-induced cytidine deaminase induces reproducible DNA breaks at many non-Ig Loci in activated B cells. *Mol. Cell* 41: 232–42.

74. Robbiani, D., A. Bothmer, E. Callen, B. Reina-San-Martin, Y. Dorsett, S. Difilippantonio, D. Bolland, H. Chen, A. Corcoran, A. Nussenzweig, and M. Nussenzweig. 2008. AID Is Required for the Chromosomal Breaks in c-myc that Lead to c-myc/IgH Translocations. *Cell* 135.

75. Robbiani, D. F., S. Bunting, N. Feldhahn, A. Bothmer, J. Camps, S. Deroubaix, K. M. McBride, I. A. Klein, G. Stone, T. R. Eisenreich, T. Ried, A. Nussenzweig, and M. C. Nussenzweig. 2009. AID produces DNA double-strand breaks in non-Ig genes and mature B cell lymphomas with reciprocal chromosome translocations. *Mol. Cell* 36: 631–41.

76. Shen, H. M., A. Peters, B. Baron, X. Zhu, and U. Storb. 1998. Mutation of BCL-6 gene in normal B cells by the process of somatic hypermutation of Ig genes. *Science* 280: 1750–2.

77. Liu, M., J. Duke, D. Richter, C. Vinuesa, C. Goodnow, S. Kleinstein, and D. Schatz. 2008. Two levels of protection for the B cell genome during somatic hypermutation. *Nature* 451: 841–845.

78. Liu, Y.-J., J. Zhang, P. Lane, E. Chan, and I. Maclennan. 1991. Sites of specific B cell activation in primary and secondary responses to T cell-dependent and T cell-independent antigens. *European Journal of Immunology* 21: 2951–2962.

79. Zhang, J., I. C. MacLennan, Y. J. Liu, and P. J. Lane. 1988. Is rapid proliferation in B centroblasts linked to somatic mutation in memory B cell clones? *Immunol. Lett.* 18: 297–9.

80. Allen, C. D., T. Okada, H. L. Tang, and J. G. Cyster. 2007. Imaging of germinal center selection events during affinity maturation. *Science* 315: 528–31.

81. Ranuncolo, S., J. Polo, J. Dierov, M. Singer, T. Kuo, J. Greally, R. Green, M. Carroll, and A. Melnick. 2007. Bcl-6 mediates the germinal center B cell phenotype and lymphomagenesis through transcriptional repression of the DNA-damage sensor ATR. *Nature Immunology* 8: 705–714.

82. Guikema, J., Linehan, Esa, Tsuchimoto, Nakabeppu, Woodland, and Schrader. 2014. Apurinic/Apyrimidinic Endonuclease 2 Regulates the Expansion of Germinal Centers by Protecting against Activation-Induced Cytidine Deaminase-Independent DNA Damage in B Cells. *The Journal of Immunology* 193: 931–939.

83. Allen, C. D., T. Okada, and J. G. Cyster. 2007. Germinal-center organization and cellular dynamics. *Immunity* 27: 190–202.

84. Lenz, G., and L. M. Staudt. 2010. Aggressive lymphomas. *N. Engl. J. Med.* 362: 1417–29.

85. Stevenson, F., S. Sahota, D. Zhu, C. Ottensmeier, C. Chapman, D. Oscier, and T. Hamblin. 1998. Insight into the origin and clonal history of B-cell tumors as revealed by analysis of immunoglobulin variable region genes. *Immunol. Rev.* 162: 247–59.

86. Küppers, R., U. Klein, M. L. Hansmann, and K. Rajewsky. 1999. Cellular origin of human B-cell lymphomas. *N. Engl. J. Med.* 341: 1520–9.

87. Basso, K., and R. Dalla-Favera. 2015. Germinal centres and B cell lymphomagenesis. *Nature Reviews Immunology* .

88. Dang, C. 1999. c-Myc Target Genes Involved in Cell Growth, Apoptosis, and Metabolism. *Molecular and Cellular Biology* 19: 1–11.

89. Vennstrom, B, D Sheiness, J Zabielski, and JM Bishop. 1982. Isolation and characterization of c-myc, a cellular homolog of the oncogene (v-myc) of avian myelocytomatosis virus strain 29. *Journal of virology* 42: 773–779.

90. Dang, C. 2012. MYC on the Path to Cancer. *Cell* 149: 22–35.

91. Fernandez, P., S. Frank, L. Wang, M. Schroeder, S. Liu, J. Greene, A. Cocito, and B. Amati. 2003. Genomic targets of the human c-Myc protein. *Gene Dev* 17: 1115–1129.

92. Nie, Z., G. Hu, G. Wei, K. Cui, A. Yamane, W. Resch, R. Wang, D. Green, L. Tessarollo, R. Casellas, K. Zhao, and D. Levens. 2012. c-Myc Is a Universal Amplifier of Expressed Genes in Lymphocytes and Embryonic Stem Cells. *Cell* 151: 68–79.

93. Bretones, G., D. Delgado, and J. León. 2015. Myc and cell cycle control. *Biochimica et Biophysica Acta (BBA) - Gene Regulatory Mechanisms* 1849: 506–516.

94. Dominguez-Sola, D., G. Victora, C. Ying, R. Phan, M. Saito, M. Nussenzweig, and R. Dalla-Favera. 2012. The proto-oncogene MYC is required for selection in the germinal center and cyclic reentry. *Nature Immunology* .

95. Calado, D., Y. Sasaki, S. Godinho, A. Pellerin, K. Köchert, B. Sleckman, I. de Alborán, M. Janz, S. Rodig, and K. Rajewsky. 2012. The cell-cycle regulator c-Myc is essential for the formation and maintenance of germinal centers. *Nature Immunology* 13: 1092–100.

96. Dib, A., A. Gabrea, O. K. Glebov, P. L. Bergsagel, and W. M. Kuehl. 2008. Characterization of MYC translocations in multiple myeloma cell lines. *J. Natl. Cancer Inst. Monographs* 25–31.

97. Zirath, Frenzel, Oliynyk, Segerstrom, Westermark, Larsson, M. Persson, Hultenby, Lehtio, Einvik, Pahlman, Kogner, P.-J. Jakobsson, and A. Henriksson. 2013. MYC inhibition induces metabolic changes leading to accumulation of lipid droplets in tumor cells. *Proceedings of the National Academy of Sciences* 110: 10258–10263.

98. Wang, H., P. Teriete, A. Hu, D. Raveendra-Panickar, K. Pendelton, J. Lazo, J. Eiseman, T. Holien, K. Misund, G. Oliynyk, M. Arsenian-Henriksson, N. Cosford, A. Sundan, and E. Prochownik. 2015. Direct inhibition of c-Myc-Max heterodimers by celastrol and celastrol-inspired triterpenoids. *Oncotarget* 6.

99. Kota, J, RR Chivukula, KA O'Donnell, and EA Wentzel. 2009. Therapeutic microRNA delivery suppresses tumorigenesis in a murine liver cancer model. *Cell* .

100. Filippakopoulos, P., J. Qi, S. Picaud, Y. Shen, W. B. Smith, O. Fedorov, E. M. Morse, T. Keates, T. T. Hickman, I. Felletar, M. Philpott, S. Munro, M. R. McKeown, Y. Wang, A. L. Christie, N. West, M. J. Cameron, B. Schwartz, T. D. Heightman, N. La Thangue, C. A. French, O. Wiest, A. L. Kung, S. Knapp, and J. E. Bradner. 2010. Selective inhibition of BET bromodomains. *Nature* 468: 1067–73.

101. Delmore, J., G. Issa, M. Lemieux, P. Rahl, J. Shi, H. Jacobs, E. Kastritis, T. Gilpatrick, R. Paranal, J. Qi, M. Chesi, A. Schinzel, M. McKeown, T. Heffernan, C. Vakoc, L. Bergsagel, I. Ghobrial, P. Richardson, R. Young, W. Hahn, K. Anderson, A. Kung, J. Bradner, and C. Mitsiades. 2011. BET Bromodomain Inhibition as a Therapeutic Strategy to Target c-Myc. *Cell* 146: 904–917.

102. Ott, C., N. Kopp, L. Bird, R. Paranal, J. Qi, T. Bowman, S. Rodig, A. Kung, J. Bradner, and D. Weinstock. 2012. BET bromodomain inhibition targets both c-Myc and IL7R in high-risk acute lymphoblastic leukemia. *Blood* 120: 2843–2852.

103. Da Costa, D., A. Agathanggelou, T. Perry, V. Weston, E. Petermann, A. Zlatanou, C. Oldreive, W. Wei, G. Stewart, J. Longman, E. Smith, P. Kearns, S. Knapp, and T. Stankovic. 2013. BET inhibition as a single or combined therapeutic approach in primary paediatric B-precursor acute lymphoblastic leukaemia. *Blood Cancer J* 3: e126.

104. Herrmann, H., K. Blatt, J. Shi, K. Gleixner, S. Cerny-Reiterer, L. Müllauer, C. Vakoc, W. Sperr, H.-P. Horny, J. Bradner, J. Zuber, and P. Valent. 2012. Small-molecule inhibition of BRD4 as a new potent approach to

eliminate leukemic stem- and progenitor cells in acute myeloid leukemia (AML). *Oncotarget* 3: 1588–1599.

105. Zuber, J., J. Shi, E. Wang, A. Rappaport, H. Herrmann, E. Sison, D. Magoon, J. Qi, K. Blatt, M. Wunderlich, M. Taylor, C. Johns, A. Chicas, J. Mulloy, S. Kogan, P. Brown, P. Valent, J. Bradner, S. Lowe, and C. Vakoc. 2011. RNAi screen identifies Brd4 as a therapeutic target in acute myeloid leukaemia. *Nature* 478: 524–528.

106. Lovén, J., H. Hoke, C. Lin, A. Lau, D. Orlando, C. Vakoc, J. Bradner, T. Lee, and R. Young. 2013. Selective Inhibition of Tumor Oncogenes by Disruption of Super-Enhancers. *Cell* 153: 320–334.

107. Mertz, J., A. Conery, B. Bryant, P. Sandy, S. Balasubramanian, D. Mele, L. Bergeron, and R. Sims. 2011. Targeting MYC dependence in cancer by inhibiting BET bromodomains. *Proceedings of the National Academy of Sciences of the United States of America* 108: 16669–74.

108. Lockwood, W., K. Zejnullahu, J. Bradner, and H. Varmus. 2012. Sensitivity of human lung adenocarcinoma cell lines to targeted inhibition of BET epigenetic signaling proteins. *Proc Natl Acad Sci* 109: 19408–19413.

109. Cheng, Z., Y. Gong, Y. Ma, K. Lu, X. Lu, L. Pierce, R. Thompson, S. Muller, S. Knapp, and J. Wang. 2013. Inhibition of BET Bromodomain Targets Genetically Diverse Glioblastoma. *Clinical Cancer Research* 19: 1748–1759.

110. Chapuy, B., M. McKeown, C. Lin, S. Monti, M. Roemer, J. Qi, P. Rahl, H. Sun, K. Yeda, J. Doench, E. Reichert, A. Kung, S. Rodig, R. Young, M. Shipp, and J. Bradner. 2013. Discovery and Characterization of Super-Enhancer-

Associated Dependencies in Diffuse Large B Cell Lymphoma. *Cancer Cell* 24: 777–790.

111. Liu, H., M. Schmidt-Supprian, Y. Shi, E. Hobeika, N. Barteneva, H. Jumaa, R. Pelanda, M. Reth, J. Skok, K. Rajewsky, and Y. Shi. 2007. Yin Yang 1 is a critical regulator of B-cell development. *Genes & Development* .

112. Zaprazna, K., and M. Atchison. 2012. YY1 controls immunoglobulin class switch recombination and nuclear activation-induced deaminase levels. *Molecular and cellular biology* .

113. Atchison, M. 2014. Function of YY1 in Long-Distance DNA Interactions. *Frontiers in Immunology* .

114. Wilkinson, F., K. Park, and M. Atchison. 2006. Polycomb recruitment to DNA in vivo by the YY1 REPO domain. *Proceedings of the National Academy of Sciences* .

115. Affar, E., F. Gay, Y. Shi, H. Liu, M. Huarte, S. Wu, T. Collins, E. Li, and Y. Shi. 2006. Essential Dosage-Dependent Functions of the Transcription Factor Yin Yang 1 in Late Embryonic Development and Cell Cycle Progression. *Molecular and Cellular Biology* .

116. Donohoe, Zhang, McGinnis, Biggers, Li, and Shi. 1999. Targeted disruption of mouse Yin Yang 1 transcription factor results in peri-implantation lethality. *Molecular and cellular biology* 19: 7237–44.

117. Perekatt, A., M. Valdez, M. Davila, Hoffman, E. Bonder, N. Gao, and M. Verzi. 2014. YY1 is indispensable for Lgr5+ intestinal stem cell renewal.

Proceedings of the National Academy of Sciences .

118. Schug, J., W.-P. Schuller, C. Kappen, M. Salbaum, M. Bucan, and C. Stoeckert. 2005. Promoter features related to tissue specificity as measured by Shannon entropy. *Genome biology* 6: R33.

119. Hsu, -W, -H Hsieh, -H Lee, -H Chao, -J Wu, -J Tseng, and -S Yeh. 2008. The Activated Notch1 Receptor Cooperates with -Enolase and MBP-1 in Modulating c-myc Activity. *Molecular and Cellular Biology* 28: 4829–4842.

120. Riggs, Saleque, Wong, Merrell, Lee, Shi, and Calame. 1993. Yin-yang 1 activates the c-myc promoter. *Molecular and Cellular Biology* 13: 7487–7495.

121. Makhlouf, M., J.-F. Ouimette, A. Oldfield, P. Navarro, D. Neuillet, and C. Rougeulle. 2014. A prominent and conserved role for YY1 in Xist transcriptional activation. *Nat Commun* 5: 4878.

122. Rosenbloom, K., C. Sloan, V. Malladi, T. Dreszer, K. Learned, V. Kirkup, M. Wong, M. Maddren, R. Fang, S. Heitner, B. Lee, G. Barber, R. Harte, M. Diekhans, J. Long, S. Wilder, A. Zweig, D. Karolchik, R. Kuhn, D. Haussler, and J. Kent. 2013. ENCODE Data in the UCSC Genome Browser: year 5 update. *Nucleic Acids Research* 41: D56–D63.

123. Grönroos, E., A. A. Terentiev, T. Punga, and J. Ericsson. 2004. YY1 inhibits the activation of the p53 tumor suppressor in response to genotoxic stress. *Proc. Natl. Acad. Sci. U.S.A.* 101: 12165–70.

124. Sui, G., E. Affar, Y. Shi, C. Brignone, N. Wall, P. Yin, M. Donohoe, M. Luke, D. Calvo, S. Grossman, and Y. Shi. 2004. Yin Yang 1 Is a Negative

Regulator of p53. *Cell* .

125. Pan, X., M. Papasani, Y. Hao, M. Calamito, F. Wei, W. J. Quinn Iii, A. Basu, J. Wang, S. Hodawadekar, K. Zaprazna, H. Liu, Y. Shi, D. Allman, M. Cancro, and M. L. Atchison. 2013. YY1 controls Igκ repertoire and B-cell development, and localizes with condensin on the Igκ locus. *EMBO J.* 32: 1168–82.

126. Pan, X., M. Jones, J. Jiang, K. Zaprazna, D. Yu, W. Pear, I. Maillard, and M. Atchison. 2012. Increased Expression of PcG Protein YY1 Negatively Regulates B Cell Development while Allowing Accumulation of Myeloid Cells and LT-HSC Cells. *PLoS ONE* 7: e30656.

127. Banerjee, A., V. Sindhava, R. Vuyyuru, V. Jha, S. Hodewadekar, T. Manser, and M. Atchison. 2016. YY1 Is Required for Germinal Center B Cell Development. *PLOS ONE* 11: e0155311.

128. Bonavida, B., and S. Kaufhold. 2015. Prognostic significance of YY1 protein expression and mRNA levels by bioinformatics analysis in human cancers: A therapeutic target. *Pharmacology & Therapeutics* 150.

129. Castellano, G., E. Torrisi, G. Ligresti, F. Nicoletti, G. Malaponte, S. Travali, J. McCubrey, S. Canevari, and M. Libra. 2010. Yin Yang 1 overexpression in diffuse large B-cell lymphoma is associated with B-cell transformation and tumor progression. *Cell Cycle* 9: 557–563.

130. Naidoo, K., V. Clay, J. Hoyland, R. Swindell, K. Linton, T. Illidge, J. Radford, and R. Byers. 2011. YY1 expression predicts favourable outcome in follicular lymphoma. *Journal of Clinical Pathology* 64: 125–129.

131. Sakhinia, E., C. Glennie, J. A. Hoyland, L. P. Menasce, G. Brady, C. Miller, J. A. Radford, and R. J. Byers. 2007. Clinical quantitation of diagnostic and predictive gene expression levels in follicular and diffuse large B-cell lymphoma by RT-PCR gene expression profiling. *Blood* 109: 3922–8.

132. Mari, S., N. Ruetalo, E. Maspero, M. Stoffregen, S. Pasqualato, S. Polo, and S. Wiesner. 2014. Structural and Functional Framework for the Autoinhibition of Nedd4-Family Ubiquitin Ligases. *Structure* 22.

133. Zhang, Y., C. Chang, D. Gehling, A. Hemmati-Brivanlou, and R. Derynck. 2001. Regulation of Smad degradation and activity by Smurf2, an E3 ubiquitin ligase. *Proceedings of the National Academy of Sciences* 98.

134. Fukunaga, E., Y. Inoue, S. Komiya, K. Horiguchi, K. Goto, M. Saitoh, K. Miyazawa, D. Koinuma, A. Hanyu, and T. Imamura. 2008. Smurf2 Induces Ubiquitin-dependent Degradation of Smurf1 to Prevent Migration of Breast Cancer Cells. *Journal of Biological Chemistry* 283.

135. Ramkumar, C., H. Cui, Y. Kong, S. Jones, R. Gerstein, and H. Zhang. 2013. Smurf2 suppresses B-cell proliferation and lymphomagenesis by mediating ubiquitination and degradation of YY1. *Nature Communications* 4: 2598.

136. Jeong, H., S. Lee, J. Yum, C.-Y. Yeo, and K. Lee. 2014. Smurf2 regulates the degradation of YY1. *Biochimica et Biophysica Acta (BBA) - Molecular Cell Research* 1843.

137. Kong, Y., H. Cui, and H. Zhang. 2011. Smurf2-mediated ubiquitination

and degradation of Id1 regulates p16 expression during senescence. *Aging Cell* 10: 1038–1046.

138. Blank, M., Y. Tang, M. Yamashita, S. Burkett, S. Cheng, and Y. Zhang. 2012. A tumor suppressor function of Smurf2 associated with controlling chromatin landscape and genome stability through RNF20. *Nature Medicine* 18: 227–34.

139. Kaneki, Guo, Chen, Yao, and Schwarz. 2006. Tumor necrosis factor promotes Runx2 degradation through up-regulation of Smurf1 and Smurf2 in osteoblasts. .

140. Schwamborn, J. C., M. Müller, A. H. Becker, and A. W. Püschel. 2007. Ubiquitination of the GTPase Rap1B by the ubiquitin ligase Smurf2 is required for the establishment of neuronal polarity. *EMBO J.* 26: 1410–22.

141. Kim, and Jho. 2010. The protein stability of Axin, a negative regulator of Wnt signaling, is regulated by Smad ubiquitination regulatory factor 2 (Smurf2). .

142. Wu, Q., J. H. Huang, E. R. Sampson, K.-O. K. O. Kim, M. J. Zuscik, R. J. O'Keefe, D. Chen, and R. N. Rosier. 2009. Smurf2 induces degradation of GSK-3beta and upregulates beta-catenin in chondrocytes: a potential mechanism for Smurf2-induced degeneration of articular cartilage. *Exp. Cell Res.* 315: 2386–98.

143. Narimatsu, M., R. Bose, M. Pye, L. Zhang, B. Miller, P. Ching, R. Sakuma, V. Luga, L. Roncari, L. Attisano, and J. L. Wrana. 2009. Regulation of planar cell polarity by Smurf ubiquitin ligases. *Cell* 137: 295–307.

144. Ramkumar, C., Y. Kong, H. Cui, S. Hao, S. Jones, R. Gerstein, and H. Zhang. 2012. Smurf2 Regulates the Senescence Response and Suppresses Tumorigenesis in Mice. *Cancer Research* 72: 2714–9.

145. Ramkumar, C., Y. Kong, S. E. Trabucco, R. M. Gerstein, and H. Zhang. 2014. Smurf2 regulates hematopoietic stem cell self-renewal and aging. *Aging Cell* 13: 478–86.

146. Serrano, M., A. Lin, M. McCurrach, D. Beach, and S. Lowe. 1997. Oncogenic ras Provokes Premature Cell Senescence Associated with Accumulation of p53 and p16INK4a. *Cell* 88.

147. Michaloglou, C., L. Vredeveld, M. Soengas, C. Denoyelle, T. Kuilman, C. van der Horst, D. Majoor, J. Shay, W. Mooi, and D. Peeper. 2005. BRAFE600-associated senescence-like cell cycle arrest of human naevi. *Nature* 436.

148. Chen, Z., L. Trotman, D. Shaffer, H.-K. Lin, Z. Dotan, M. Niki, J. Koutcher, H. Scher, T. Ludwig, W. Gerald, C. Cordon-Cardo, and P. Pandolfi. 2005. Crucial role of p53-dependent cellular senescence in suppression of Pten-deficient tumorigenesis. *Nature* 436: 725–730.

149. Pollock, P., U. Harper, K. Hansen, L. Yudt, M. Stark, C. Robbins, T. Moses, G. Hostetter, U. Wagner, J. Kakareka, G. Salem, T. Pohida, P. Heenan, P. Duray, O. Kallioniemi, N. Hayward, J. Trent, and P. Meltzer. 2002. High frequency of BRAF mutations in nevi. *Nature Genetics* 33.

150. Bauer, J., J. Curtin, D. Pinkel, and B. Bastian. 2006. Congenital

Melanocytic Nevi Frequently Harbor NRAS Mutations but no BRAF Mutations. *Journal of Investigative Dermatology* 127.

151. Schmitt, C., J. Fridman, M. Yang, S. Lee, E. Baranov, R. Hoffman, and S. Lowe. 2002. A Senescence Program Controlled by p53 and p16INK4a Contributes to the Outcome of Cancer Therapy. *Cell* 109.

152. Wilson, A., M. Murphy, T. Oskarsson, K. Kaloulis, M. Bettess, G. Oser, A.-C. Pasche, C. Knabenhans, R. MacDonald, and A. Trumpp. 2004. c-Myc controls the balance between hematopoietic stem cell self-renewal and differentiation. *Gene Dev* 18: 2747–2763.

153. Zhao, Lwin, Zhang, Huang, Wang, Marquez, Chen-Kiang, Dalton, Sotomayor, and Tao. 2013. Disruption of the MYC-miRNA-EZH2 loop to suppress aggressive B-cell lymphoma survival and clonogenicity. *Leukemia* 27: 2341–2350.

154. Emadali, A., S. Rousseaux, J. Bruder‐Costa, C. Rome, S. Duley, S. Hamaidia, P. Betton, A. Debernardi, D. Leroux, B. Bernay, S. Kieffer‐Jaquinod, F. Combes, E. Ferri, C. McKenna, C. Petosa, C. Bruley, J. Garin, M. Ferro, R. Gressin, M. Callanan, and S. Khochbin. 2013. Identification of a novel BET bromodomain inhibitor‐sensitive, gene regulatory circuit that controls Rituximab response and tumour growth in aggressive lymphoid cancers. *EMBO Molecular Medicine* 5: 1180–1195.

155. Yang, Y., A. L. Shaffer, N. C. Emre, M. Ceribelli, M. Zhang, G. Wright, W. Xiao, J. Powell, J. Platig, H. Kohlhammer, R. M. Young, H. Zhao, Y. Yang, W. Xu, J. J. Buggy, S. Balasubramanian, L. A. Mathews, P. Shinn, R. Guha, M. Ferrer, C. Thomas, T. A. Waldmann, and L. M. Staudt. 2012. Exploiting

synthetic lethality for the therapy of ABC diffuse large B cell lymphoma. *Cancer Cell* 21: 723–37.

156. Rai, D., S. Karanti, I. Jung, P. L. Dahia, and R. C. Aguiar. 2008. Coordinated expression of microRNA-155 and predicted target genes in diffuse large B-cell lymphoma. *Cancer Genet. Cytogenet.* 181: 8–15.

157. Henssen, A., T. Thor, A. Odersky, L. Heukamp, N. El-Hindy, A. Beckers, F. Speleman, K. Althoff, S. Schäfers, A. Schramm, U. Sure, G. Fleischhack, A. Eggert, and J. H. Schulte. 2013. BET bromodomain protein inhibition is a therapeutic option for medulloblastoma. *Oncotarget* 4: 2080–95.

158. Shimamura, Chen, Soucheray, and Carretero. 2013. Efficacy of BET bromodomain inhibition in Kras-mutant non–small cell lung cancer. .

159. Mehra, S., H. Messner, M. Minden, and R. S. Chaganti. 2002. Molecular cytogenetic characterization of non-Hodgkin lymphoma cell lines. *Genes Chromosomes Cancer* 33: 225–34.

160. Epstein, A. L., R. Levy, H. Kim, W. Henle, G. Henle, and H. S. Kaplan. 1978. Biology of the human malignant lymphomas. IV. Functional characterization of ten diffuse histiocytic lymphoma cell lines. *Cancer* 42: 2379–91.

161. Gaidano, G., N. Z. Parsa, V. Tassi, P. Della-Latta, R. S. Chaganti, D. M. Knowles, and R. Dalla-Favera. 1993. In vitro establishment of AIDS-related lymphoma cell lines: phenotypic characterization, oncogene and tumor suppressor gene lesions, and heterogeneity in Epstein-Barr virus infection. *Leukemia* 7: 1621–9.

162. Schneider, B., S. Nagel, M. Kaufmann, S. Winkelmann, J. Bode, H. G. Drexler, and R. A. MacLeod. 2008. T(3;7)(q27;q32) fuses BCL6 to a non-coding region at FRA7H near miR-29. *Leukemia* 22: 1262–6.

163. Farrugia, Duan, Reis, and Ngan. 1994. Alterations of the p53 tumor suppressor gene in diffuse large cell lymphomas with translocations of the c-MYC and BCL-2 proto-oncogenes. .

164. Chen, Foreman, SantAngelo, and Krangel. 2016. Yin Yang 1 Promotes Thymocyte Survival by Downregulating p53. *The Journal of Immunology* 196: 2572–2582.

165. Rickert, R., J. Roes, and K. Rajewsky. 1997. B Lymphocyte-Specific, Cre-mediated Mutagenesis in Mice. *Nucleic Acids Research* 25: 1317–1318.

166. Crouch, E., Z. Li, M. Takizawa, S. Fichtner-Feigl, P. Gourzi, C. Montaño, L. Feigenbaum, P. Wilson, S. Janz, N. Papavasiliou, and R. Casellas. 2007. Regulation of AID expression in the immune response. *The Journal of Experimental Medicine* 204: 1145–1156.

167. Sernández, I., V. de Yébenes, Y. Dorsett, and A. Ramiro. 2008. Haploinsufficiency of Activation-Induced Deaminase for Antibody Diversification and Chromosome Translocations both In Vitro and In Vivo. *PLoS ONE* .

168. Muzumdar, M., B. Tasic, K. Miyamichi, L. Li, and L. Luo. 2007. A global double‐fluorescent Cre reporter mouse. *genesis* 45: 593–605.

169. Victora, G., T. Schwickert, D. Fooksman, A. Kamphorst, M. Meyer-Hermann, M. Dustin, and M. Nussenzweig. 2010. Germinal Center Dynamics Revealed by Multiphoton Microscopy with a Photoactivatable Fluorescent Reporter. *Cell* 143: 592–605.

170. Nicholson, D., A. Ali, N. Thornberry, J. Vaillancourt, C. Ding, M. Gallant, Y. Gareau, P. Griffin, M. Labelle, Y. Lazebnik, N. Munday, S. Raju, M. Smulson, T.-T. Yamin, V. Yu, and D. Miller. 1995. Identification and inhibition of the ICE/CED-3 protease necessary for mammalian apoptosis. *Nature* 376: 37–43.

171. Vermes, Haanen, and Reutelingsperger. 2000. Flow cytometry of apoptotic cell death. *Journal of Immunological Methods* 243: 167–190.

172. Schrader, C., E. Linehan, A. Ucher, B. Bertocci, and J. Stavnezer. 2013. DNA polymerases β and λ do not directly affect Ig variable region somatic hypermutation although their absence reduces the frequency of mutations. *DNA Repair* 12: 1087–1093.

173. Roderick, J. E., J. Tesell, L. D. Shultz, M. A. Brehm, D. L. Greiner, M. H. Harris, L. B. Silverman, S. E. Sallan, A. Gutierrez, A. T. Look, J. Qi, J. E. Bradner, and M. A. Kelliher. 2014. c-Myc inhibition prevents leukemia initiation in mice and impairs the growth of relapsed and induction failure pediatric T-ALL cells. *Blood* 123: 1040–50.

174. Xu, Sharp, Yao, Segal, Ang, Khaw, Aubrey, Gong, Kelly, Herold, Strasser, Roberts, Alexander, Burns, D. Huang, and Glaser. 2016. BET inhibition represses miR17-92 to drive BIM-initiated apoptosis of normal and transformed hematopoietic cells. *Leukemia* .

175. Ceribelli, M., P. Kelly, A. Shaffer, G. Wright, W. Xiao, Y. Yang, L. Griner, R. Guha, P. Shinn, J. Keller, D. Liu, P. Patel, M. Ferrer, S. Joshi, S. Nerle, P. Sandy, E. Normant, C. Thomas, and L. Staudt. 2014. Blockade of oncogenic IκB kinase activity in diffuse large B-cell lymphoma by bromodomain and extraterminal domain protein inhibitors. *Proceedings of the National Academy of Sciences* 111: 11365–11370.

176. Cinar, M., F. Rosenfelt, S. Rokhsar, J. Lopategui, R. Pillai, M. Cervania, A. Pao, B. Cinar, and S. Alkan. 2015. Concurrent inhibition of MYC and BCL2 is a potentially effective treatment strategy for double hit and triple hit B-cell lymphomas. *Leukemia Research* 39: 730–738.

177. Johnson-Farley, N., J. Veliz, Bhagavathi, and J. Bertino. 2015. ABT-199, a BH3 mimetic that specifically targets Bcl-2, enhances the antitumor activity of chemotherapy, bortezomib and JQ1 in “double hit” lymphoma cells. *Leukemia & Lymphoma* 56: 2146–2152.

178. Allen, C., M. Ansel, C. Low, R. Lesley, H. Tamamura, N. Fujii, and J. Cyster. 2004. Germinal center dark and light zone organization is mediated by CXCR4 and CXCR5. *Nature Immunology* 5: 943–952.

179. Bannard, O., R. Horton, C. Allen, J. An, T. Nagasawa, and J. Cyster. 2013. Germinal Center Centroblasts Transition to a Centrocyte Phenotype According to a Timed Program and Depend on the Dark Zone for Effective Selection. *Immunity* 39: 912–924.

180. Hanahan, D., and R. Weinberg. 2011. Hallmarks of Cancer: The Next Generation. *Cell* 144: 646–674.

181. Wiesner, S., A. Ogunjimi, H.-R. Wang, D. Rotin, F. Sicheri, J. Wrana, and J. Forman-Kay. 2007. Autoinhibition of the HECT-Type Ubiquitin Ligase Smurf2 through Its C2 Domain. *Cell* 130: 651–662.

182. Vega, Jazirehi, Huerta-Yepez, and Bonavida. 2005. Rituximab-induced inhibition of YY1 and Bcl-xL expression in Ramos non-Hodgkin's lymphoma cell line via inhibition of NF-kappa B activity: role of YY1 and Bcl-xL in Fas resistance and chemoresistance, respectively. *J Immunol* .

183. Leverson, Zhang, Chen, Tahir, Phillips, Xue, Nimmer, Jin, Smith, Xiao, Kovar, Tanaka, Bruncko, Sheppard, Wang, Gierke, Kategaya, Anderson, Wong, Eastham-Anderson, M. Ludlam, Sampath, Fairbrother, Wertz, Rosenberg, Tse, Elmore, and Souers. 2015. Potent and selective small-molecule MCL-1 inhibitors demonstrate on-target cancer cell killing activity as single agents and in combination with ABT-263 (navitoclax). *Cell Death & Disease* 6: e1590.